MICROFLUIDICS DEVICES FOR *DROSOPHILA*-BASED DRUG DISCOVERY ASSAYS

By

REZA GHAEMI

B.Sc., M.Sc.

A Thesis

Submitted to the School of Graduate Studies

in Partial Fulfilment of the Requirements for the Degree of

Doctor of Philosophy in Mechanical Engineering

McMaster University

Microfluidics devices for *Drosophila*-based drug discovery assays

McMaster University DOCTOR OF PHILOSOPHY (2017)

Hamilton, Ontario, Canada

TITLE: Microfluidics devices for *Drosophila*-based drug discovery assays

AUTHOR: Reza Ghaemi

B.Sc. (Sharif University of Technology)

M.Sc. (McMaster University)

SUPERVISOR: Professor P. Ravi Selvaganapathy

NUMBER OF PAGES: xx, 133

ABSTRACT

Drosophila melanogaster has long been a preferred model organism for the study of developmental, genetic, and biochemical processes. They have only four chromosomes and a comparably simple morphology. Given that 60% of *Drosophila* proteins share homologs with humans, this allows for the effective study of biological processes that are of importance in human and vertebrate models. The conventional drug discovery assays using *Drosophila* are manual and require skill operator, which makes them expensive and unsuitable for high-throughput screening. Hence, technologies to address the existing challenges involved in the conventional *Drosophila*-based assays (either in embryonic or larva stage) would greatly facilitate drug discovery process. In this thesis, microfabrication and microfluidics engineering approaches have been utilized in *Drosophila*-based assays due to their potential to obtain high accurate positioning and reagent delivery in a low-cost, rapid and potentially automated manner. At embryonic stage, the first microinjector that allow one to precisely insert a long taper microneedle laterally and at various positions inside the length of the *Drosophila* embryo (up to 250μm) was developed. Using this device, it was demonstrated that the cardioblast migration velocity is modified in a dose sensitive manner to varying doses of injected Sodium Azide (NaN3). At larva stage, a systematic analysis of various mechanical constrictions incorporated into microfluidic channels were conducted. This could allow one to find an optimized design for rapid mechanical immobilization of larvae for whole-CNS imaging. The optimal immobilization mechanism has been used for immobilization and live-intact fluorescence functional imaging of *Drosophila* larva's CNS in response to controlled acoustic stimulation using a Genetically Encoded Calcium Indicator (GECI) probe, called GCaMP5. The microfluidics clamps developed could immobilized *Drosophila* larvae for only whole-CNS imaging and they cannot allow one to capture neuronal responses at single-neuron resolution, which requires stronger immobilization. In this thesis, a simple microfluidic device, which employed an interesting strategy to completely immobilize the brain and the CNS of a live, fully-functioning *Drosophila* larva was demonstrated. This enables one, for the first time, to imaging throughout these organs at a single neuron resolution. None of the mechanical immobilization methods available currently are capable of immobilization of the brain and the CNS of a live fully functioning *Drosophila* larva for intact imaging at a single neuron resolution. The application of this platform was not limited to brain and CNS imaging and it can potentially being used to record neuronal events at different organs such as gut, intestine and hearts in a fully intact manner.

ACKNOWLEDGMENT

There have been many people who have walked alongside me during this journey that I would like to thank each and every one of them.

Firstly, I would like to express my sincere gratitude to my supervisor professor Ravi Selvaganapathy for the continuous support of my Ph.D. study and related research, for his patience, motivation, and immense knowledge. At many stages in the course of this research project I benefited from his advice, particularly so when exploring new ideas. His positive outlook and confidence in my research inspired me and gave me confidence.

Besides my advisor, I would like to thank the rest of my thesis committee: Professor Ching and Professor Jacobs for their insightful comments and encouragement, but also for the hard question which incented me to widen my research from various perspectives.

My sincere thanks also goes to my fellow labmates, Dr. Balaji G. Iyengar and Dr. Pouya Rezai, for the stimulating discussions, for the sleepless nights we were working together before deadlines, and for all the fun we have had (e.g. Watching *Famile door* and listening to great *Jazz music*) along this journey.

To the technicians in the Department of Mechanical Engineering Joe Verhaeghe, Mark Mackenzie, Ron Lodewyks, John Colenbrander, Michael Lee, Dan Wright who provided valuable help at many points during this thesis. To Doris Stevanovic and Zhilin Peng in CEDT, Department of Engineering Physics, for their training and suggestions in microfabrication process.

To my colleagues and friends of CAME, Russel, Leo, Ali, Jun, Rana, Mohammadhossien, Pedram, Shayan, Aliakbar, Celine, Aditya, Monika, Yujie, Prker and to the co-authors of my papers, Meryl, Pouya, Ana, Qanber, and to my always there friend Kia. I thank them for their companionship and for providing a so pleasurable and friendly working atmosphere. The moments of leisure shared together helped to overcome some more difficult moments. I am also thankful for their always prompt help, whenever I needed it.

Last but not the least, I would like to thank my family: my parents (Ostad and Gigil) and to my brothers (Masoud, Behrouz, Abolfazl and Hamid) and sister (Fariba) and to my Parents-in-law (Mr. Rafiei Nejad and Mrs. Sefidi) and Family-in-law for supporting me spiritually throughout writing this thesis and my life in general.

Above all I would like to thank my wife Shirin Banoo for her love and constant support, for all the late nights and early mornings over the past few years. Shirin has made countless sacrifices to help me get to this point. But most of all, thank you for being my best friend. I owe you everything.

Without such a team behind me, I doubt that I would be in this place today.

Contents

List of Figures

NOMENCLATURE

2D	2 Dimensional
3D	3 Dimensional
ANOVA	Analysis Of Variance
ATP	Adenosine Triphosphate
C. elegans	Caenorhabditis Elegans
CB	Cardioblasts
CCD camera	Charge Coupled Device Camera
CCM	Collective Cell Migration
CM	Center Of Mass
CNS	Central Neuronal System
CPS	Cephalo-Pharyngeal Skeleton
DI water	Deionized Water
DNA	Deoxyribonucleic Acid
DOF	Degree Of Freedom
DV	Dorsoventral
eGFP	Enhanced Green Fluorescent Protein
ETC	Electron Transport Chain
FACS	Fluorescence-Activated Cell Sorting
F-actin	Actin Filaments
FOV	Field Of View
G- actin	Globular Actin
GECI	Genetically Encoded Calcium Indicator
GFP	Green Fluorescent Protein
GRNs	Gustatory Receptor Neurons
HCS	High-Content Screening
HF	Hydrofluoric Acid
HTS	High-Throughput And
MEMS	Microelectromechanical Systems
OD/ID	Outer Diameter / Inner Diameter
ORNs	Olfactory Receptor Neurons
PDMS	Polydimethylsiloxane
RNAi	RNA Interference
ROI	Region Of Interest
siRNA	Small Interfering Rna
SOG	Subesophageal Ganglion
VNC	Ventral Nerve Cord

Chapter 1

INTRODUCTION

1. Microfabricated and Microfluidics devices for *Drosophila*-based drug discovery assays

1.1.Drug discovery

The drug discovery process starts with the identification of a target protein, which is implicated in a particular disease. Once the protein is identified then libraries of chemical compounds are screened against this target to identify a few candidates that bind to it effectively in order to modify its functioning. Then, the candidate chemical molecules are optimized through medicinal chemistry to enable easy administration, better distribution in the body, reduce toxic side effect and finally, tested on animal models [1] such as mice, rats, pigs and monkeys. Drug discovery process is long (~12-15 years) and expensive ($0.5-$1 billion dollars) [1].

High-throughput and high-content screening (HTS and HCS) are powerful tools in the initial stages of the drug discovery process, especially at the stage of lead identification and optimization, where millions of chemical compounds can be assayed against the target molecules to identify a few drug candidates. Mostly, HTS and HCS processes are microwell array-based *in-vitro* assays. These assays are simple to implement and have been automated for high throughput. However, they usually do not represent the complexity of biological processes in multicellular organisms particularly in distribution, metabolism and toxicity of the drug candidate. Therefore, in many instances, highly promising lead compounds have failed at subsequent stages of testing. To address this problem, whole organisms can be used, which screens for not only efficacy of a drug

candidate but also identifies any potential issues with administration, distribution, metabolism, and toxicity. Modern drug discovery process uses model organisms such as *Drosophila*, *C. elegans*, mice, rats or pigs as biomimics of human physiology in order to perform whole organism testing [2].

1.2. *Drosophila* as model organism

Drosophila melanogaster (fruit fly) is a well established model organism for human diseases at the molecular genetic level. Presently, significant amount of effort has been invested in using *Drosophila* for understanding of neurobiological development, gene regulations, physiological, behavioral or biochemical processes [3]-[5] at the molecular level and the correlation of these processes to disease development in mammals or humans (e.g. molecular underpinnings of aging, tumor formation, alcohol intoxication, neurodegeneration, and memory loss). This is because of *Drosophila* genome is ~70% homologous disease related genes as human genome and many of the fundamental biological processes are shared. In addition, the *Drosophila* could be genetically manipulated to introduce transgenes that will then mimic specific human condition. New genetic tool developed for *Drosophila* also allow one to easily track and studies the functionality of the target gene via advanced optical methods available for live imaging of biological processes.

Similar to other insects, *Drosophila*'s life cycle passes through embryonic, larvae and pupa stages prior to formation of adult flies as shown in FIG. 1. 1. It begins when the female fly lays her embryos on a moisturized substrate. After 24 hours, the embryos hatch into 1st instar larvae. Next, they molt into the 2nd and 3rd instar larvae after 48 hours in each stages. After the first three days, *Drosophila* larvae enter the pupa stage and stay in it for the next 6 days in order to develop into adult flies.

As a model organism, each developmental stage of the *Drosophila*, has been used to study specific biological processes. *Drosophila* embryo has been used to study and understand the mechanisms of embryogenesis by geneticists and developmental biologists due to advantages such as small size (150µm diameter and 600µm length), short

generation time (~24 hr from embryo to 1st larva and), transparent shell (chorion), and large brood size [6]. *Drosophila* larvae (~600 µm-thick and 4mm-long in 3rd instar stage) are also used for different genetic and neuronal studies as they contain different types of sensory neurons that are patterned in a segmental configuration. *Drosophila* larvae sense various environmental stimuli (e.g. mechanical, visual and chemical) and transmit the neuronal signals to the central nervous system (CNS) as a feedback to the brain to control the stereotypic motor behaviors. This simple architecture allow researchers to explore and study the numerous developmental-genetic and neurobiological conditions primarily through deploying surgical, histological, transgenic and behavioral methods. Various age-related neurodegenerative diseases such as Alzheimer's and Parkinson's diseases have been studied using larvae's behavioral response to external stimuli.

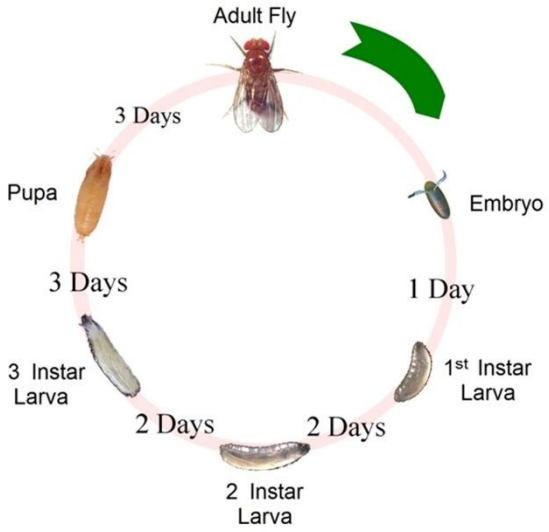

FIG. 1. 1: The *Drosophila* life cycle consists of a number of stages: embryogenesis, three larval stages, a pupal stage, and (finally) the adult stage

The adult *Drosophila* fly has been used in both primary screens and secondary validation of biologically active compounds mainly in the area of neurodegenerative diseases [7]. The fly shares many genetic similarities with humans and have a number of structures that perform similar functions as human organs like the brain, lung, gut, kidney, heart and reproductive tract. Therefore, transgenic flies that incorporate the features of human diseases have been created to study disease mechanisms. These fundamental studies have

been mainly applied in the areas of neurodegeneration (Alzheimer's and Parkinson's diseases), triplet repeat expansion diseases, sleep disorders and seizure disorders, cancer, cardiovascular, inflammation/infectious Diseases, metabolic disorders and diabetes [7].

1.3.Technological challenges in *Drosophila* assays

Assays performed using *Drosophila* as a model organism usually require four unit operations, namely: sorting, positioning, drug delivery and post exposure screening as depicted in FIG. 1. 2.

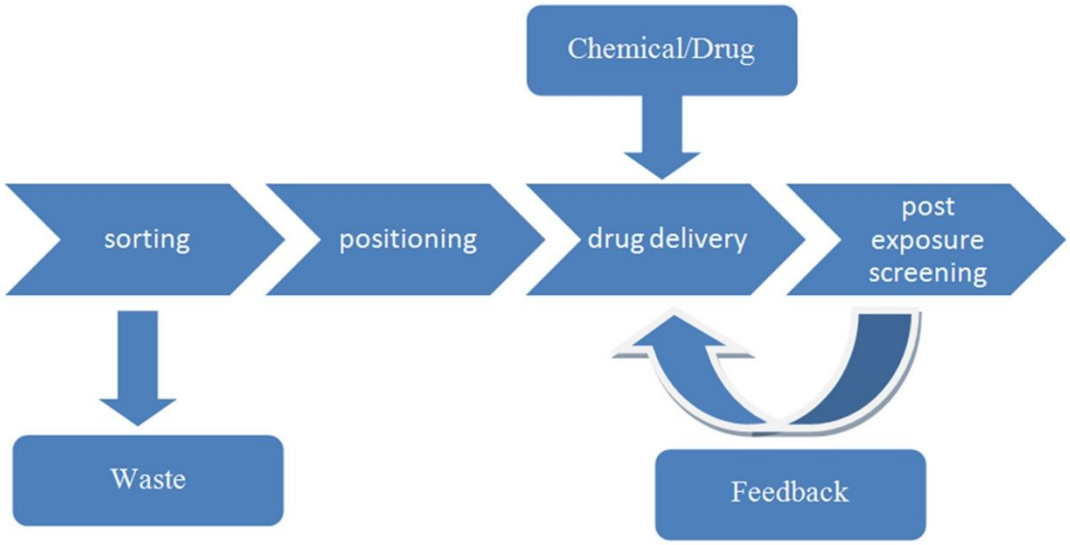

FIG. 1. 2: General scheme of drug discovery assays performed on model organisms such as *Drosophila*.

First, the desired stage of *Drosophila* (i.e. Embryo, 1st, 2nd and 3rd instar larva, pupa and adult fly) is sorted out from a mixed population growing on the food media. Next, the animal is positioned and aligned so that appropriate and defined dose of various drug candidates can be delivered to it. Subsequently, the drug candidates are delivered by various methods depending on the stage of the animal. In the case of the embryo, the drug is directly injected into the embryo, while for the larvae, it can be either be directly injected or mixed with food media that is either solid or liquid. Adults can have drug delivered as an aerosol or gas, or mixed with food substrate, as a direct application on an exposed nerve cord, or as an injection. Finally, the treated organism is monitored and

examined, in order to investigate the effect of the drug candidates on the animal. This investigation procedure can be performed via different assays including live imaging, electrophysiology or behavioral assays.

A common issue in all of the unit operations is in controlling the movement and position of the organism. For instance, when *Drosophila* embryo is used in an assay, the shape of the embryo creates numerous difficulties in accurately orienting and positioning the embryo for either microinjection or observation under a microscope. Similarly, in assays that image the internal organs of the *Drosophila* larva, a live organism that instinctively moves all the time has to be immobilized for observation. The most common technique used for the larva is to dissect it [8] so that movement-based artifacts can be eliminated. In this process, the mobile larva is pinned onto a soft substrate, its body wall cut and the desired organs isolated for observation. Subsequently, the dissected larva is exposed to the drug candidates and observed under the microscope or probed using electrophysiology. Although larva's dissection assays successfully remove the locomotion artifacts and creates great access to the target organ, it does not represent a true in-vivo assay as removal of other internal organs and disruption of the neuronal network due to dissection prevents observation of a systemic response in these assays. Additionally, the need of a skilled operator and possibility of human errors involved in every dissection, make the process very slow and unsuitable for high-throughput drug screening protocols. Alternatively researchers glue the animals (larva and the adult fly) to the surface to immobilize them to perform the drug discovery process. This process is time-consuming and tedious. In addition to human errors, gluing the organism is also an irreversible process it does not allow one to use the sample for other assays, which assessing behavior of these animals. Similarly, nearly all drug delivery and post-exposure processes (e.g. behavioral studies, live imaging protocols and electrophysiology protocols) are currently performed manually on open agar gel surfaces in a Petri dish environment. However, manual operation on open agar gel surfaces create conditions that may be variable and dependent on the skill of the operator that could potentially have significant influence on the assay, in particular *Drosophila* biological responses which

could in turn lead to large variations and complexity in the results. Therefore, the key challenges associated with conventional drug discovery assays are low throughput, poor performances and low efficiency, time consuming and complex procedure. Additionally, some experiments that might help researchers to answer critical biological questions, cannot be performed due to the lack of technology. For instance, deep microinjection into the *Drosophila* embryo using conventional microinjection system, is not possible as the taper angle of the microneedles are large and deep insertion of the needle into the embryo could potentially affect the viability of the embryo.

1.4.Current Microfluidics technology for *Drosophila* assays

Recently, some microfluidic devices have been developed for automating some or several of the unit operations of *Drosophila* drug discovery assays, which are capable of either overcoming the above mentioned challenges or simplifying them in a manner that drug discovery processes can be done in a more automated and high-throughput manner. In case of *Drosophila* embryo, microdevices were designed for sorting, self-assembly of embryos and morphogenesis as well as for developmental studies [9][14]. Microinjection is a well-established method to delivery desire transgenic construct or toxin into the embryo. In the recent past, a few microdevices [13]-[14] have been developed to automate or simplify the microinjection process. However, they were not capable to perform deep and localize microinjection, which is desirable in some applications such as toxicological and developmental studies. In contract to *Drosophila* embryo, less attention have been paid to the *Drosophila* larva. Immobilization of *Drosophila* larvae is more difficult than *C. elegans* as it exerts stronger force. Complicating matters further, the internal organs of interest such as the CNS capsule that needs to be visualized can loosely move inside the hemolymph-filled body cavity even if the outer body is completely immobilized by encapsulation. Recently, mechanical encapsulation and CO_2 aesthetic exposure [15][16] approaches have been used to immobilize *Drosophila* larva. They allow whole-larval body compression inside the chip so that neuronal transport processes and sensory neuron regeneration upon injury can be visualized. Both these devices reduce

the movement artifacts as compared to the freely moving larva but do not eliminate them. The use of anesthetic leads to spurious neurobehavioral responses and the use of encapsulation prevents the exposure of the larva to external sensory stimulus.
Therefore, at the current microfluidics technology developed for the *Drosophila* assay, cannot be used for the applications that required deep microinjection into the embryo or

2. Research objective and aims

The primary objective of this thesis is the development microfluidic devices that could address some of the key outstanding challenges involved in the *Drosophila* assays such as deep embryo microinjection and in-vivo live imaging of *Drosophila* CNS. The aims of the thesis was categorized into two groups based on the *Drosophila* stages: (i) microfluidic devices for *Drosophila* embryonic studies and (ii) *Drosophila* larvae studies. Therefore, the research aims of this thesis can be listed as below.
i-1: A microfluidic microinjector for toxicological and developmental studies of embryos
ii-1: Characterization of microfluidic clamps for immobilizing and of *Drosophila* larvae
ii-2: Microfluidic devices for imaging neurological response of *Drosophila* larvae's CNS to auditory stimulus
ii-3: A Microfluidic devices for imaging of *Drosophila* larva at single neuronal resolution

3. Thesis outline

This thesis contains 7 chapters presented in a "sandwich Thesis" format. An introduction chapter (Chapter 1) and a summary chapter (Chapter 7) with the overall conclusions and recommendations are included. The contents of Chapters 2-6 have been mainly extracted from a number of published or under review articles. The following chapters of this thesis are summarized as:
Chapter 2: This chapter reviews the current microfluidics technologies used for the *Drosophila* assays with primary application towards drug discovery for human diseases. In this chapter, the microdevices were categorized based on the stage of the *Drosophila*

that have been used. In the first part, Microfluidic devices used for *Drosophila* embryogenesis have been reviewed. These devices were mainly used for three different application such as sorting, positioning (self-aligning) and microinjection. In The second part, Microfluidics devices for *Drosophila* larval assays, which were mostly used for live imaging of *Drosophila* larvae have been examined. In the third part, devices that were used for adult *Drosophila* assays have been highlighted.

Chapter 3: As described section 2, a low cost microinjector, which could deeply insert the microneedle, >100µm into the embryo without damaging it, would be ideal for the application that required reagent delivery at multiple locations inside the embryo. This technical challenge was addressed in this chapter and the first microinjector that allow one to precisely insert a long taper microneedle laterally and at various positions inside the length of the *Drosophila* embryo (up to 250µm) was developed. The conceptual design of the microinjector following with method of device fabrication and experimental setup, have been described in this chapter. This design could be used to precisely insert a long taper microneedle laterally and at various positions inside the length of the *Drosophila* embryo. It also could deliver regent accurately via pressure pulses. Therefore, the characterization of the complaint system and delivery system have been presented. The device has been used to study the effect of toxins on cardiogenesis in *Drosophila* embryos and the effect of the sodium azide (NaN_3) on the heart development of the *Drosophila* embryo have been studied. This device can be potentially used for other embryonic assays that need accurate delivery of the regents to a specific location within the embryo.

Chapter 4: As described section 2, *Drosophila* larva is highly mobile and its internal organs cannot be sharply imaged without complete immobilization. Currently, a systematic study on immobilization of the *Drosophila* larva has not been performed. In this chapter, a systematic analysis of various mechanical constrictions incorporated into microfluidic channels were conducted. This could allowed us to find an optimized design for rapid mechanical immobilization of larvae for whole-CNS imaging. The clamping and immobilization processes were characterized by imaging and movement measurement of

larvae's CNS. The performance of optimal design have been compared to other immobilization technique (Gluing) and the strength points of the design have been presented. The optimal design that contained two 3D constrictions inside a narrowed channel significantly decreased the internal CNS movements.

Chapter 5: in this chapter, the optimal immobilization mechanisms (Pneumatic Chip) developed in the previous chapter have been used for immobilization and live-intact fluorescence functional imaging of *Drosophila* larva's CNS in response to controlled acoustic stimulation. The Pneumatic Chip allowed automated animal loading, immobilization and unloading and it held larva under positive fluid pressure to reduce the CNS movement entirely. In order to examine the acoustic properties of Pneumatic Chip on the larva's neuronal response another immobilization chip (FlexiChip) has been developed. The FlexiChip allowed for manual loading, unloading and immobilization. Both chip designs allowed the stable recording of GCaMP5 fluorescence activity in the CNS, without the use any anaesthetic drugs that could affect animals' neurophysiological status. In the method section, the fabrication design and experimental setup used for the controlled acoustic exposure was described. A Genetically Encoded Calcium Indicator (GECI) probe, called GCaMP5, have been used to optically record the response of the CNS to auditory stimuli.

Chapter 6: Both microfluidics clams used in the previous chapter could immobilize *Drosophila* larvae for only whole-CNS imaging and they cannot allow one to capture neuronal responses at single neuron resolution, which requires stronger immobilization. In this chapter, the first microfluidics device for immobilization and intact-live imaging of the single neuron in the larva's CNS and body wall has been developed. In this novel design, unlike the current mechanical immobilization technique that compress the entire body or a portion of the body, the immobilization of the larva was achieved by bending the larva's body. The conceptual design of the mechanism following with method of device fabrication and experimental setup, have been described in this chapter. This device can be used for to record the neuronal activities in response to various external

stimuli. It also can be used for the live neuroblast imaging in the brain and CNS of *Drosophila* larva, where single neuron resolution is required.

Chapter 7: In this chapter, a summary of the conclusions and discussions presented in the previous chapters of this thesis have been presented, which is followed by the research contributions and recommendations for the future work. As shown in this thesis, Microfluidics technology provides an elegant tool to make *Drosophila* assays easy and quick to perform in an automated manner and potentially at high throughput. The future work of this thesis can be dived into two avenues. In the first road, the current devices can be modified for different assays. For instance, different imaging systems such as epifluorescent, confocal, two-photon, light sheet require different setups for imaging. The current immobilization devices developed in this thesis were greatly compatible with epifluorescent and confocal microscopy. However, they can be modified for two-photon and light sheet microcopy, which involved more complex challenges. In the second road, other bio-applications can be performed with the existing devices. For example, the embryo microinjector can used for creating transgenic embryos or immobilization mechanisms can be used for neuronal imaging of the CNS when it exposed to different stimulates such as heat, light, or electrical/magnetic field.

4. Contributions

Thesis contributions to the general body of knowledge can be categorized into the Innovative techniques and the application assay sections. In the innovative techniques, novel devices have been developed for (i) the deep microinjection of the *Drosophila* embryo and (ii) intact immobilization of *Drosophila* larvae. In this these, a simple compliant mechanism based PDMS-microinjection system has been demonstrated. Small taper angle microneedles have been fabricated for microinjection of the embryo, which could allow one to deeply deliver the reagent into the embryo. The immobilization of the embryo has been achieved via a form fitting passive immobilization chamber, which could stop the embryo's movements during the needle insertion. In contrast to the existing

microfluidics microinjector, the fabrication of the microinjector did not require semiconductor manufacturing facilities and it is mainly based on conventional soft photolithography process, which could significantly reduce the cost of the fabrication. In this thesis, a series of the microfluidics clams have been characterized and three microfluidics devices have optimized for rapid loading and intact live imaging of the *Drosophila* larvae's internal organs. Two of the devices were suitable for whole-CNS imaging of *Drosophila* larvae with high rate of viability. The third device could generate stronger immobilization, which could be great for high-resolution imaging of the single neurons. However, the viability of the larvae were significantly decreased by using the bending immobilization technique.

At an application level, the microinjector has been used in toxicological studies of the *Drosophila* larvae. In this assay, the effect of sodium azide (NaN3), a cytochrome oxidase inhibitor, on heart development during embryogenesis has been examined. Using this microinjector, it has been shown that the cardioblast migration velocity is modified in a dose sensitive manner to varying doses of injected Sodium Azide (NaN3) and, for the first time the effect of the toxin on heart assembly, have been quantified. The Pneumatic Chip and FlexiChip have used for the visualization of neuronal activities using a Genetically Encoded Calcium Indicator (GECI) probe, called GCaMP5, in response to auditory stimuli. Both chip designs allowed the stable recording of GCaMP5 fluorescence activity in the CNS. We report an optimal GCaMP5 response at 200 Hz. These larval lab-on-chip platforms allow the integration of functional imaging with a sensory-motor response. The bending immobilization mechanisms allowed us to take the first intact-live imaging of the CNS neurons when it was exposed to the chemical stimulates (NaN_3) as single neuronal resolution. All the devices in this thesis have been developed with a common aim of being integrated into an automated high throughput microfluidic lab-on-a-chip assay at a later stage. The utilization of the outcomes of this thesis is proposed in the applications such as drug screening, toxicology, transgenesis and many more application.

The following describes my contributions to the articles constituting Chapters 2-6, which

consists of three articles that have been published (two regular journal papers and one review journal paper), one regular article that has been submitted in *lab-on-a-chip (LOC)* and one article under preparation for submission that address the key objectives of this study. The tittle and the authors of the papers are listed as below:

1. Reza Ghaemi, and Ponnambalam R Selvaganapathy. "***Microfluidic devices for automation of assays on Drosophila melanogaster for applications in drug discovery and biological studies***." Current pharmaceutical biotechnology 17.9 (2016): 822-836.

2. Reza Ghaemi, Pouya Arefi, Ana Stosic, Meryl Acker, Qanber Raza, J. Roger Jacobs and Ponnambalam Ravi Selvaganapathy. "***A microfluidic microinjector for toxicological and developmental studies of cardiogenesis in Drosophila embryos***". This chapter contains a submitted regular journal article (at *journal of lab-on-a-chip (LOC)*

3. Reza Ghaemi, Pouya Rezai, Fatemeh Rafiei Nejad, Ponnambalam R Selvaganapathy, "***Characterization of microfluidic clamps for immobilizing and imaging of Drosophila melanogaster larva's central nervous system***", Biomicrofluidics 11 (3), 034113-1 034113-14

4. Reza Ghaemi, Pouya Rezai, Balaji G. Iyengar, and Ponnambalam Ravi Selvaganapathy. "***Microfluidic devices for imaging neurological response of Drosophila melanogaster larva to auditory stimulus***." Lab on a Chip 15, no. 4 (2015): 1116-1122.

5. Reza Ghaemi, Ana Stosic, Meryl Acker, J. Roger Jacobs and Ponnambalam Ravi Selvaganapathy, "***A Microfluidic devices for imaging of Drosophila larva's CNS at single neuronal resolution in response to chemical stimulate***". under preparation for submission.

5. A Note to the Reader

Different portion of this chapter have been taken and permission is granted for the following subject to the conditions outlined below:

Microfluidic Devices for Automation of Assays on Drosophila Melanogaster for Applications in Drug Discovery and Biological Studies" by Reza Ghaemi and P. Ravi Selvaganapathy to the journal Current Pharmaceutical Biotechnology

To be used in the following manner:

1) *Bentham Science Publishers grants you the right to reproduce the material indicated above on a one-time, non-exclusive basis, solely for the purpose of thesis writing. Permission must be requested separately for any future or additional use.*
2) *For an article, the copyright notice must be printed on the first page of article or book chapter. For Figures, photographs, covers, or tables, the notice may appear with the material, in a footnote, or in the reference list.*

References

[1] Hughes, J. P.; Rees, S.; Kalindjian, S. B.; Philpott, K. L. Principles of early drug discovery. *British journal of pharmacology*, 2011, 162(6), 1239-1249.

[2] Cockburn, I.; Henderson, R. Racing to invest? The dynamics of competition in ethical drug discovery. *Journal of Economics & Management Strategy*, 1994, *3*(3), 481-519.

[3] Baier, A.; Wittek, B.; Brembs, B. *Drosophila* as a new model organism for the neurobiology of aggression?. *Journal of Experimental Biology*, 2002, 205(9), 1233-1240.

[4] Stewart, B. A.; Atwood, H. L.; Renger, J. J.; Wang, J.; Wu, C. F. Improved stability of *Drosophila* larval neuromuscular preparations in haemolymph-like physiological solutions. *Journal of Comparative Physiology A*, 1994, 175(2), 179-191.

[5] Rockwell, R. F.; Grossfield, J. *Drosophila*: behavioral cues for oviposition. *American Midland Naturalist*, 1978, 361-368.

[6] Markow, T. A.; Beall, S.; Matzkin, L. M. Egg size, embryonic development time and ovoviviparity in *Drosophila* species. *Journal of evolutionary biology*, 2009, 22(2), 430-434.

[7] Pandey, U. B.; Nichols, C. D. Human disease models in *Drosophila* melanogaster and the role of the fly in therapeutic drug discovery.*Pharmacological reviews*, 2011, 63(2), 411-436.

[8] Brent, J. R.; Werner, K. M.; McCabe, B. D. *Drosophila* larval NMJ dissection. *Journal of visualized experiments: JoVE*, 2009, (24).

[9] Furlong, E. E.; Profitt, D.; Scott, M. P. Automated sorting of live transgenic embryos. *Nature biotechnology*, 2001, 19(2), 153-156.

[10] Chen, C. C.; Zappe, S.; Sahin, O.; Zhang, X. J.; Fish, M.; Scott, M.; Solgaard, O. Design and operation of a microfluidic sorter for *Drosophila* embryos. *Sensors and Actuators B: Chemical*, 2004, 102(1), 59-66.

[11] Bernstein, R. W.; Zhang, X.; Zappe, S.; Fish, M.; Scott, M.; Solgaard, O. Characterization of fluidic microassembly for immobilization and positioning of *Drosophila* embryos in 2-D arrays. *Sensors and Actuators A: Physical*, 2004, 114(2), 191-196.

[12] Chung, K.; Kim, Y.; Kanodia, J. S.; Gong, E.; Shvartsman, S. Y.; Lu, H. A microfluidic array for large-scale ordering and orientation of embryos.*Nature methods*, 2011, 8(2), 171-176.

[13] Zhang, X.; Scott, M. P.; Quate, C. F.; Solgaard, O. Microoptical characterization of piezoelectric vibratory microinjections in *Drosophila* embryos for genome-wide RNAi screen. *Microelectromechanical Systems, Journal of*, 2006, 15(2), 277-286.

[14] Delubac, D.; Highley, C. B.; Witzberger-Krajcovic, M.; Ayoob, J. C.; Furbee, E. C.; Minden, J. S.; Zappe, S. Microfluidic system with integrated microinjector for automated *Drosophila* embryo injection. *Lab on a Chip*, 2012, 12(22), 4911-4919.

[15] Ghannad-Rezaie, M.; Wang, X.; Mishra, B.; Collins, C.; Chronis, N. Microfluidic chips for in vivo imaging of cellular responses to neural injury in *Drosophila* larvae. *PloS one*, 2012, *7*(1).

[16] Mondal, S.; Ahlawat, S.; Koushika, S. P. Simple microfluidic devices for in vivo imaging of C. elegans, *Drosophila* and zebrafish. *Journal of Visualized Experiment: JoVE* , 2012, (67), e3780-e3780.

Chapter 2

MICROFLUIDIC DEVICES FOR AUTOMATION OF ASSAYS ON *DROSOPHILA* MELANOGASTER FOR APPLICATIONS IN DRUG DISCOVERY AND BIOLOGICAL STUDIES.

Compete citation:

Ghaemi, Reza, and Ponnambalam R Selvaganapathy. "*Microfluidic devices for automation of assays on Drosophila melanogaster for applications in drug discovery and biological studies."* Current pharmaceutical biotechnology 17, no. 9 (2016): 822-836.

Copyright:

Relative Contributions:

Ghaemi, R.: Reviewed the cited papers and wrote the drafts of the manuscript including all figures and text.

Selvaganapathy P.R.: Supervisor of R. Ghaemi, revised the drafts of the manuscript and was responsible for the final draft submittal to the journal.

1. Introduction

One of the central themes of biological research is to understand the mechanisms of human diseases and to develop new and successful treatments to mitigate them. Once the mechanism of a disease process or a target biomolecule that could influence the disease has been identified, thousands of chemical compounds available in chemical libraries of drug companies are screened against the target and assayed for their ability to bind as part of the drug discovery process [1]. However, a simple binding efficiency test does not represent the biological complexity of an organism and therefore the candidates that perform well in those assays often end up failing in the subsequent tests on animals and humans. Due to the vast complexity of the cellular and molecular processes and the ethical issues related to testing of unproven drug candidates on humans, researchers have focused on a number of model organisms, which are also complex enough to address many of the questions relevant to human biology. *Drosophila melanogaster* is a well established model organism for studying human diseases at the cellular and molecular/genetic level. *Drosophila* larvae have also been used to understand the biological mechanisms underlying neurological responses to external stimuli such as chemicals, temperature and light. Such behavioral assays when combined with molecular/cellular imaging can provide powerful tools to elucidate the origins and mechanism of such responses [2] as well as study the influence of drug candidates on the response. Traditional methods of screening of *Drosophila* involve exposure of the model animal/organism to individual chemicals/drugs on culture plates (e.g., 96-well plate), while monitoring the subsequent effects on growth, movement and other processes by visual inspection (e.g. Green fluorescent protein (GFP) tag imaging, behavioral and locomotion assays) [3]. However, these methods remain mostly manual, low-throughput and remain expensive to perform. In addition, manual handling of mobile live micrometer-scale organisms such as *Drosophila* requires skill and experience on the part of the user. Automation of unit operations of these assays such as positioning the organism, microinjection and post-exposure manipulation and studies such as imaging and behavioral studies could lead to higher throughput and lower cost of these assays, facilitating their use at an early stage in the drug discovery process. Recently,

microfabricated lab-on-chip devices have been developed to perform assays on various model organisms such as *Caenorhabditis elegans* [4]-[6] and Zebrafish. These techniques have also been extended for assays on *Drosophila* [7]-[9]and is the main theme of this paper.

2. Microfluidic devices for *Drosophila* embryogenesis

Drosophila embryo with a typical size of 150µm-diameter and 500µm-length is an ideal model organism for development studies and genetics due to its short development time (24hr), transparent body and low number of cells (~6000 after cellularization) [10]. In the recent past, several microfluidic devices have been developed to automate various aspects of Petri dish based embryogenesis assays. The main focus of the recent work can be categorized into three areas, namely: Microsystems for embryo (1) sorters, (2) positioners, and (3) microinjection.

2.1. Sorters

There is a significant need to sort *Drosophila* embryos based on their genetic profile and modifications therein. Typically, the successfully modified embryos have fluorescent protein tags, which are then used as a marker for sorting process. Furlong et al. [11] presented a microfluidics-based device that automatically separates *Drosophila* embryos of one genotype from a larger population of embryos, based on the intensity of fluorescent protein marker. Their design of the optical system for sorting is shown in FIG. 2. 1. In this design, a batch of embryos, which are suspended in buffer, is continuously moved into an optical cuvette/channel (0.4 mm square glass tube) via a peristaltic pump at a fixed rate (~6 ml/min). The dimension of the optical cuvette was well designed in order to restrict the embryos' motion into two possible orientations. When the embryos travel through the optical cuvette, they are exposed to an argon laser beam (488 nm), which excites the fluorescent marker in the modified embryos resulting in emission of light at a slightly different frequency. After passing the emitted light through an aspheric condenser lens, a plano-convex focusing lens, and two dichroic mirrors (optical cutoff at 498 nm and 520 nm), the intensity of the emitted light were measured by three photodetectors. One diode

was used to measure light intensify, which has passed through the lenses, to detect the position of each passing embryo. While two other diodes were used to detect the GFP signal (PMT-1) and the background fluorescence or autofluorescence emanating from the yolk of the embryo (PMT-2). This configuration allows one not only to detect the existing of an embryo in the optical cuvette, it also could detect the different level of GFP signal. As a result, embryos with different level of the Green Fluorescent Protein (GFP) signal could be easily detected and the feedback was sent to a mechanical switch to sort the embryos in different chambers. The mechanical switch is based on a magnetic actuation mechanism where a rare-earth neodymium super magnet is suspended between two electromagnets. Electric current applied to one of the electromagnets pulls the super magnet towards it which deflects a small thin membrane between two channels closing one and keeping the other open. The mechanical switches can operate with speed of 10 ms/switch to open/close the channels which allowed a throughput of 100 embryos/s. However, other requirements such as time required to wash unwanted embryos reduced the sorting speed 15 embryos/s.

The results showed that the machine sorts 15 live *Drosophila* embryos per second with more than 99% accuracy. This sorter was used to select one genotype from a large population of embryos. Flies that contain lethal mutations are crossed with those that contain balancer chromosome (multiply inverted chromosomes that minimize recombination events which lead to lethal mutations) along with GFP marker gene. In the resultant flies, only 25% will contain the homozygous mutation of interest. Using the GFP marker the authors distinguished this minority population from their balancer containing siblings among the living embryos and used it for sorting and obtaining large quantities of mutant embryos. Such sorting and collection of mutant embryos can facilitate whole genome wide gene expression analysis of mutants using DNA microarrays that are important to understand the molecular effects of losing a gene function. This device could be used in the assays, where rapid fluorescence-activated cell sorting (FACS) is required. Study of the transgenic efficiency and sorting of the embryos transgenic process are examples of biological processes that this design could be greatly used.

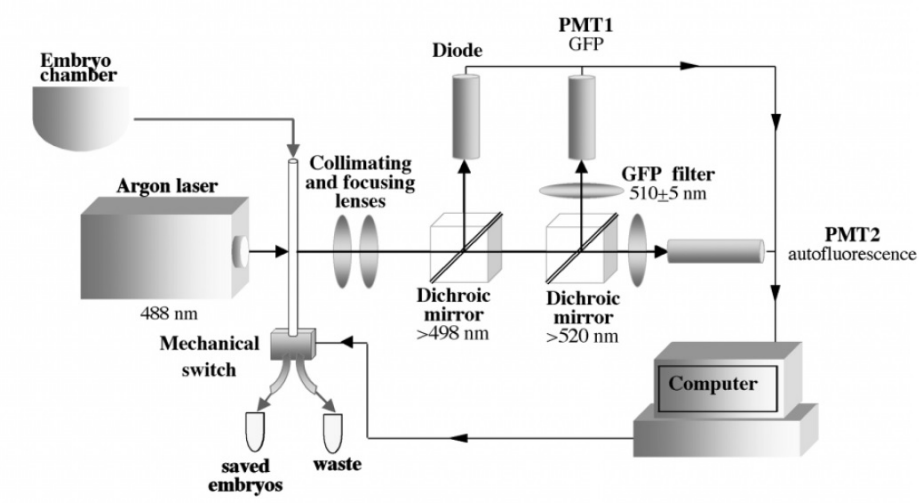

FIG. 2. 1: Sorting embryos based on their expression of GFP. When the embryos pass through the laser beam, the emitted light was collected by three diodes, which are responsible for detecting the existing of the embryo in the optical cuvette GFP and autoflorescent signal. The feedback of the diodes then was sent to the mechanical switch to sort different genotypes into different chamber [11].

In another recent work, Chen et al. [12] demonstrated a device that uses fluidic drag instead of a mechanical switch to selectively sort *Drosophila* embryos into different outlets. The microfluidic design as shown in FIG. 2. 2, consisted of three regions: three inlets, a detection chamber and two outlets. One inlet was used to flow in the embryos suspended in buffer into the detection chamber. While the other two inlets (control inlets) were design to selectively switch the main flow into one of the outlets by changing their pressures appropriately and in synchrony. It was reported that the shortest switching time achieved experimentally was limited by the response time (5ms) of electromagnetic three-way valve used to control the pressure. However, simulations showed that with an optimized chamber length of 500 μm in the microfluidic device and a faster switch valve, the shortest switching time could potentially be reduced to 357 μs with a control pressure of 20kPa.

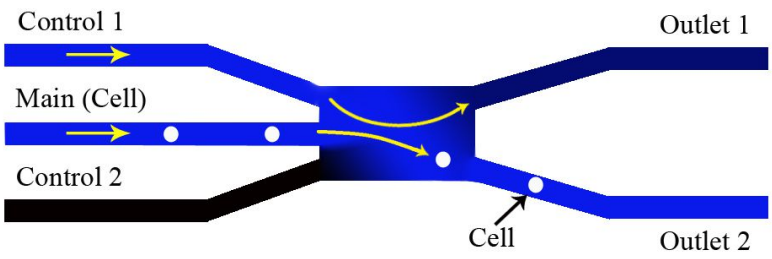

FIG. 2. 2: The schematic of the drag based *Drosophila* embryo sorter with. By controlling the pressure of the channel "Control 1" and "Control 2", the main flow, which contains the embryos can be selectively leaded into channel "Outlet 1" or "Outlet 2"

Although the authors have not shown any practical biological application of this is device such as sorting mutants from a population, this device has a great potential for being used in such sorting assays, automating the sorting and achieving high-throughput. These two microfluidic devices [11]-[12] could successfully load and sort *Drosophila* embryo based on the optical feedback from fluorescent probes expressed in the embryo. The designs also can be easily modified for other cell types (e.g. zebra fish embryo) as well as other micro model organism like *C. elegans*. After 2004, there has been a paucity of investigations into development of new sorting technologies for *Drosophila* embryo. This lack of interest may be because current technology provide sufficient capabilities for biological researchers. However, sorting technologies have been developed for other model organisms such as *C. elegans* and the readers are referred to an extensive review by Yanik *et. al* [13]. Some of these technologies can be applied with some modifications for *Drosophila* embryo or larval sorting.

2.2. Positioning and aligning

The important part of drug delivery and post-exposure analysis of the embryos is to position them accurately in a defined location for injection and to orient them precisely for imaging. Unlike other model systems such as zebrafish embryos which are spherical in shape, the *Drosophila* embryo has an asymmetric ovaloid shape (see FIG. 2. 3) that is flat on one side and has a distinct curvature on the other. Also, the developing internal organs

are not symmetrically located about the central axis thereby requiring a preferred orientation for clear and accurate imaging in various embryogenesis' assays. Currently, embryos are positioned and oriented manually on a cover glass and attached firmly to a substrate using an "embryo glue" [14] which is made by dissolving a small amount of adhesive tape into a solvent such as heptane. Over the past few years, investigators have used microfluidics and its capability to overcome the changes involved in the manual positioning of the embryo and to automate the process.

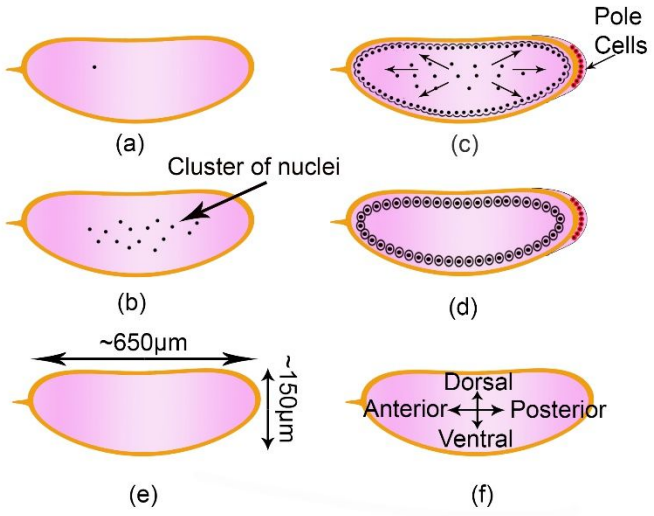

FIG. 2. 3: The cellular configuration and the ovaloid shape of the *Drosophila* Embryo in early development. (a) Single nuclei of newly laid embryo. (b) Early nuclear divisions occurs inside the common cytoplasm roughly every ten minutes. (c) All nuclei subsequently move to the periphery to form pole cells, which will eventually become germ line cells. (d) Other nuclei at the periphery cellularize simultaneously to form ~6000 cells for the next stage of the development. (e) The overall dimension of the embryo when its chorionic layer has been removed. (f) Directional nomenclature of the *Drosophila* embryo

In a pioneering demonstration, Bernstein et al. [15] used microfluidic self-assembly method using surface tension forces to position and immobilize of *Drosophila* embryos in precise 2-D arrays for high throughput microinjection. In this design, an array of gold/chromium (Au/Cr) pads were patterned photolithographically onto oxidized silicon wafers as shown in FIG. 2. 4. They exposed this surface to 1mM octadecanethiol in ethanol buffer, which led to functionalization of gold regions with organic molecules making it

hydrophobic while the oxide substrate remains hydrophilic. After a rinse in ethanol the samples were covered with a film of low toxicity oil (polychlorotrifluoro-ethylene based oil) that is regularly used to protect *Drosophila* embryos from dehydration during injection experiments and hatching. *Drosophila* embryos were then dispensed onto the substrate after which it was submerged in water. The introduction of water created a two phase solution and confined the hydrophobic polychlorotrifluoro ethylene based oil to the Au pads. Since the embryo had a greater affinity to this oil than water, it automatically assembled on to the precisely defined pads. The excess embryos were then washed out by a gentle rinse.

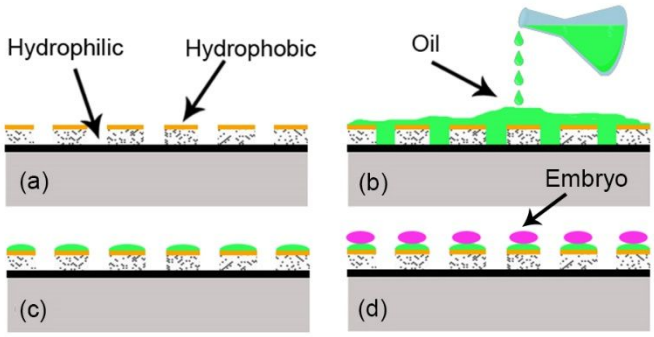

FIG. 2. 4: Schematic process flow for the described fluidic microassembly immobilization technique [15]

The authors also characterized the effect of four different geometry of the pads on the immobilization yield, the number of misplaced embryos, alignment properties and adhesion force of the embryos. An array of rectangular pads (250µm×400µm) immobilized ~120 embryos simultaneously with an yield of 85% and an adhesion force of 36 ± 22µN. About 40% of the self-assembled embryos were aligned within ±9° of the long axis of the immobilization sites. In order to accelerate drug discovery process and rapidly examine the effect of specific drug on the genotype/phenotype of *Drosophila* as a model organism, high-throughput embryo screening is required. Various assays have been implemented in order to internally (e.g. Microinjection) or externally (drug exposure technique) perturbate the genetic expression and biomolecular composition of the embryo. The main requirement of these assays is precise immobilization and manipulation of the embryo over the process.

This novel technique significantly increased the throughput with which a large number of embryos could be positioned for drug delivery or microscopic inspection. A drawback of this device is that it still required manual orientation of the embryo on an individual basis so that its major (posterior-interior) and minor (perpendicular to the substrate) axis' are appropriately oriented for imaging or injection. Although the device can be used to accurately to rapidly position the embryos for drug discovery assays, the authors have not yet implemented a practical biological assay on it.

To address this problem, Chung et al. [16] developed another microfluidic device that uses the flow itself to passively orient hundreds of embryos vertically for imaging. The design consists of a serpentine fluid-delivery manifold and an array of cross-flow channels (FIG. 2. 5a). The serpentine channel (700-μm wide) allows embryos of any orientation to move easily through it as it is wider than the length of the major axis of the embryo (~500μm). The design of each cross-flow channel involved a truncated conical embryo trap connected to a narrowing channel and a long and narrow resistance channel. When the embryos are loaded into the manifold and approach to an empty trap, the flow through the trap will automatically lead them into the trap and position them vertically due to the pressure driven flow (FIG. 2. 5b). The shape of the trap is such that it only allows embryos in the proper orientation to enter the trap. This orientation of embryo was achieved mainly because of the presence of a significant Dean flow (Dean Number >100). Dean flow is a secondary non-axial flow, which is caused due to the curvature of the channel. It also maximizes loading efficiency since an embryo has many opportunities to be in contact with an empty trap. Afterward, the positioned and oriented embryos would be ready for live imaging from the top.

In this device, hundreds of embryos were successfully oriented vertically just in a few minutes which is a great achievement for high-throughput analysis of the dorsoventral (DV) patterning signals in embryogenesis studies. More than 90% of the ~ 700 traps were found to be filled. It allows one to obtain DV axis data from multiple embryos, which was previously possible for only a few embryos.

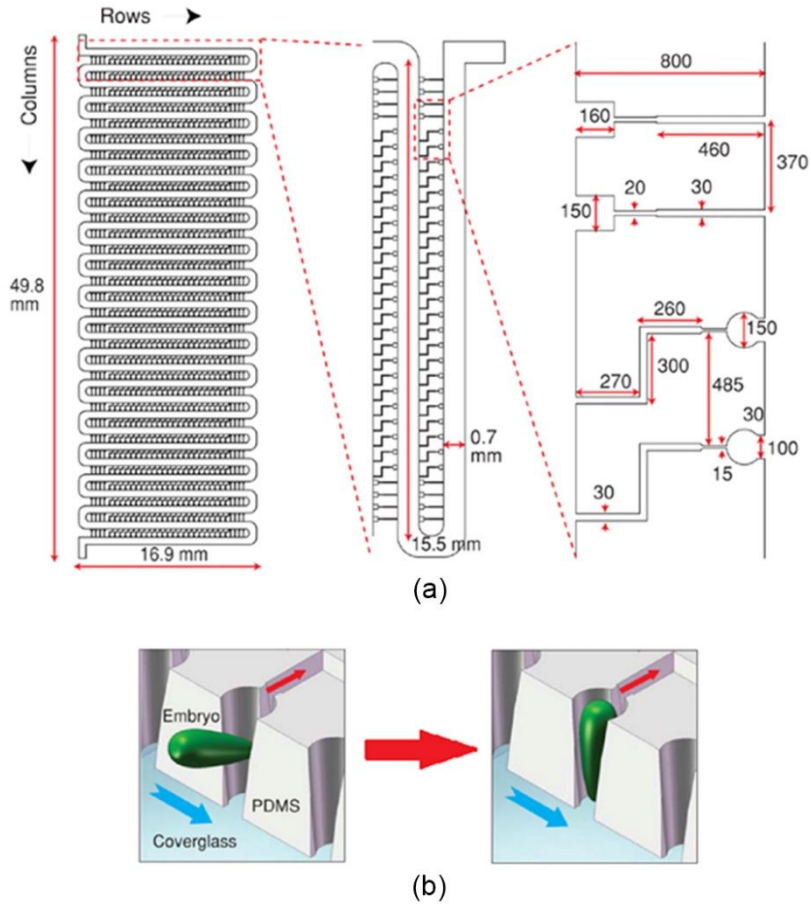

FIG. 2. 5: large-scale positioning and vertical orientation of fruit fly embryos. A. Schematic of the design consists of a serpentine fluid-delivery manifold and an array of cross-flow channels. B. Schematics, which shows how the embryo was loaded and immobilized into the embryo chamber [16].

As a biological application, this device has been used to quantify morphogen gradients in *Drosophila* embryos and allow one to screen nuclear divisions in live embryos and the dorsoventral patterning system, in a high-throughput manner. The live confocal imaging of the embryo in the ventral-to-dorsal (DV) direction can show the spatial extent of the dorsoventral patterning gradient in the embryo (see FIG. 2. 6a). The data shown in FIG. 2. 6 indicates how this gradient changes gradually with distance from the pole of the embryo during the last division cycle before cellularization. However, the device is not capable of orienting the embryo along the posterior - interior axis as the shape of the embryo is

identical along that axis. In addition, this device could not perform horizontal positioning of the embryos, which is required for other embryogenesis assays.

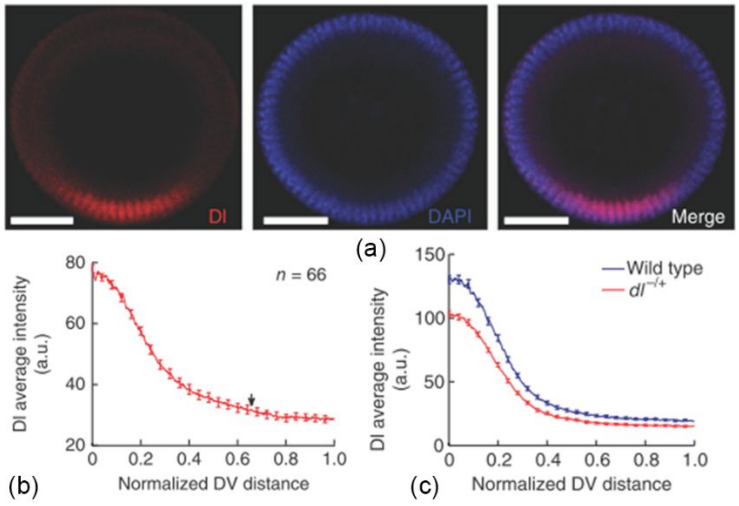

FIG. 2. 6: Spatial extent of the Dl gradient. (a) Confocal images of loaded embryos into the microfluidics chip stained for Dl and stained with DAPI. The merged picture is shown here. (b) Average intensity of the gradients of nuclear Dl in wildtype embryo. The arrow denotes the dorsoventral (DV) position beyond which the nuclear Dl gradient can be assumed flat. (c) Quantitative average gradients of the pairwise comparison of Dl gradients in wild-type and mutant backgrounds (dl−/+ females).[23]

2.3. Microinjection

Transgenesis is an important method to modify the genome of the *Drosophila* for genetic and developmental biology studies. Microinjection is an established and reliable method to deliver transgenic constructs and other reagents to specific locations in the *Drosophila*'s embryo. The current method for embryo microinjection requires expensive multi degree of freedom (DOF) micromanipulator, detailed alignment procedure of the posterior and a skilled operator which makes the microinjection process slow and not suitable for scale to high throughput wide-genome screening assays. The transfection efficiency of current microinjection methods is also very low (1% to 10% of surviving adult flies). Microelectromechanical systems (MEMS) technology could be used to integrate microneedles with actuators and sensing mechanisms so that automated, high-throughput microinjections could be performed. Recently many microfabricated injectors have been

developed for *Drosophila* embryo in order to improve the transfection efficiency, throughput and accuracy mainly by reducing the injection time and improving the reliability through automation.

Zhang et al. [17] designed a piezoelectric vibratory microinjector for genome-wide RNAi screens on *Drosophila* embryos, which could minimize the force needed for penetration the embryo. This was achieved by creating a high speed oscillation of the needle alone the penetration. The MEMS based microinjection device consisted of a micromachined silicon-nitride probe with an integrated force sensor (FIG. 2. 7). The optical force sensor consists of two aligned but separate micro-gratings called "index grating "and "scale grating ". The scale grating is fixed on the actuator and is used to measure the displacement. The index grating is connected to the microinjector and is suspended by four cantilever springs with known spring constants. The relative motion of the index grating with respect to the scale grating, measured optically, provides the displacement and the a measure of the penetration force at the injector tip. In this design, the microinjector device was ultrasonically agitated by a piezoelectric actuator to reduce the penetration force.

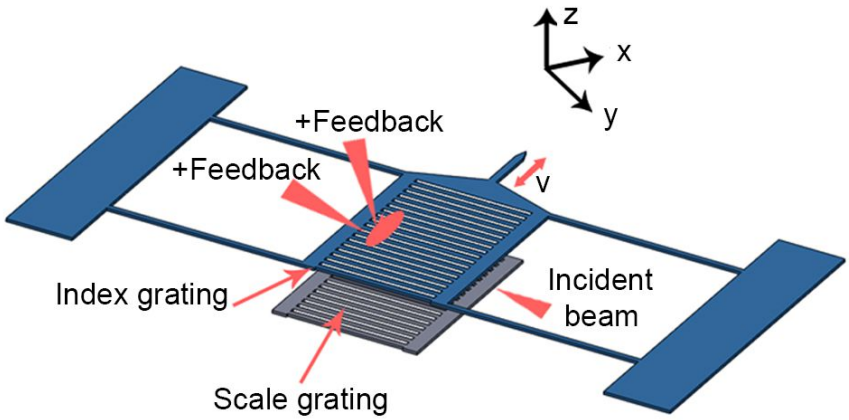

FIG. 2. 7: The force encoder is composed of a fixed scale grating and the index grating attached to the microneedle. The force sensor measures microinjector displacement and penetration force

The results indicated that due to a smaller tip size (with a 30 µm probe tip) and ultrasonic vibration involved in mechanism, the penetration force on a *Drosophila* embryo was

approximately a fourth of the force required for a microinjector without ultrasonic vibration and tip diameter of ~75 μm. This can dramatically reduce the damage to the embryo and increase the viability. This setup leads to a shorter embryo deformation before needle insertion, a faster injection rate, and minimal membrane damage due to closed loop control (optical sensor and microinjector) in the design. It also allows one to control the microneedle insertion depth, which is usually a challenge in manual injection and is dependent on the skill of the trained researcher. This microinjector successfully injected 100 embryos within 7 minutes using a piezoresistive pressure sensor to control the injected volume, which would be suitable method for wide-genome screen assays. However, the drawback of this device is that the microinjector needs to be integrated with automatic high degree of freedom (DOF) micromanipulator to accurately position embryos in order to potentially create tool for high throughput injections. Although the mechanics of the device has been validated and no practical biological application has been demonstrated, this device can be potentially used for high-throughput microinjections of *Drosophila* embryos for genome-wide RNA interference (RNAi) screens in the field of drug discovery.

In order to integrate and automate the needle insertion within the device, Delubac et al. [18] have designed a device with a fixed microneedle and have used microfluidic flow to bring and insert the needle into the embryo for injection. Their device is fabricated in glass and Silicon using conventional microfabrication approaches (see FIG. 2. 8). In this device, a surface micromachined silicon nitride microneedle suspended inside a microchannel and used for injection. Embryos are sequentially loaded into the channel and oriented for needle insertion using a sheath flow such that embryo's posterior end faces the microneedle. Once oriented, embryos are pushed towards the needle which inserts into them in a similar fashion as the previous device. Then the reagent is delivered into the embryo using a pressure pulse to the microchannel attached to the microneedle. The total time from loading and injection was 2sec.

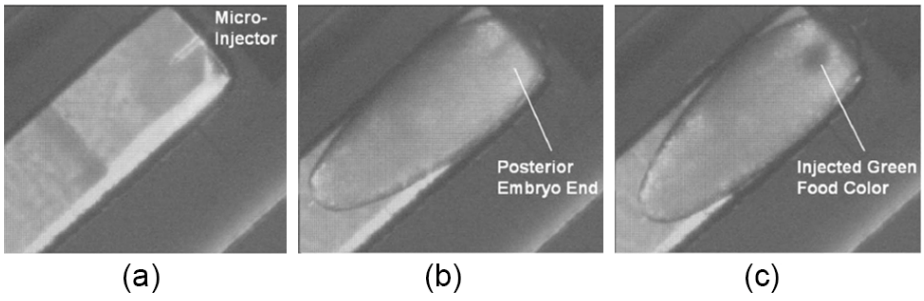

FIG. 2. 8: Images of an embryo arriving at the injector and being injected with green food color [18]

To examine the effect of mechanical stress on embryo viability, the authors loaded and then unloaded the embryos inside the channels and subsequently stored under a 1 mm thick Klearol oil film in a humid environment (surrounded by water in a closed container). The results showed a survival of 93% of embryos. The author used suppression of eGFP (Enhanced Green Fluorescent Protein) expression by a siRNA (Small Interfering RNA) that blocks the expression of the eGFP as a way of demonstrating injection efficiency. The embryos were monitored for about 4hr (16–22hr old) old post fertilization and they showed that after injection of siRNA against eGFP, 90% of embryos exhibited entirely suppressed or lack of fluorescence as shown in FIG. 2. 9. This system allowed the authors to inject 231 embryos within ~14 min (~3-4 s for each embryo). The device was suited for performing automated screens (e.g. wide-genome screening assays) based on *Drosophila* embryos as well as generation of transgenic *Drosophila* lines. One of the drawbacks of this device is that the length of the needle, which penetrates into the embryo, is fixed. Therefore, the device is unable to deliver the reagent at locations inside the embryo other than that determined by the microneedle length. Moreover, for different transgenic application, the needle should be inserted from the posterior of the embryo. Therefore, embryos should be loaded into the channel from the posterior to interior that may require a pre-processing of the embryos.

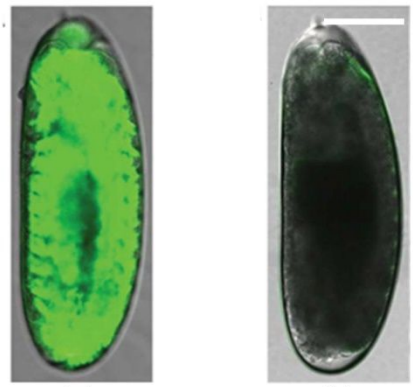

FIG. 2. 9: Fluoroscent images showing the presence of GFP signal throughout the 4 hr old non-injected embryos (a) in contrast with the embryo after injection of siRNA against GFP marker (b). 90% of the embryo exhibited almost completely suppressed or lack of fluorescence as shown. Scale bars: 100 μm. [25]

Pressure driven flow is a conventional method to deliver the reagent when the microneedle is inserted into the embryo. This technique is simple, fast and easy to perform in micro-scale format devices. However, the backpressure and the pressure shock that it usually imposed inside the embryo during the delivery can cause a large displacement of the biochemical composition and distribution inside the embryo. Since the gradient of material inside the embryo is critical for variability and development of the embryo, microinjection with pressure driven flow may decrease its viability after injection. Electrokinetic flow is another option for ionic reagent delivery into the embryo. In order to create electrokinetic flow for microinjection, an electrical potential is apply inside the reagent chamber and on the target. When the needle is inserted into the target, the electrical pathway will be closed and ions inside the reagent will migrate to the negative pole, which can cause electrical current from the reagent chamber to the target. Noori et al. [9] demonstrate a microfluidic microinjector with electroosmotic flow delivery of the methylene blue dye into the zebra fish embryo.

3. Microfluidics devices for *Drosophila* larval assays

Two of the main categories of assays performed on the larval stage of *Drosophila* are based on 1) assessing their behavior such as movement, feeding and digging or 2) imaging internal organs such as the heart, central nervous system and the brain and assessing their functioning both in response to exposure of various chemicals, drugs or environmental cues. Assessing behavior can be performed by capturing videos of the behavior of the animals in specific environments or when exposed to external stimuli and using image processing software to automate the analysis of their behavior. Imaging functioning of internal organs such as neuronal responses in the central nervous system and the brain to external stimuli is challenging because the larva in its natural state is constantly digging and burrowing.

3.1. Neuronal imaging

In order to perform neuronal imaging (live fluorescent imaging from the neuronal activities), the larva is usually immobilized. Conventional immobilization methods use anesthetics [19]-[20], which is suitable for study of various organs such as the heart but may not be suitable for others such as neuronal assays. Preferably, immobilization should be quick, easy to perform and reversible while still allowing the larva to respond to sensory stimulus as if it were unconstrained. In this section we review several microfluidic devices that have been developed to immobilize *Drosophila* larvae for neuronal imaging.

Ghannad-Rezaie et al. [19] designed two different devices, one for short-term (up to 1 hour) and one for long-term (up to 12 hours), for non-invasive and chemical-free immobilization of 3rd instar larvae. These devices were a great tool for high resolution live imaging in *Drosophila* using microfluidic chips. The first design simply contains a micro chamber and a vacuum network. The micro chamber (3.5 mm long, 1.5 mm wide and 140 μm thick) was appropriately designed to closely fit the body of an early-stage 3rd instar larva (see FIG. 2. 10a). In order to reversibly seal the micro chamber with the substrate (cover glass here), the micro chamber was surrounded by a microfluidic network, which was held under constant vacuum during the experiment. Then a mild suction was applied

from the inside of the microchamber to deflected/compress the PDMS membrane on the larva. When the membrane was deflected, it compressed the larva inside the chamber, which leads to the complete immobilization of the larva. This configuration allows the larva to be oriented such that internal body structures such as the central nervous system is close to the bottom cover slip and results in high resolution imaging. They also show that this purely mechanical immobilization approach can keep 90% of larvae alive for continuous immobilization periods of up to 1 hour. In order to increase the immobilization time longer than 1hr, they designed a second double layer architecture microfluidic chip shown in FIG. 2. 10b. Similar to the first chip, a micro chamber that fits the size of a larva was designed. A CO_2 micro chamber (170 µm thick) was added on top of the immobilization chamber. These two were separated by a 10 µm thick PDMS membrane for well-controlled delivery of CO_2/air mixture. The CO_2 acted as an anesthetic and immobilized the larva. The positive pressure applied to the top chamber to flow the CO_2 was also used to deflect the PDMS membrane, which also contributed to the immobilization.

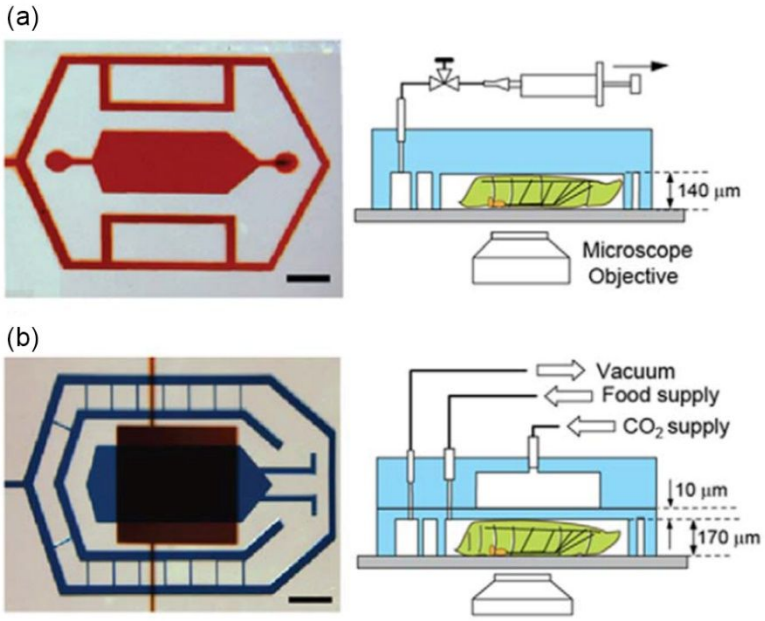

FIG. 2. 10: A. Schematic of the single-layer PDMS microfluidic device that utilizes a shallow (140 mm thick) immobilization microchamber to fix a 3rd instar larva in the vertical direction. Scale bar, 1 mm (B) Schematics of the two-layer immobilization chip. Scale bar, 1 mm [19].

In these designs, mechanical encapsulation or CO_2 anesthetic exposure allows the whole larval body to be immobilized inside the chip so that neuronal transport processes and sensory neuron regeneration upon injury can be visualized. Both these devices reduce the movement artifacts as compared to the freely moving larva but did not eliminate them. In particular, internal structures such as the central nervous system and the brain are still mobile and they move when the larva flexes its muscles. Also, the use of anesthetic leads to spurious neurobehavioral responses and the use of encapsulation prevents the exposure of the larva to external sensory stimulus. Finally, the fabrication of two layer PDMS device as well as using active mechanism for immobilization adds to the complexity of construction and operation of the device. The design with exposure of CO_2 can be used for many *Drosophila* assays, which requires long-term immobilization of the larva for high resolution imaging. For instance, this device could be used in the study of neuronal degeneration after injury which is a process that occurs over ~5 hr and therefore requires long term immobilization. Ghannad-Rezaie et al. studied the subcellular responses of the larval neurons to axotomy (neuronal injury) over time. They found that the proximal stump was inactivated for the first seven hours after injury. New axonal sprouting was observed between 7 and 12 hours after injury. GFP-tagged version of the F-actin binding protein moesin were also used to visualize F-actin location as shown in FIG. 2. 11. They found that F-actin was mainly dynamic in the range of 10 and 11 hours after injury, which was obtained by quantitative measurement of the proximal stump of the injured axon (FIG. 2. 11b). They also found that this device could not only be used for studying degeneration of neurons but also regeneration. In addition, these immobilization methods could also be used to image other organs such as the heart upon exposure to various chemicals and drug candidates. Although the authors have not shown any capability of the device for high-throughput live imaging assays, the design of the device is amenable for parallel imaging of multiple organisms to increase the throughput of the assay.

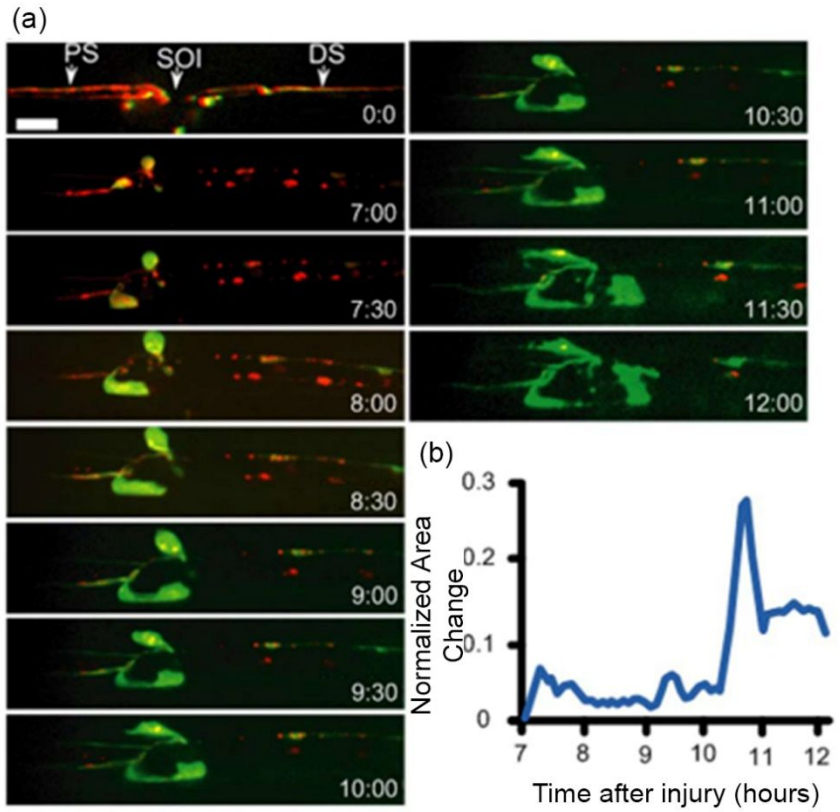

FIG. 2. 11: (a) Live imaging of the proximal stump for 5 hr (7 -12 hours after laser axotomy) visualized in a single enteric motoneuron. Scale bar, 10 mm. (b) Significant movement in the proximal stump can be seen after 10.5 hr after injury by quantitative (normalized) area of the proximal stump over time [19].

Mondal et al. [20] have also developed similar microfluidic device where, the immobilization of the *Drosophila* larvae were achieved by mechanically compressing a thin layer of the PDMS on the larvae located in a micro chamber as Ghannad-Rezaie et al. [20] designed previously (see FIG. 2. 12). However, nitrogen gas was used instead of CO_2/air mixture to pressurize and bend the PDMS membrane on the larvae, which leads to pure mechanical immobilization with no chemical anesthesia effects.

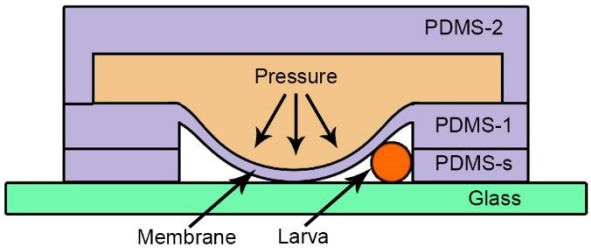

FIG. 2. 12: Design and operation of a pneumatic immobilization system for larva. The membrane seperating the top and bottom channels is deflected under pressure to immobilize the larva in the channel.

Ardeshiri et al. [21] recently developed a microfluidics device, which can not only immobilize the larva but could also orientate it in the desired directions for live imaging of the heart activity. In this design (shown in FIG. 2. 13), the microfluidics device composed of two guide channels and a larva chamber between them. The core of the microfluidics design (see FIG. 2. 13) consists of a channel for placing the larva, six side-channel for applying suction to immobilize the larva after loading and two others for introducing the chemical stimuli. In order to orient the larva in the desired direction, two glass capillary have been placed in side of the guide channels through which suction is applied to hold the head and the tail. This arrangement could allow one to rotate the larva into the desired orientation by rotating the glass capillaries. When the larva was well orientated, the suction was applied from the side channels to fully immobilize the larva.

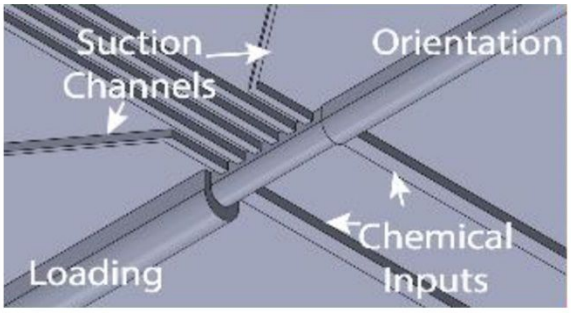

FIG. 2. 13: schematic of the Microfluidic chip used for fly larva orientation and imaging of cardiac activities when it was exposed to the Sodium Azide (NaN_3) via chemical inputs [21]

In this device, the effects of the Sodium Azide (NaN_3) on the heartrate have been investigated. The results showed that the heart rate was significantly decreased from ~170 to ~25 beats/min, when the larva was exposed to NaN_3 with rate of 1ml/min over 10 minutes. The advantage of this design is the ease of orientation and the ability to reuse the device. This allows precise exposure of the larva to different chemicals while an internal organ such as the heart is monitored. However, it requires active feedback and control of the rotation of the larva and application of suction for operation. Furthermore, chemical exposure of the larva is limited to the outer body of the larvae. This could be a limitation when ingestion of the chemical involved is desired as the route for delivery. High-throughput exposure assays is also fairly difficult to achieve with this design as manual rotation of the larvae have to be performed one at a time.

4. Devices for adult *Drosophila* assays

Among the various stages of the *Drosophila* used in research, the adult fly has been used in a significant majority of studies. The adult fly is used in behavioral studies involving vision, oviposition, auditory and navigation that require a fully developed organism. It is in the final and more advance stage of the *Drosophila* life cycle, which allow one to investigate wider range of biological assays, which might not be possible to perform in the younger stage (e.g. vision, oviposition auditory, navigation assays). Due to their larger size (3mm length and 2mm width without considering the wings) the adult fly can be handled in millimeter scale devices that could be machined conventionally. They also operate using air as the fluid medium rather than water which is the operating fluid in most microfluidic devices. Finally, most of the assays using the adult fly is behavioral in nature rather than imaging-based as they are not transparent like the larva or the embryo.

Oviposition (egg-laying behavior) assays are an example of behavioral assays that have been automated. Leung et al. [22] have developed an agar-polydimethylsiloxane device for quantitative investigation of oviposition behavior of adult *Drosophila* melanogaster. In this design, a custom-patterned through-hole PDMS membrane has placed on top of the agar plate (see FIG. 2. 14a). Based on the pattern of the PDMS membrane, defined amount of

the agar juice would be exposed to the flies. In order to allow the fly to lay eggs on the substrate, 45 flies (25 female and 20 male) were held inside a stock bottle and inverted onto the oviposition substrate (see FIG. 2. 14b). This design allows them to simply study the oviposition behavior and viability of the flies based on the amount of exposed agar juice to the stock. They found that flies avoided lying egg on pure PDMS and on top of substrates with 0.5 mm diameter agar exposure areas. However, for hole size from 2 mm and above, the ovipositioning have been observed and beyond 4mm hole size, the oviposition behavior became similar to a normal agar substrate. The design of the device and the fabrication method make it amenable for adaption to high-throughput ovipositioning assays.

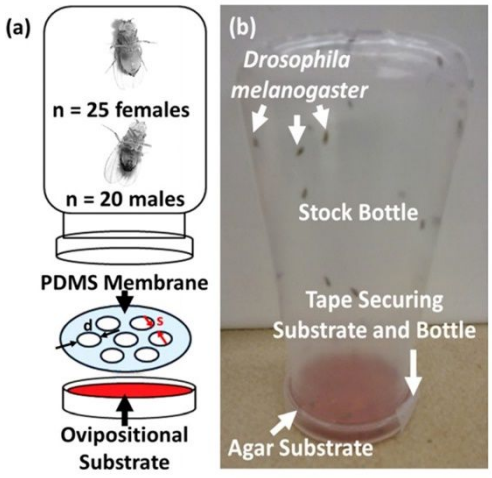

FIG. 2. 14: (a) Schematic of the experimental setup for ovipositional setup. (b) The setup consisted of 45 flies (25 female and 20 male) in a stock bottle capped onto an oviposition substrate [22]

Feeding behavior assays have also been performed using microfluidic technology. Choudhury et al. [23] developed a microfluidic capillary feeder with integrated activity monitoring chamber for *Drosophila* studies. In this design as shown in FIG. 2. 15, an array of the monitoring chamber has been created. In each chamber, there are two capillary channels, one for food and the other for water. The capillary feeder was connected to the feeding cups which can keep the food required for a day. The fly chamber also connected to the humidity chamber via evaporation holes as shown in FIG. 2. 15. When the various types of adult flies have been placed inside the chamber, flies started to feed from the outlet

of the vertical feeding channel. Their feeding behavior such as the amount of the consumed food can be monitored and recorded by CCD camera located in front of the devices. Then, the video was analyzed in order to characterize the feeding behavior of the flies based on the strain that they were selected. Although author have not shown any high-throughput application of the device for drug discovery assays, this system could be potentially used with suitable modification to explore different feeding behavior in adult fly in a high-throughput manner, variations in dosage and the concentration of the food by creating larger platform of the design. However, the system is limited to one type of the food at the time and the confined environment in the feeding chambers is different from the natural environment to which the flies are accustomed.

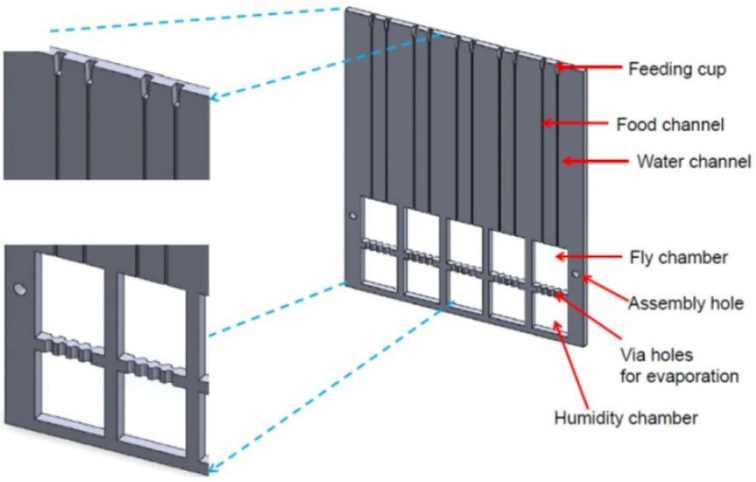

FIG. 2. 15: schematic of main layer of the chip. In each chamber there are two microfluidic channel feeders. The bottom humidity chamber with water inside maintains higher humidity within the chamber and decreased fluid evaporation [23].

References

[1] Drews, J. Drug discovery: a historical perspective. *Science*, 2000, *287*(5460), 1960-1964.

[2] Atwood, H. L.; Govind, C. K.; Wu, C. F. Differential ultrastructure of synaptic terminals on ventral longitudinal abdominal muscles in *Drosophila* larvae. *Journal of neurobiology*, 1993, *24*(8), 1008-1024.

[3] Skehan, P.; Storeng, R.; Scudiero, D.; Monks, A.; McMahon, J.; Vistica, D.; Warren, J.T.; Bokesch, H.; Kenney, S.;Boyd, M. R. New colorimetric cytotoxicity assay for anticancer-drug screening. *Journal of the National Cancer Institute*, 1990, *82*(13), 1107-1112.

[4] Rezai, P.; Salam, S.; Selvaganapathy, P. R.; Gupta, B. P. Electrical sorting of Caenorhabditis elegans. Lab on a chip, (2012) 12(10), 1831-1840.

[5] Hulme, S. E.; Whitesides, G. M. Chemistry and the worm: Caenorhabditis elegans as a platform for integrating chemical and biological research. *Angewandte Chemie International Edition*, 2011, *50*(21), 4774-4807.

[6] Mondal, S.; Ahlawat, S.; Rau, K.; Venkataraman, V.; Koushika, S. P. Imaging in vivo neuronal transport in genetic model organisms using microfluidic devices. *Traffic*, 2011, *12*(4), 372-385.

[7] Ghannad-Rezaie, M.; Wang, X.; Mishra, B.; Collins, C.; Chronis, N. Microfluidic chips for in vivo imaging of cellular responses to neural injury in *Drosophila* larvae. *PloS one*, 2012, *7*(1).

[8] Heckscher, E. S.; Lockery, S. R.; Doe, C. Q. Characterization of *Drosophila* larval crawling at the level of organism, segment, and somatic body wall musculature. *The Journal of Neuroscience*, 2012, *32*(36), 12460-12471.

[9] Noori, A.; Selvaganapathy, P. R.; Wilson, J. Microinjection in a microfluidic format using flexible and compliant channels and electroosmotic dosage control. *Lab on a Chip*, 2009, 9(22), 3202-3211.

[10] Markow, T. A.; Beall, S.; Matzkin, L. M. Egg size, embryonic development time and ovoviviparity in *Drosophila* species. *Journal of evolutionary biology*, 2009, 22(2), 430-434.

[11] Furlong, E. E.; Profitt, D.; Scott, M. P. Automated sorting of live transgenic embryos. *Nature biotechnology*, 2001, 19(2), 153-156.

[12] Chen, C. C.; Zappe, S.; Sahin, O.; Zhang, X. J.; Fish, M.; Scott, M.; Solgaard, O. Design and operation of a microfluidic sorter for *Drosophila* embryos. *Sensors and Actuators B: Chemical*, 2004, 102(1), 59-66.

[13] Yanik, M. F.; Rohde, C. B.; and Pardo-Martin, C.; Technologies for micromanipulating, imaging, and phenotyping small invertebrates and vertebrates. *Annual review of biomedical engineering*, 2011, 13, 185-217.

[14] Ashburner, M. *Drosophila. A laboratory handbook* ; Cold Spring Harbor Laboratory Press, 1989.

[15] Bernstein, R. W.; Zhang, X.; Zappe, S.; Fish, M.; Scott, M.; Solgaard, O. Characterization of fluidic microassembly for immobilization and positioning of *Drosophila* embryos in 2-D arrays. *Sensors and Actuators A: Physical*, 2004, 114(2), 191-196.

[16] Chung, K.; Kim, Y.; Kanodia, J. S.; Gong, E.; Shvartsman, S. Y.; Lu, H. A microfluidic array for large-scale ordering and orientation of embryos.*Nature methods*, 2011, 8(2), 171-176.

[17] Zhang, X.; Scott, M. P.; Quate, C. F.; Solgaard, O. Microoptical characterization of piezoelectric vibratory microinjections in *Drosophila* embryos for genome-wide RNAi screen. *Microelectromechanical Systems, Journal of*, 2006, 15(2), 277-286.

[18] Delubac, D.; Highley, C. B.; Witzberger-Krajcovic, M.; Ayoob, J. C.; Furbee, E. C.; Minden, J. S.; Zappe, S. Microfluidic system with integrated microinjector for automated *Drosophila* embryo injection. *Lab on a Chip*, 2012, 12(22), 4911-4919.

[19] Ghannad-Rezaie, M.; Wang, X.; Mishra, B.; Collins, C.; Chronis, N. Microfluidic chips for in vivo imaging of cellular responses to neural injury in *Drosophila* larvae. *PloS one*, 2012, *7*(1).

[20] Mondal, S.; Ahlawat, S.; Koushika, S. P. Simple microfluidic devices for in vivo imaging of C. elegans, *Drosophila* and zebrafish. *Journal of Visualized Experiment: JoVE* , 2012, (67), e3780-e3780.

[21] Ardeshiri, R.; Amini, N.; and Rezai, P. In: International Conference on Miniaturized Systems for Chemistry and Life Sciences :A microfluidic device to screen chemicals on *Drosophila* melanogaster larvae for cardiac system toxicity, Proceeding of 19th International Conference on Miniaturized Systems for Chemistry and Life Sciences, Gyeongju, Korea, October 25-29.

[22] Leung, J. C.; Taylor-Kamall, R. W.; Hilliker, A. J.; Rezai, P. Agar-polydimethylsiloxane devices for quantitative investigation of oviposition behaviour of adult *Drosophila* melanogaster. *Biomicrofluidics*, 2015, 9(3), 034112.

[23] Choudhury, D.; Navawongse, R.; Raczkowska, M.; Wang, Z.; Claridge-Chang, A.. In: International Conference on Miniaturized Systems for Chemistry and Life Sciences : Microfluidic capillary feeder with integrated activity monitoring chamber for *Drosophila* studies, 19th International Conference on Miniaturized Systems for Chemistry and Life Sciences , Gyeongju, Korea, October 25-29..

Chapter 3

A MICROFLUIDIC MICROINJECTOR FOR TOXICOLOGICAL AND DEVELOPMENTAL STUDIES OF CARDIOGENESIS IN *DROSOPHILA* EMBRYOS

Complete citation:

Ghaemi, Reza, Pouya Arefi, Ana Stosic, Meryl Acker, Qanber Raza, Roger Jacobs and Ponnambalam Ravi Selvaganapathy. "*A microfluidic microinjector for toxicological and developmental studies of cardiogenesis in Drosophila embryos*", submitted to journal of Lab on a Chip, 2017. Received (in July, 2017).

Relative Contributions:

Ghaemi, R.: Performed all experiments, interpretation and analysis of the data and wrote the drafts of the manuscript including all figures and text.

Arefi, P.: Helped in performing the confocal imaging of the injected embryos and control samples and performed filopodia analysis.

Stosic, A.: Helped in performing the confocal imaging and sample preparations.

Acker, M.: Helped in performing the viability test and sample preparations.

Raza, Q.: Assisted in performing proof of concept experiments and consults in the development of assays.

1. Introduction

Microinjection is a common method used to deliver chemicals, biomolecules and toxins to specific locations inside the embryo in order to probe or perturb the biochemical networks inside the embryo or an organism. Capillary microinjection has been used extensively to introduce material into small organisms such *C. elegans* worm or zebrafish, Xenopus and *Drosophila* embryos. One of the main applications of microinjection is creating transgenic organisms. Transgenic *Drosophila* are generated by injecting foreign genetic material into the pre-cellular embryo so that it can be incorporated into the germline cell genome. Applications of microinjection are not limited to transgenics. The chemical composition of the embryo can be perturbed by injecting various toxins/chemicals to study the response of the embryo. Injection of toxins and drugs into transgenic *Drosophila* embryo that contain fluorescent cell lineage or morphology markers, reporters of protein location or those that fluoresce in response to physiological signals enable functional study of drug responses in living, intact embryos. In these assays, a known volume and concentration of a selected toxin would be delivered into a specific location of the embryo via microinjection.

Conventional microinjection systems required a high degree-of-freedom micropositioner in order to hold the embryo, align the microneedle with targeted location and insert it into the embryo. This approach is complex, time consuming and requires a skilled operator, which makes the process slow and expensive to perform. Additionally, the microneedle used in conventional microinjection have a steep taper angle of over 30^{o} which can create significant damage to the embryo, if the microneedle was inserted too deeply. Therefore, conventional microinjection needles are not appropriate to deliver small volumes of chemicals (drugs or toxins) to specific tissues deep inside the embryo.

Recently, a few microinjectors have been developed for the injection of microorganisms such *C. elegans*, zebrafish embryo and *Drosophila* embryo [1]-[6]. These devices aim to simplify the needle insertion procedure and improve repeatability. However, these designs are not suited to perform deep needle insertion or precise positioning of the delivery

location within the embryo, either because of the large taper angle of the needle or the mechanism of the needle insertion. Additionally, they require active immobilization mechanisms (e.g. flow induced drag force) to hold the embryo for needle insertion, which adds more complexity to the operation. Finally, these devices and their microneedles are often fabricated through semiconductor manufacturing processes, which required expensive fabrication equipment. Therefore, a low cost microinjector, which could deeply insert the microneedle, >100µm into the embryo without damaging it, would be ideal for the application that required reagent delivery at multiple locations inside the embryo.

In this chapter, we demonstrate the first microinjector specifically designed to accommodate a small taper angle microneedle for toxicological and developmental studies of cardiogenesis in *Drosophila* embryos. The device immobilizes the embryos using a form fitting passive immobilization chamber, allows easy needle penetration and enables a wide range of needle motion and positioning inside the embryo. In order to demonstrate the applicability of this microinjector in toxicological studies, the effect of sodium azide (NaN3), a cytochrome oxidase inhibitor, on heart development during embryogenesis has been examined.

2. Method

2.1. Design of the Microfluidic chip

The microinjector system is composed of six components, which includes the embryo chamber, microneedle, needle channel, top and bottom needle aligner and compliant mechanism, as shown FIG. 3. 1a-b. The embryo chamber was designed to fit the form of an average fly embryo and passively immobilize it (FIG. 3. 1a). Based on this criterion, the width, length and depth of the embryo chamber were determined to be 150µm, 600µm and 150µm respectively. A microneedle made of fused glass capillary (outer diameter of 90µm) is placed inside the needle channel (150 µm depth and 100µm width). The needle channel connects with one end of the embryo chamber where the posterior end of the embryo will be placed via an opening (50µm length and 40µm width) with depth of 150µm (FIG. 3. 1b).

The width of the opening (40µm) was designed to restrict the lateral movement of the needle in the range of ±20 µm from the centre line of the embryo posterior.

The depth of the needle channel and its alignment to the embryo chamber were determined to ensure that the needle is displaced in the vertical direction to penetrate the posterior end of the embryo. Since both the depth of the needle channel and embryo chamber are 150µm, an embryo placed inside the chamber, will have ideal injection point at its posterior end located between 60µm to 90µm from the bottom of the needle channel (see FIG. 3. 1c). Therefore, two aligners (top and bottom needle aligner) in the needle channel were designed to restrict the motion of the microneedle in the vertical direction. The bottom aligner was a step (60µm), which was made of Polydimethylsiloxane (PDMS) (FIG. 3. 1d). This step was integrated into the mold used to make the needle channel and embryo chamber. The top aligner consists of two fused silica rods (90 µm diameter with the length of 0.6mm) that could be slid into precise position into appropriately placed grooves (1mm length with cross section of 90µm *x* 90µm) in the PDMS top layer.

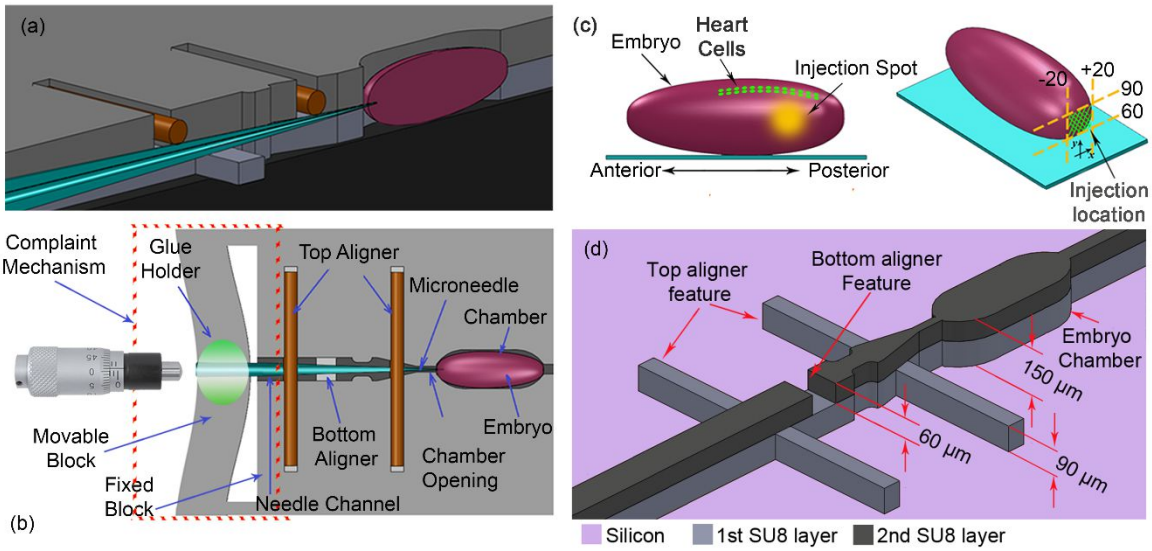

FIG. 3. 1: Schematic of the *Drosophila* embryo microinjector. (a) The 3D cross-section of the microneedle channel which shows the details of the needle aligners. (b) The top view of the microinjector. (c) The schematic of the *Drosophila* embryo that shows the direction and the dimension of the injection location. (d) 3D schematic of the master mold which shows the epoxy-based negative photoresist (SU8) layers on the silicon wafer. The first and SU8 layer has 90µm and 60µm, respectively. By casting PDSM on this mold, a 60µm step inside the needle channel and a 90µm channel on top of the needle channel could be created.

This simple arrangement is suitable to reliably align the microneedle to the posterior of the embryo. Furthermore, the use of the top and bottom aligners enable smooth friction free motion of the needle inside the needle channel in a controllable and well aligned manner. While the tip of the microneedle and its shank are able to freely move inside the needle channel, the tail end of the needle capillary is fixed on to the movable block that is attached to a complaint mechanism (FIG. 3. 1b), The compliant mechanism (a movable block and two posts), allows relative motion of the movable block with respect to the fixed block when the movable block is pushed using a micropositioner. Since the tail end of the needle capillary is attached to the movable block, its motion is transduced into the motion of the needle tip inside the embryo chamber. This system has high compliance in one direction and high stiffness in other directions which allows precise unidirectional motion. The movable block is pushed using a precise (5µm resolution) micropositioner which then moves the tip of the needle precisely.

2.2. Device fabrication

2.2.1. *Master mold fabrication*

The devices were made by soft lithographic fabrication using Polydimethylsiloxane (PDMS). Photolithography process was used to fabricate an epoxy master mold to cast PDMS. First, an epoxy based photoresist (SU8 3035 MicroChem Corp.) was spun on a 3" silicon wafer to obtain a layer thickness of 90 µm. Next, this photoresist layer was exposed to the first layer pattern which forms the shape of the embryo chamber, needle channel and the top aligners, as shown in FIG. 3. 1d. Subsequently, the second layer of SU8 with the thickness of 60µm was spun on top of the first layer. The second layer was exposed to a pattern, whose shape consisted of the embryo chamber, the needle channel and the bottom aligner feature, as shown in FIG. 3. 1d.Using the two layer lithography process, the mold for the microfluidic substrate was fabricated incorporating the embryo chamber (depth of 150 µm), needle channel (depth of 150 µm), bottom needle aligner (height of 60µm) and grooves for the top needle aligner (depth of 90µm), as schematically shown in FIG. 3. 1d.

2.2.2. PDMS casting

PDMS (10:1 ratio base: regent, SYLGARD® 184, Dow Corning Corporation) was cast on the fabricated master mold and cured at 70 °C for 2 h. The cured PDMS was peeled off from the mold and the region between the fixed and the movable blocks with the dimension 2×10mm2, was cut to form the compliant mechanism.

2.2.3. Microneedle fabrication

Needles with tip sizes in the range of 3-6 µm and taper length of ~250µm, were selected to minimize embryo damage, while being large enough to allow reagent delivery into *Drosophila* embryo. In conventional embryo microinjection, Borosilicate capillaries (OD/ID of 1000/500µm) are used for needle fabrication. However, the integration such needles into microfluidic devices is challenging as the size of needle shank is significantly larger than the size of normal microfluidic channels (the channel dimensions are in range of 100µm). To address this problem, fused silica microcapillaries with OD/ID of 90/20 µm were chosen for needle fabrication as shown in FIG. 3. 2. This selection allows a simple and easy integration of the needle with microfluidic devices. In order to fabricate fused silica microcapillaries, a custom-built needle puller was designed (see FIG. 3. 2a), which allows to fabricate conical microneedle with tip sizes in the range of 3 µm to 6 µm. The needle puller consists of three components: a fixed clamp, a movable clamp and a piezo torch. In this method, first, the fused silica capillary with the length of 15cm, was attached to the fixed and movable clamps, where the centre of the capillary was aligned with the piezo torch. Since, the movable clamp can freely move on the slider in vertical direction, a certain pulling force was generate along the capillary. Therefore, the weight of the movable clamp defines the amount of the pulling force, which can be adjusted in this design by adding defined weight to the movable clamp. Next, the piezo torch was turned on and the capillary was exposed to its flame (1300ºC), that heated the capillary at its centre. When the temperature of the capillary was reached to the glass softening point temperature, the pulling force (25g) caused creep and pulled (necking) the capillary into two pieces. The bottom piece with the length of ~10cm was used for the microinjection. In order to store

and transfer the reagent after needle insertion, the tail of the microneedle was attached to the 15mm capillary tube (OD/ID of 1000/500µm) by using epoxy glue as shown in FIG. 3. 2b. In this design, 2.5µL of the reagent can be filled inside the chamber. Finally, the tip of the needle was dipped into the 30% Hydrofluoric acid (HF) for 25s second in order to open any potential blockage during the pulling process.

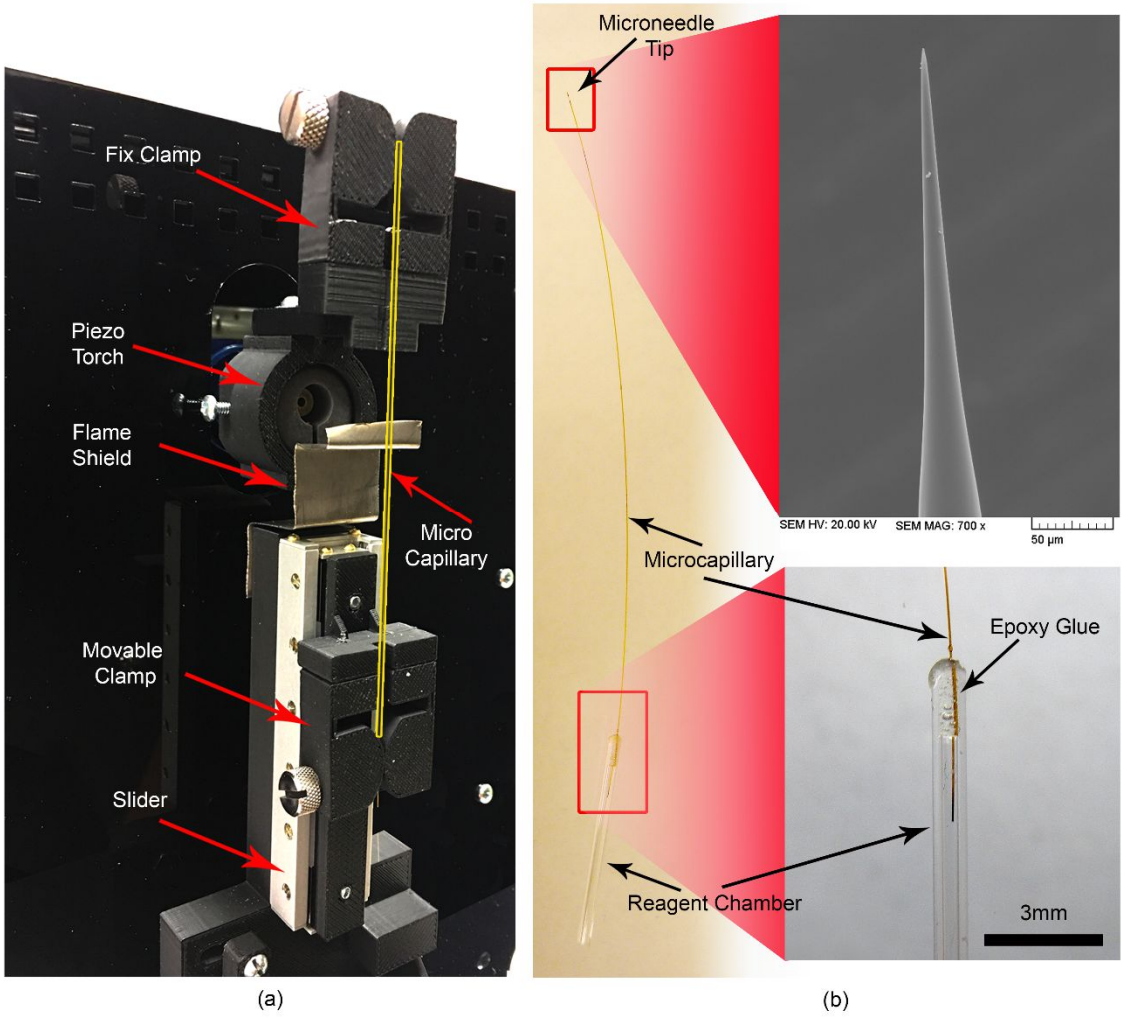

FIG. 3. 2: (a) Custom-built microneedle puller used for microneedle fabrication. (b) Fused silicon microneedle fabricated with a custom-made needle puller. The microneedle was connected to 15mm capillary tube (OD/ID of 1000/500µm) by using epoxy glue to form the reagent chamber. The tip of the microneedles can be adjusted between 3-6µm.

2.2.4. Device assembly

First, the PDMS chip was bonded (80s, 50W, plasma oxygen) to a glass slide to form a stable substrate for operation. Before the complete bonding could occur, the bottom of the compliant actuator part was detached from the glass slide to allow the free movement of the compliant system relative to the embryo chamber (see FIG. 3. 3). Next, the microneedle was gently placed on the PDMS chip, inside the needle channel. The tip of the microneedle is positioned approximately between the chamber opening and the top needle aligner channel. Subsequently, the top needle aligners were placed into the designed channels. Then, the microneedle was glued into the complaint mechanism using a droplet of 1:10 PDMS as shown in FIG. 3. 3. Finally, the reagent chamber was attached to the glass slide using tape.

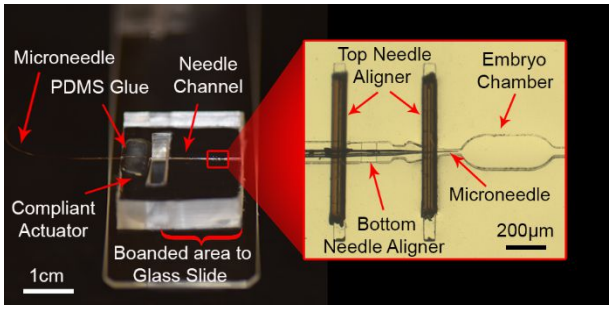

FIG. 3. 3: Assembled microinjector, which was bonded partially to a glass slide. The top needle aligners were gently placed on the needle, after the needle was positioned inside the needle channel.

2.3. Embryo and reagent preparation

*Tup-GFP[*7] males, containing a GFP reporter driven by *tailup* regulatory sequence, were crossed with virgin *yw* females. Embryonic CBs of the progeny were visualized during cardioblast migration. A new applejuice-agar plate was substituted onto the house containing the adult flies 19 hours before injection, and this plate was used for a 2-hour collection of the progeny. Stage 12 – 13 embryos were manually rolled on double sided tape to remove chorion. The embryos will then be double-checked under a dissection scope for green fluorescence and verified for the correct developmental stage before transfer onto the microfluidic chip for injection.

In order to prepare 50Mm, 0.958gr of Rhodamine B powder (Sigma-Aldrich Co. LLC.

PN: 83689) was dissolved into 40ml sterilized DI water. Similarly, 1.3mg of NaN3 powder (Sigma-Aldrich Co. LLC. PN: S2002) was dissolved into 1ml sterilized DI water to make 20mM sodium azide solution.

2.4. Experimental setup

The setup is composed of four major components: microfluidic chip, needle actuation mechanism, drug delivery system and the optical microscope as shown in FIG. 3. 4. The microfluidic chip described in previous section was placed into the device holder under a Leica M165 fluorescent dissecting microscope and viewed under 10x magnification. A single microfluidics microinjector can be used for minimum of 50 microinjections and the device with loaded reagent can be used for another day, if the device was kept at 4^{o} C fridge. However, the reagent used for a single chip cannot be replaced with another reagent. In order to move the needle precisely, a manual micropositioner (with resolution of 5µm motion) has been assembled with device holder and then coupled with the compliant mechanism. For the reagent delivery system, a Tygon tube was connected to the reagent chamber, which was connected to a solenoid valve, pressure regulator (1:24 reduction factor) and pressurized air tank (6000kPa). Subsequently, the flow of pressurized air was controlled via a solenoid valve.

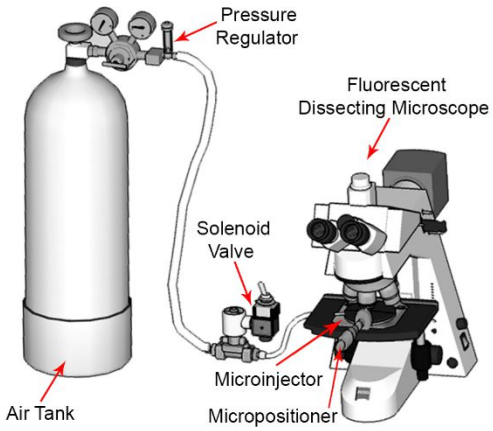

FIG. 3. 4: The experimental setup used for microinjection of the *Drosophila* embryo, which was built on a custom-made 3D printer part.

2.5. Embryo imaging

The embryo staging for time-lapse confocal imaging was followed based on hanging drop method[8]. An imaging chamber was prepared by placing a layer of moistened tissue paper in the well. A 5µl drop of halocarbon oil (chlorotrifluoroethylene polymer), manufactured by Halocarbon Products Corp, was placed on a 22mm *x* 40mm cover slip, and the injected embryo was removed from the microfluidic chip and placed into the oil using tweezers. The embryo was then oriented with its dorsal side towards the glass, and the cover slip was inverted onto the depression slide, with the embryo hanging in oil over the depression in the slide[8]. The coverslip was immobilized with Mylar tape. The embryos were visualized using a Leica LP5 confocal microscope, and z-stacks of 28 optical sections comprising 36µm were taken 30 minutes apart. The images were blurred and processed as a 3D projection of all slices using the LSM software. Cardioblast migration velocity was determined using ImageJ.

2.6. Data analysis and statistics

A pair of CBs, aligned linearly on contralateral rows of the dorsal vessel, were identified at segment A4. The difference in initial and final distance between these cells were obtained and divided by the 30 minute period during which the embryo was imaged. A one-way ANOVA was performed to test for significance amongst three or more treatments. In addition, a T-test assuming unequal variance was performed to test for a significant difference in CB migration velocity amongst each pair of treatments. Differences were accepted as significant when $P<0.05$.

3. Results and discussion

3.1. Characterization of mechanical system

3.1.1. Fluorescent dye injection

In order to demonstrate the operation of the microinjector, a fluorescent dye (50mM Rhodamine B) was injected into the embryo. First, the embryo was prepared (see section 2.3) and was gently rolled into the embryo chamber such that its posterior was positioned close to the needle as shown in FIG. 3. 5a. Next, the needle was actuated manually by a simple micropositioner (Starrett, 463P Micrometer Head) in order to penetrate the chorionic layer of the embryo (see FIG. 3. 5b-c and supplemental video S1). It should be noted, that the high aspect ratio of the needle formed using the custom needle puller was sharp and caused minimal deflection of the chorionic layer for successful injection. The microneedle used in conventional microinjection typically have larger taper angle compared to this microcapillary needle (see FIG. 3. 5d-f), which can cause significant damage to the embryo, especially in the assays that require deep (>200µm) needle insertions, as shown in supplement video S2. After inserting the microneedle inside the embryo, 40pL of Rhodamine B was injected at a position approximately 200µm inside the embryo using a pressure pulse of 250kPa with duration of 4 seconds (supplemental video S3). The fluorescent images (excited by 540 nm light and is detected at 620nm) of the embryo before injection, 1min and 30min after injection have been captured and shown in FIG. 3. 5g-k. It should be noted that while the embryo is the same in these images its orientation is different due to rotation after unloading the embryo from the embryo chamber and imaging setup. The mean gray value of the pixels along the posterior to anterior (550µm), which represent the intensity of the detected light, have been measured using ImageJ and were plotted in FIG. 3. 5. The results shows that the Rhodamine B was successfully transferred into the embryo as the signal intensity have been increased significantly at the posterior of the embryo immediately after injection. The intensity at the anterior end is similar to that of the uninjected embryo. After, 30 min, the intensity at the posterior end decreases considerably but is still above the baseline while the intensity in

the anterior end increases indicating that the dye has diffused throughout the embryo in that duration of time. These experiments demonstrate that small volume injections at precise locations inside the embryo can be performed using this device. Although, in this current demonstration, the location and the type of the injected dye have been selected arbitrarily for visualization purposes, the location of the needle tip inside the embryo can be precisely controlled to deliver controlled quantities of various reagents at any location along its central axis

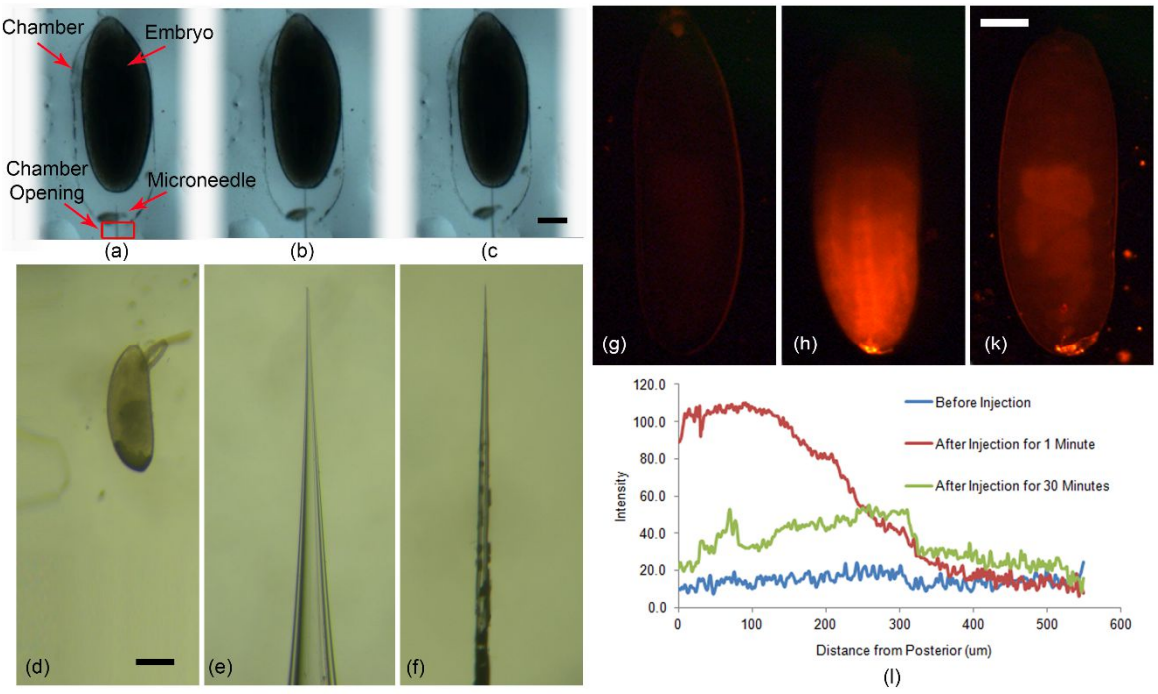

FIG. 3. 5: (a-c) Image sequence of the needle insertion into the embryo, before (a), during (b) and after (c) penetrating the embryo (Scale bar = 80 µm). (d-f) size comparison between (d) *Drosophila* embryo, (e) Conventional microneedle and (f) fused silica microneedles designed in this method. The tape angle of the conventional microneedle are significantly larger than the fused silica microneedles which can cause more damage to the embryo in the injections that require deep needle insertion (Scale bar = 80 µm). (g-k) Fluorescent images (excited by 540nm and detected at 620nm) of the embryo in three different states: before injection (g), 1 minute (h) and 30 minutes (k) after injection. The embryo is the same in these image, while, the orientation of the embryo might not be the same (Scale bar = 80 µm). (l) The intensity of the fluorescent dye alone a midline from posterior to anterior at these different time points.

3.1.2. Characterization of complaint mechanism

The performance of the compliant mechanism attached to the micropositioner was characterized by applying a known displacement to the micropositioner and measuring the actual movement of the microneedle tip inside the embryo chamber. The needle motion was recorded under microscope and then, the videos were analysed to obtain needle displacement by using ImageJ. The movement of the needle either in the presence of the embryo or in its absence, were the same as the stiffness of the embryo was significantly lower than the microneedle and complaint system. The results plotted in FIG. 3. 6 shows the displacement applied by the micropositioner (x-axis) and the resultant normalized needle motion as measured through image analysis (y-axis). It can be seen that the microneedle can be moved in a controllable and repeatable manner by using a micropositioner and a compliant mechanism. The relationship between the displacement of the needle tip and that of the micropositioner is initially linear till a displacement of 200µm after which it plateaus. This may be because the stiffness of the micropositioner was not constant and varied with the displacement. This mechanism allows precise manual positioning of the needle tip and precise locations inside the embryo guided by observation under the microscope for localized delivery of reagents. The alignment of the needle with the embryo and the single degree of freedom motion allowed by the device are critical in enabling precise positioning.

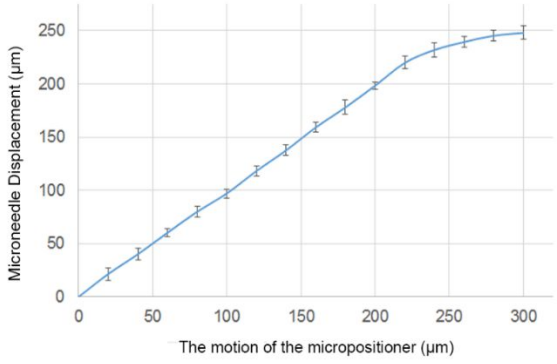

FIG. 3. 6. The characterization of the compliant mechanism. The error bar represent the standard deviation (SD) of the data in each repeat.

3.1.3. Characterization of regent delivery system

Pressure driven flow has been used to deliver reagents from the reagent chamber through the microneedle into the embryo. The volume of reagent delivery can be controlled by changing the pressure level as well as the duration of the pressure pulse. In order to characterize the reagent delivery system, the volume delivered by 200kPa pressure pulse with duration of 4s have been measured for 5 different microneedles. To do this, firstly, microneedles with inner diameter of ~5µm and taper length ~250µm were fabricated by pulling 90/20µm (ID/OD) fused silica capillary as discussed in section 2.2.3. Next, the needle chamber was loaded with 50mM Rhodamine B and connected to a solenoid valve. The tip of the microneedle was placed inside a halocarbon oil reservoir so that the ejected liquid forms a spherical drop due to surface tension, making it easier to measure its volume. The volume delivered in each pulse was calculated by simply measuring the diameter of the droplet and calculating the volume of the sphere. The experiment was repeated for five different microneedles and the result is plotted in FIG. 3. 7. The results show that the delivery system was consistently able to deliver ~30±10pL (~0.3% of the embryo's volume[9]) per pulse, which is in the range suitable for injection into the embryo. Higher volumes can be injected using multiple pulses.

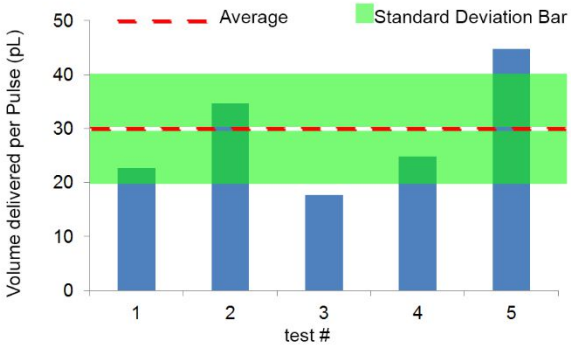

FIG. 3. 7: The volume delivered by five different microneedles, when a pressure pulse of 200kPa with duration of 4s have been applied to into the reagent chamber.

3.2. Effect of NaN3 on CB migration velocity

The *Drosophila* heart, also called the dorsal vessel, is a linear tube composed of two contralateral rows of cells and is responsible for the circulation and flow of hemolymph[10]. The dorsal vessel is divided into ten segments, with each segment containing four to six pairs of cardioblasts (CB), which are aligned on contralateral sides of the heart tube and are responsible for generating contractile force.

The heart arises from two bilateral rows of cardioblasts (CB) that migrate dorsally towards the midline and contact their contralateral partners to form the dorsal vessel[11] (see supplementary video S4). This process occurs by the collective cell migration (CCM) of cardial cells and requires coordinated cell to cell and cell to ECM signalling[10]. CCM occurs in conjunction with the dorsal closure of the overlaying ectoderm, and is thus facilitated by association between CBs and ECM basal to the ectoderm. During this processes, actin-based filopodia and lamellipodia extend from the leading edge of CBs, making contact with contralateral cells and aiding in dorsal vessel closure and alignment[12]. Furthermore, actin polymers are important in cytoskeleton organization and cell adhesion, and have been shown to localize at the leading edge of migration cells[13]. Therefore, actin plays a direct role in ensuring the cohesive migration of a group of cells and the dorsal closure of the overlaying ectoderm. The actin filaments (F-actin) that are involved in migration and adhesion arise from the polymerization of globular actin (G-actin). This requires energy in the form of ATP that is produced through biochemical processes in the electron transport chain (ETC), which necessitates the functionality of cytochrome oxidase, which can be inhibited by metabolic toxins.

Sodium azide (NaN3) is a potent metabolic toxin with a multitude of dosage dependent effects. Sodium azide has been used as an herbicide and has also been shown to cause hypotension by inducing blood vessel dilation in human[14]. In addition, azide is a soluble and membrane permeable toxin which dissociates from sodium and competitively binds cytochrome oxidase at the site of oxygen binding. As a result, sodium azide is a potent

cytochrome oxidase inhibitor, which is the last enzyme in the electron transport chain and is responsible for transferring electrons onto oxygen and forming water molecules[15]. The inhibition of this enzyme prevents the function of the electron transport chain and significantly reduces ATP production. Further, the toxicity of sodium azide is dosage dependent, in large part because of its competitive pattern of inhibition. As ATP is required for the formation and stabilization of F-actin, delivery of surpra-threshold sodium azide may limit F-actin in the cell and disturb migratory and cell adhesion processes associated with these filaments. It is important to note, however, that ATP is used in many processes throughout the cell, including key signalling cascades, and a reduction in its abundance can alter cellular dynamics in ways other than actin filament inhibition.

In order to observe the effect of sodium azide on dorsal vessel formation and heart development during embryogenesis, embryos were microinjected with 40pL of varying concentrations of NaN3. Cardioblast migration was then monitored over 30 minutes and migration velocity was measured at segment A4 (see FIG. 3. 8). All the concentrations were mixed with 50mM Rhodamine B (mixing ration of 4:1 of Sodium Azide and Rhodamine B) as a tracer to visualize the delivery process under fluorescent microscopy. The CB migration velocity in uninjected embryos was calculated for comparison with injected treatments as shown in FIG. 3. 8.

An ANOVA was performed, and a significant difference in mean CB migration velocity was obtained amongst the treatment groups at A4 (P <0.001). Subsequently, a T-test was performed for the mean velocities at A4, and injection with either 50mM or 100mM NaN3 (dissolved in saline) was shown to significantly ($p<0.001$) decrease migration velocity compared to uninjected embryos. Further, CB migration towards the midline was completely stopped in embryos injected with 100mM NaN3, showing a significant ($p<0.001$) difference compared to 50mM NaN3 injected groups, which maintained migration towards the midline. In the absence of any NaN3, injection of Rhodamine B dissolved in water did not alter CB migration velocity when compared to uninjected embryos. Further, no significant difference was observed between the 0.05mM, 5mM, 10mM NaN3, and uninjected embryos. Qualitatively, there was no change in the alignment

or morphology of the cardioblasts during development in any of the treatment groups (see FIG. 3. 9). Therefore, NaN3 was shown to reduce CB migration velocity at concentrations above 10mM in a dose-dependent manner.

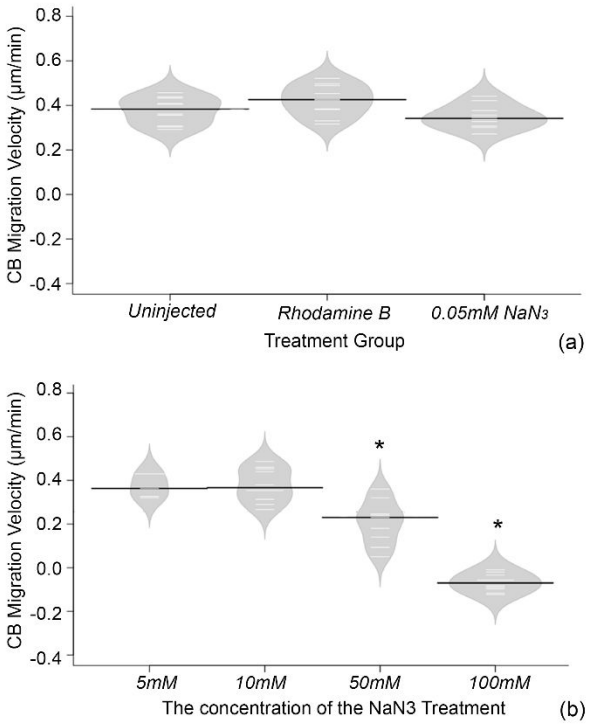

FIG. 3. 8: CB migration velocity is reduced in response to NaN3 in a dose-dependent manner. Mean CB migration velocities of stage 13/14 embryos injected with Rhodamine B or NaN3 dissolved in water (A), and embryos injected with NaN3 dissolved in saline (B). Injection with just Rhodamine B shows no difference in velocity compared to uninjected embryos. Embryos injected with 50mM NaN3 show a significantly ($p<0.001$) decreased CB migration velocity compared to uninjected embryos. Further, 100mM NaN3 injected embryos show a significantly ($p<0.001$) decreased velocity compared to 50mM NaN3, with a complete arrest of migration. Black horizontal lines represent mean values and the grey shaded area represents sample distribution.

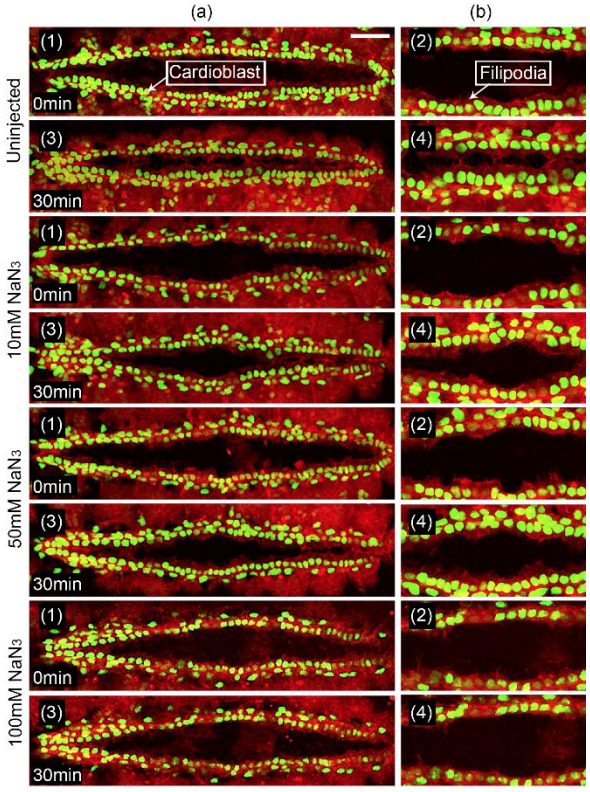

FIG. 3. 9: NaN3 is effective in disrupting dorsal vessel formation in a dose-dependent manner. Dorsal projections (enlarged in 2 and 4) of stage 13/14 embryos taken at 0 and 30 minutes, showing cardioblasts labeled with Tup-GFP (green) and actin network labelled with dMef-GAL4 regulated UAS-moesin-mCherry (red). Cardioblast migration velocity is reduced in embryos injected with 50mM NaN3 and completely stopped in embryos injected with 100mM NaN3. Filopodia numbers also decreased over time in both the 50 mM and 100 mM NaN3 injected embryos, Cardioblasts and filopodia are labelled on the figures of uninjected embryo (1 and 2).

Furthermore, in order to observe the effect of NaN3 on the leading edge during dorsal vessel formation, filopodia number was monitored over 30 minutes (segments A4-A2) in injected and uninjected embryos, and percentage change in filopodia number per segment was calculated (see FIG. 3. 10). A Mann-Whitney U test was performed for mean ranks, and embryos injected with either 50mM or 100mM NaN3 showed a significantly ($p<0.05$) greater reduction in the number of filopodia after 30 minutes compared to uninjected samples, decreasing by 29% in 50mM and by 38% in the 100mM injected groups. Injection with 10mM NaN3 did not show a significant difference compared to uninjected samples, and no significant difference was detected between the 50mM and 100mM NaN3 groups.

NaN3 was shown to significantly reduce filopodia number at concentrations above 10mM.

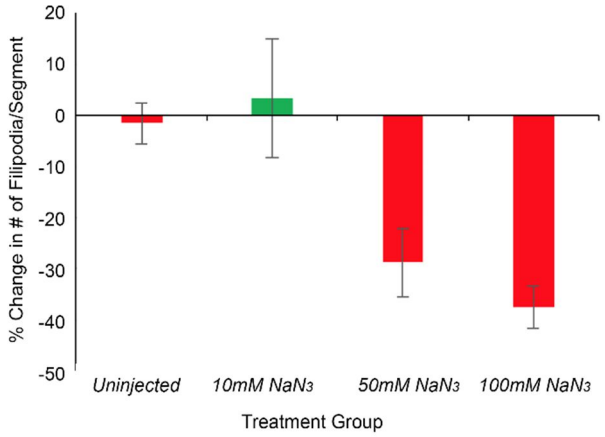

FIG. 3. 10: NaN3 decreases number of filopodia and leading edge activity over time (30 minutes). Change in the mean number of filopodia per segment across segments A4-A2 measured in embryos injected with varying concentrations of NaN3. Injection with 50mM and 100mM NaN3 results in a greater decrease ($p<0.05$) in number of filopodia per segment compared to uninjected (0mM) embryos. The error bar represent the standard deviation (SD) of the data in each group.

Overall, injection with NaN3 decreased the migration velocity of CBs and number of filopodia, disrupting dorsal vessel formation in a dose-dependent manner. As ATP is required for the formation of actin polymers, it is likely that the suspension of the electron transport chain via inhibition of cytochrome oxidase would depress overall actin polymerization and inhibit collective cell migration. Furthermore, sub-threshold (0.05mM, 5mM, 10mM NaN3) injected embryos and Rhodamine B (0mM NaN3) injected embryos showed comparable CB migration velocities to uninjected samples, indicating that the injection mechanism/apparatus itself is not responsible for the disruption observed in CB migration. It is important to note, however, that ATP is used in a variety of processes and a decrease in its abundance can disrupt many cellular functions. As a result, further experimentation using embryos that label the actin filaments of CBs is required to examine the effect of NaN3 on F-actin decrease[12].

3.3. Viability test

The effect of the needle insertion on the viability of embryos was investigated by testing the viability of n=20 embryos (collected from four sets (n=5) of embryos). This experiment was performed by loading the embryo into the chamber and inserting the microneedle 150µm into the embryo for 10s in order to mimic the injection process. Then, the embryos were unloaded from the chamber and placed on the agar plate to measure their viability. After 24hrs, the number of the embryos that successfully hatched to become first instar larva was counted for each set and the results was compared with the control samples, which were dechorionated, but not injected. The results (see FIG. 3. 11) shows that the number of the viable embryos, which moved from the embryo to the larval stage, were 80%. This indicated that the needle insertion reduced the viability from average of 18 viable embryos to 16, in compared to the control. However, this efficiency might be sufficient for various embryonic assays including microinjection assays.

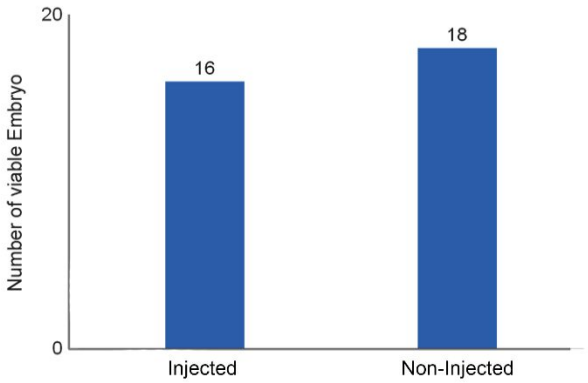

FIG. 3. 11: Viability test after needle insertion compared to not inserted control worms.

References

[1] Ghaemi, R., Tong, J., Selvaganapathy, P.R. and Gupta, B.P., "Microfluidic Device for Microinjection of *C. elegans*", The 17th International Conference on Miniaturized Systems for Chemistry and Life Sciences, μTAS 2013 Conference, Freiburg, Germany, 27-31 October 2013.

[2] Zhao, X., Xu, F., Tang, L., Du, W., Feng, X., Liu, B.F. (2013) Microfluidic chip-based *C. elegans* microinjection system for investigating cell-cell communication in vivo. Biosens. Bioelectron., 50, 28–34

[3] Noori, A., Selvaganapathy, P.R. and Wilson, J. (2009) Microinjection in a microfluidic format using flexible and compliant channels and electroosmotic dosage control., Lab on a Chip 9, 3202-3211.

[4] Delubac, D., et al. (2012) Microfluidic system with integrated microinjector for automated *Drosophila* embryo injection." Lab on a Chip, 12, 4911-4919.

[5] Bernstein, R.W., Scott, M., and Solgaard, O., "BioMEMS for high-throughput handling and microinjection of embryos." Photonics Asia 2004. International Society for Optics and Photonics, 2004.

[6] Zhang, X., et al. (2006) Microoptical characterization of piezoelectric vibratory microinjections in *Drosophila* embryos for genome-wide RNAi screen. Journal of microelectromechanical systems, 15, 277-286.

[7] Tao, Y., and Schulz, R.A.. "Heart development in *Drosophila*." Seminars in cell & developmental biology. Vol. 18. No. 1. Academic Press, 2007.

[8] Reed, B.H., Mcmillan, S.C. and Chaudhary, R. (2009). The Preparation of *Drosophila* Embryos for Live-Imaging Using the Hanging Drop Protocol. Journal of Visualized Experiments JoVE, (25). doi:10.3791/1206

[9] Markow, T.A., Beall, S., and Matzkin L.M.. (2009) Egg size, embryonic development time and ovoviviparity in *Drosophila* species. Journal of evolutionary biology, 22, 430-434.

[10] Vanderploeg, J., and Jacobs, J.R.. (2015) Talin is required to position and expand the luminal domain of the *Drosophila* heart tube. Developmental biology, 405, 189-201.

[11] Vanderploeg, J. and Jacobs, J.R. (2016). Mapping heart development in flies: Src42A acts non-autonomously to promote heart tube formation in *Drosophila*, Veterinary Sciences (in press).

[12] Raza, Q. and Jacobs, J.R. (2016). Guidance signaling regulates leading edge behavior during collective cell migration of cardiac cells in *Drosophila*. Developmental Biology 419:285-297.

[13] Lucas, E.P., et al. (2013) The Hippo pathway polarizes the actin cytoskeleton during collective migration of *Drosophila* border cells, The Journal of cell biology 201, 875-885.

[14] Chang, S., and Lamm, S.H. (2003) Human health effects of sodium azide exposure: a literature review and analysis. International journal of toxicology 22, 175-186.

[15] Stannard, J.N., and Horecker, B.L. (1948). The in vitro inhibition of cytochrome oxidase by azide and cyanide. Journal of Biological Chemistry, 172, 599-608.

Chapter 4

CHARACTERIZATION OF MICROFLUIDIC CLAMPS FOR IMMOBILIZING AND IMAGING OF *DROSOPHILA MELANOGASTER* LARVA'S CENTRAL NERVOUS SYSTEM

Complete citation:

Ghaemi, Reza, Pouya Rezai, Fatemeh Rafiei Nejad, and Ponnambalam Ravi Selvaganapathy. "*Characterization of microfluidic clamps for immobilizing and imaging of Drosophila melanogaster larva's central nervous system.*" Biomicrofluidics 11, no. 3 (2017): 034113.

Relative Contributions:

Ghaemi, R.: Performed all experiments, interpretation and analysis of the data and wrote the drafts of the manuscript including all figures and text.

Rezai, P.: Helped and consulted in the design chips and revised the final draft.

Rafiei Nejad, F.: Helped and assisted for data analysis.

1. Introduction

As a model organism, each developmental stage of the *Drosophila* has specific applications. The focus of the previous chapter was on a microfabricated device for microinjection of the *Drosophila* embryo. While, in the upcoming chapters, the microfluidics devices have been developed to address technical challenges involved in the larva assays. At the larval stage, *Drosophila* contains different types of sensory neurons, which are formed in a segmental arrangement (FIG. 4. 1). They allow the larvae to sense various environmental cues (e.g. mechanical, visual and chemical) and transmit signals to the central nervous system (CNS) to generate response signals for stereotypic motor behaviors [1]-[3]. This simple neural circuit is used for studying numerous developmental-genetic and neurobiological problems primarily through deploying surgical, histological, transgenic and behavioral methods [4], [5].

The larva is a mobile organism and is constantly moving and seeking food. However, in a variety of live imaging protocols, the larva should be completely immobilized. Additionally, the digging and burrowing behaviour exhibited by the larva even when it is physically held stationary makes the high-resolution neuroimaging study of the larva's CNS very challenging. This challenge is associated with the anterior structure of *Drosophila* that includes the cephalo-pharyngeal skeleton (CPS) and sets of skeletal muscles, which are segmentally connected to the body wall. The CPS is actuated by specialized muscles to cause digging into food substrates [6]. In order to perform *in* vivo imaging in *Drosophila*, the digging and burrowing movement has to be eliminated and the whole-larva body should be made completely stationary during the imaging.

Although conventional immobilization protocols, which use dissection or anaesthetic drugs [7] (chloroform, and isofluorane), efficiently stop the CPS motion, they also attenuate neural activities and affect animals' neurophysiological status. The larvae can also be attached to a substrate using an adhesive or glue in order to immobilize without anaesthetics. However, adhesive attachment is an irreversible method, which does not allow one to perform further behavioural or developmental studies on the mobile larva.

Ideally, immobilization has to be performed in a simple and reversible manner while still allowing sensory stimulus to affect the larva. Recently, miniaturized microfluidic devices have been developed for immobilization of microorganisms, and these devices could be used for this purpose.

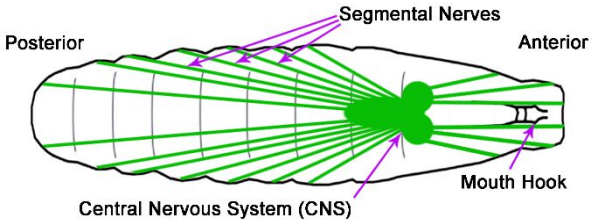

FIG. 4. 1: Schematic of a 3rd instar larva expressing GFP in all cholinergic neurons as driven by Cha-Gal4, UAS-GFP transgenes.

Microfluidic lab-on-chip devices are increasingly being used for studying model organisms such as *Caenorhabditis elegans* [8]-[10] and *Drosophila* [11]-[14]. These devices have the ability to automate immobilization of these small organisms and can be applied for *in vivo* visualization and tracking of cellular and physiological responses. Microfluidic-based immobilization techniques for *C. elegans* have been well developed using chemical (CO_2) or mechanical (tapering microchannels or encapsulation using deflectable PDMS membranes) approaches [15]-[19].

Furthermore, various microfluidic devices have also been developed for improving the throughput of the assays performed on embryo [20]-[27] such as microinjection [20]-[24], self-assembly of eggs and morphogenesis [25]-[26] and developmental studies [27]. However, very few devices have been developed for on-chip larval studies. Immobilization of *Drosophila* larvae is more complex than other small model organisms such as *C. elegans* due to the stronger forces that the larva is capable of generating. The strong forces are a result of the size and the number of muscles in the larva compared to *C. elegans*. In addition, the internal organs of the larva can loosely move inside its hemolymph-filled body cavity even if the outer body is completely immobilized by encapsulation. This makes the visualization of organs such as the CNS, brain and gut even more difficult. Moreover, the *Drosophila* larvae use a peristaltic type of motion as compared to other micro model

organisms such *C. elegans*, which also makes its immobilization more complex.

Recently, mechanical encapsulation [11], CO_2 anaesthetic exposure [12] and mechanical clamp [13] have been used to immobilize the body wall of the *Drosophila* larva in order to visualize the internal organ of interest such as CNS inside the body. They allow whole-larva body compression inside the chip so that neuronal transport processes [11], sensory neuron regeneration upon injury [12] and cardiac activities can be visualized. Mechanical encapsulation can efficiently reduce the larva's motion for a short period. However, it cannot allow one to capture high-resolution images of the internal organs such as CNS over long period. The CO_2 exposure combined with mechanical capsulation can increase the duration of the immobilization. However, the use of anaesthetic leads to spurious neurobehavioral responses and the use of encapsulation prevent the exposure of the larva to external sensory stimulus.

To address the abovementioned challenges associated with microfluidic-based *Drosophila* larva immobilization techniques, we recently developed a 3D mechanical clamp to immobilize the larva for imaging neurological response of *Drosophila* melanogaster to auditory stimulus [13]. However, a systematic study on immobilization of the *Drosophila* larva has not been performed. Here, a systematic analysis of various mechanical constrictions incorporated into microfluidic channels were conducted in order to optimize the process of rapid loading and mechanical immobilization of *Drosophila* larvae with proper orientation for CNS imaging. The immobilization designs were studied by quantitative imaging and movement assessment of the CNS through expression of genetically encoded Calcium sensor GCaMP5 [28]. The devices are engineered to first stop the larva's whole body locomotion and then immobilize the internal organs of interest such as CNS that may move due to ongoing motor movements and the resulting internal hemolymph displacements. The larva-lab-on-a-chip platform will also be useful for studying CNS responses to sensory cues including sound, chemosensory, light, and electric/magnetic fields.

2. Materials and methods

2.1 Animal preparation

Larvae of the genotype w, Cha-Gal4/CyO; UAS-GCaMP5/TM3, Sb were used for CNS activity imaging in response to external stimulations. In this protocol, hetereozygotes and homozygotes were not separated before testing. Expression of the GCaMP5 GECI was conducted using the Gal4/UAS system [29]. Through standard fly crosses, a stable fly stock was created containing two transgenes, namely: 1. Cha-Gal4 - A promoter sequence of CholineAcetyltransferase (Cha) driving the expression of the Gal4 transcription factor [30] and 2. UAS-GCaMP5 – a transgene contains the binding sites for the Gal4 transcription factor [28]. Thus, in the Cha-Gal4/CyO; UAS-GCaMP5/TM3 strain, all sensory and central neurons that express the CholineAcetyltransferase gene express the GCaMP5 calcium sensor. The GCaMP calcium sensor is circularly permuted protein containing the Green Fluorescent Protein (GFP), Calcium binding protein called Calmodulin, and the M13 (Calmodulin binding) peptide [31]. Influx of Ca^{2+} during neuronal activity triggers a conformational change of GCaMP so that solvent access to the chromophore is prevented and thus resulting in higher level of fluorescence [32]. GCaMP5 is a recently developed high signal-to-noise ratio calcium sensor [28]. This genotype was generated through a standard genetic crossing scheme. Larvae in the 3rd instar stage were isolated using a fine brush and washed with distilled water and dried on a tissue paper before loading into the chips.

2.2 Experimental setup

The experimental setup (FIG. 4. 2) consisted of four modules, i.e. pneumatic system, optical system, the microfluidic devices and image acquisition and processing software. The fluidic system, which was used to introduce the larva into the device and pressurize it during imaging, consisted of a pressurized air tank regulated at 400kPa pressure with a regulator (2000 series regulator, ARO, Ingersoll Rand, USA) and a solenoid valve

(S10MM-30-12-3, 3-way normally closed, Pneumadyne, Inc., USA). The optical system and digital camera (Flea3 FLs-U3-32S2C, Point Grey Research, Inc. Canada) were used to image and record the immobilization process. The dissecting microscope (S8 APO, Leica, Canada) with low magnification was used to image and record the loading of the larvae and the fluorescent microscope (Model 500 LumaScope, Etaluma, Inc, CA) with higher magnification (40x objective) was used to record the CNS motions in GFP mode. The image acquisition software (flyCapture2©, Etaluma© and Labview©) was used for image recording and data analysing. The microfluidic device was mounted on the dissection microscope to observe the animal loading and record the whole-larva body movement. A fluorescent microscope (Excitation 457-493nm; Emission 508-552nm) was used to record CNS movements.

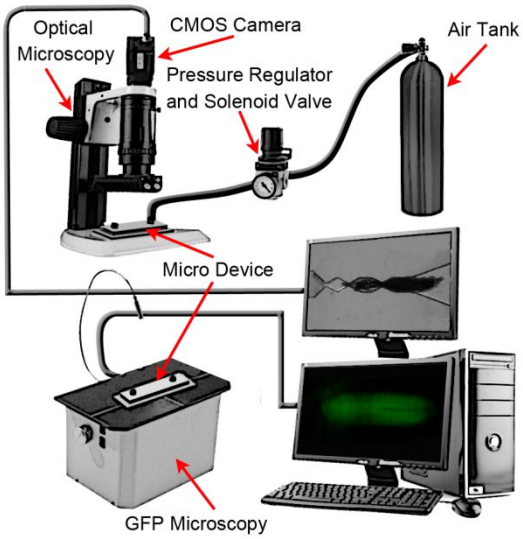

FIG. 4. 2: The experimental setup used for larva loading, sequential image recording and processing. The experimental setup consisted of four modules, i.e. fluidic unit (Air tank, pressure regulator and solenoid valve), optical system (Optical microscope, CMOS camera and GFP microscope), microfluidic devices (Micro device) and image acquisition software (ImageJ).

2.3 Device fabrication

The devices for immobilization of *Drosophila* larvae were fabricated by casting Polydimethylsiloxane (PDMS, Sylgard SYLGARD® 184, Dow Corning, USA) on 3D

printed master mold. First, the 3D mold was designed in Solidworks software and converted into a STL format. A 3D printer (Projet HD 3000 from 3D Systems, Material: VisiJet® EX200 Plastic) was used to print the design from the STL file in hard plastic part. Next, 1cm silicone tubes (3/16"ID x 5/16"OD, Cole-Parmer Canada Inc.) were placed on the reservoirs as the inlet/outlet. Subsequently, the uncured PDMS (10:1 ratio base:agent) was poured on the mold and then cured at room temperature for 24hr. Finally, the cured PDMS was peeled off and bonded to the glass slides (80s, 50W, plasma oxygen) to form a complete device.

2.4 Data acquisition and processing

Image sequences captured for each larva were quantified by Labview© software to measure the movement of the whole body and CNS movement during the time that larva tried to release itself from the trap. The RGB image sequences (2 f/s) for each video were converted to 8-bit grey scale images. Then, the pixel value of 255 was assigned for the larva's body or its CNS, while the background was adjusted to the pixel value of 0. Subsequently, the pixel centre of mass of both larva's body and its CNS were measured in the entire image stack and recorded.

3. Results and discussion

The *Drosophila* larva is highly mobile and its internal organs cannot be sharply imaged without complete immobilization. The locomotion of the larva follows a characteristic pattern which can be observed by tracking the larva's centre of the mass (CM) over time as shown in FIG. 4. 3. As described in section 2.4, the CM of the larvae was determined by recording an image sequence (0.2s intervals) of the larvae's locomotion inside a 2mm×2mm first. Next, the images were converted to a binary images with the larvae as white (255) and the background was black (0). Then, the CM of larva was calculated by finding the centre of the white region using ImageJ. The larva crawls using a repetitive cycle of motion called strides, where each stride is composed of two phases [2]. In the first phase called visceral pistoning movement, the head, tail and gut move slowly forward due

to the internal muscle contractions in the head and tail, while most of the abdominal segments remain firmly attached to the substrate. This results in the forward motion of the centre of mass of the larva as shown in FIG 3. In the second phase, the tail and head are attached to the substrate and the peristaltic motion of the body wall moves the abdominal segments in the direction of the crawling. The CM of the larva remains nearly stationary in this phase as shown in FIG. 4. 3. A suitable device that will immobilize the larva for imaging has to stop or interrupt this pistoning motion of the larva. Furthermore, the internal organs of interest such as the brain or the CNS capsule that need to be imaged are loosely attached to the outer body wall and are free to move inside the hemolymph-filled body cavity. Therefore, even if the outer body is completely immobilized by encapsulation, the contraction of internal muscles due to the digging and burrowing behaviour can induce hemolymph motion resulting in movement of the loosely held organs. Consequently, a desired immobilization system should be able to not only immobilize whole-larva body movements, but also inhibit the motion of internal organs such as CNS. In the rest of the paper, a set of microfluidic clamps for immobilizing and in-vivo imaging of *Drosophila* larva's internal organs such as CNS have been examined and characterized.

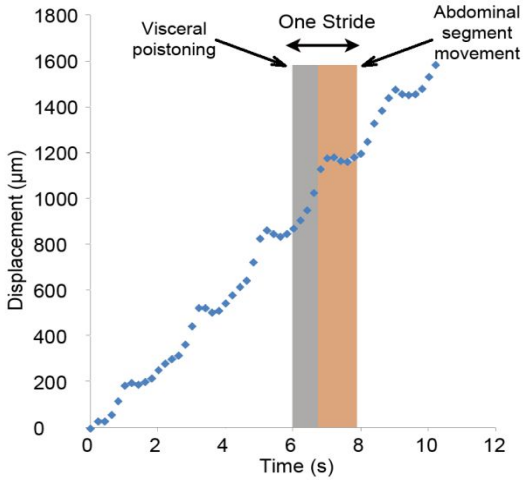

FIG. 4. 3: Linear periodic crawling of 3rd instar *Drosophila melanogaster* larva inside a channel. Crawling is composed of repetitive cycles of motion called strides. The strides can be divided into two phase: (i) movement of the center of mass and (ii) abdominal segment movement.

3.1 Narrowed channel immobilization

Imaging *Drosophila* larva is challenging due to the loose movement of the internal organs inside the hemolymph-filled body cavity even if the outer body is completely immobilized. Any immobilization mechanism should first be capable of inhibiting whole-larval body motion. The first design considered was a tapered (guide) channel with a constriction (narrow channel) at its end, which is similar to that used to immobilize *C. elegans* [16]. The design of the chip consisted of an inlet port for animal loading into the device ('inlet' in FIG. 4. 4a), a channel for transporting the animal towards the narrowed channel that was designed to immobilize the larvae for imaging and an outlet for ejecting the tested animal upon completion of each experiment. The inlet and narrowed channel were connected via guide channel. The gate at the end of the narrowed channel was designed such that it allows only the head of the larva to pass through the narrowed channel. The cross section of the tapered channel was 600×500 μm^2 (width×depth) at its wide end and reduced to 200×500 μm^2 at its narrow end. A further section of the channel with a uniform cross section of 200×500μm^2 and a length of 500μm forms the constriction gate (see the side view in FIG. 4. 4a). This dimension of the channel enable us to compress and flatten a 700μm×3mm (diameter×length) larva into the constriction gate for body immobilization and CNS imaging.

In order to test the design, a 3D printed master mold was fabricated and PDMS was cast and cured on top of it to form the channel structure as discussed in the Materials and Methods section. Then this structure was bonded with a glass slide (75mm×25mm) to form the complete device. *Drosophila* larvae (3rd instar) were washed from the food medium onto a petri dish with DI water. Next, by using a soft brush, a larva was picked from the dish and loaded into the chip at the inlet. The larva was pneumatically (0.2bar pressure pulse) moved to the guide channel near entrance region of the narrow channel as shown in FIG. 4. 4b-1.The pressure was removed to allow the larva orient and crawl voluntarily into the trap as shown in the sequence images in FIG. 4. 4b-2 to 4b-4. The voluntary movement allowed the head of the larva to orient forward and also ensured proper axial orientation for suitable imaging of the CNS. The self-orientation process usually took up to 30s, but

robustly created the desired orientations after immobilization. In rare cases, it was observed that the larvae attempted to exit from the inlet channel. After achieving the proper orientation, the animal was then pneumatically pushed further inside the trap using a 0.8bar continuous pressure which was stopped when the head of the larvae reached to the end of the trap (FIG. 4. 4b-5 and 4b-6) which completely immobilized the outer body of the animal.

After loading and immobilizing the 3rd instar larvae (n=10) inside the narrowed channel, image sequences (2 f/s) of the whole-larva body movements were recorded until they could release themselves from the trap. Then, the movement of the CM of the larvae (representing their locations) were calculated by using a custom-made image processing code in the LabVIEW© software. Using this data, the horizontal movement of the CM vs. time was plotted for all 10 larvae as shown in FIG. 4. 4c. The data reveals that the displacement of the CM from the original position increased over time for all larvae, which indicated that the larvae actively attempted to release themselves from the trap. This behaviour caused erratic back and forth motions of the CM of the larvae which would induce movement of the internal organs such as the CNS, making it difficult to obtain good images of this organ with the current design. The back and forth motion is similar to the digging and burrowing behaviour of the larva.

In order to quantify the ability of the immobilization mechanism to hold the larva in place for imaging purposes, the time that the larva was present in the field of view of a CNS imaging setup (FOV of ~1000×800 μm2 in 40x objective lens) was calculated. Such quantification is useful in comparison of the various immobilization schemes to identify the best performing ones. In a typical imaging setup for whole-CNS imaging, the proper field of view is ~1000×800 μm2 as the CNS is approximately 600μm long and 200μm wide. Therefore, a CM movement of more than 500μm in either direction was considered out-of-range and the time that this movement happened was designated as the release time. A total of ten 3rd instar larvae were analysed and their release times are plotted in FIG. 4. 4d.

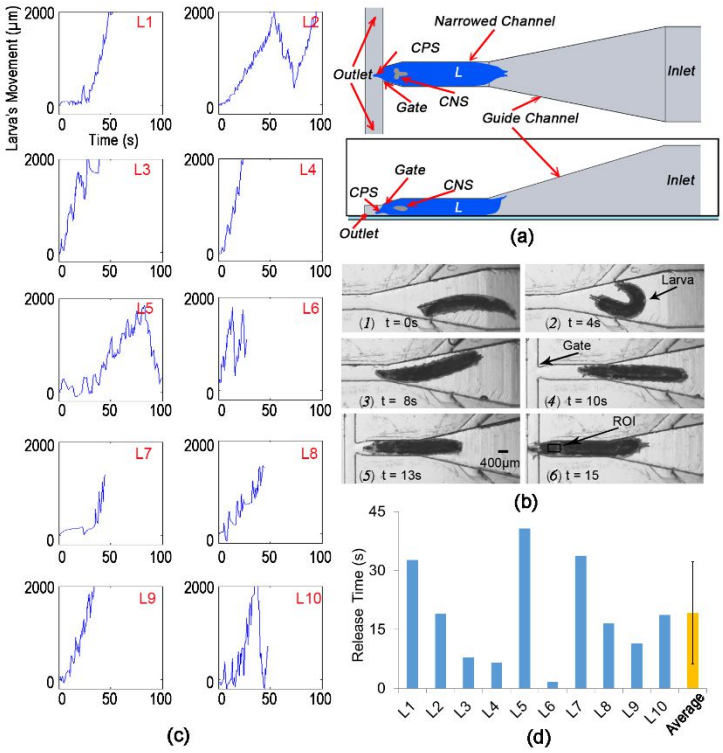

FIG. 4. 4: (a) Schematic design of the narrowed channel chip (not to scale) – top view (top image) and side view (bottom). (b) Steps to load a 3rd instar *Drosophila* larva using the narrowed channel chip. (1-4) larva swam freely into the trap, (5-6) larva was pneumatically moved into the trap and immobilized. (c)The movement of the center of mass (CM) for ten different larvae over time, inside the narrowed channel. (d) The release time of ten different 3rd instar larvae from the narrowed channel trap. By defining a threshold of 500 μm on the larva's CM displacement, the releasing time of each larva was calculated. In average, the narrowed channel was not able to immobilize the larvae more than ~20s. Scale bar=400 μm for all figures.

The results showed that the narrow channel was capable of immobilizing the body of the whole-larva for only 20s on an average. However, the required time for high resolution CNS imaging when the larva is exposed to external stimulus is usually more than 1 minute [13]. Therefore, the narrow channel design was found to be not suitable for whole-larva body immobilization for imaging purposes. An alternate design which could improve the whole body immobilization was required. Also, the longitudinal contraction of the abdominal muscle segments which was a critical mechanism in larva locomotion and

digging behaviour was found to be the crucial factor that facilitated the release of the larva from the trap. A modified configuration which could impede the segmental contraction, in addition to compressing its body, might be more suitable for immobilization.

3.2. 2D segmental pinning

Unlike *C .elegans,* which has rounded cylindrical body shape, *Drosophila* larva consists of mouth hook, two thoracic segments (T2, T3), seven abdominal segments (A1-7) and tail on its body. Muscle contraction patterns in abdominal segments cause a pistoning action that results in the *Drosophila* larva's forward and reverse crawling. The narrow channel immobilization approach demonstrated that disruption of this muscle contraction is critical if the larval body is to be immobilized. Therefore, the second device was designed in order to introduce segmental constrictions along the body designed to disrupt transmission of abdominal constriction along the body of the larva. Similar to the first chip, the second design consisted of an inlet port, inlet channel, a channel with 2D segmental pinning for immobilization, a gate to only allow the head to pass through it and an outlet for ejecting the tested animal (schematically shown in FIG. 4. 5a). The key design modification here was addition of three equispaced 2D protrusions to the narrowed channel that served as pinning points for the larva. The spacing between the protrusions were closely matched with abdominal segment lengths on the larva's body (indicated in FIG. 4. 5a). Therefore, when the larva was loaded into the trap, the segmental protrusions would latch into the larva's abdominal segments and potentially restrict larva's locomotion more efficiently.

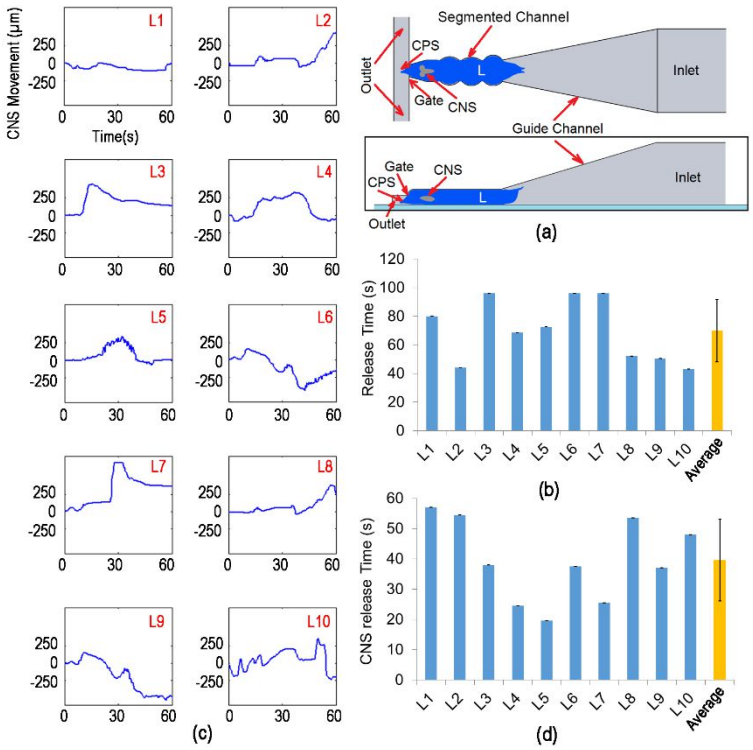

FIG. 4. 5: (a) Schematic design of the immobilization channel with 2D segmental pinning structure (not to scale) – top view (top image) and side view (bottom image). (b) The releasing time of ten different 3rd instar larvae from the 2D segmented channel. The segmented channel could improve the immobilization time from the average of ~20s (in narrowed channel) to ~70s. (c) The CM movement of the larva's CNS for 10 different larvae over time, inside the 2D segmented channel. (d) The CNS resealing time of ten different 3rd instar larvae from the narrowed channel with 2D segmental pinning structure. By defining a threshold of 200 μm on the larva's CNS displacement, the CNS releasing time of each larva was calculated. In average, the 2D segmented channel was not able to immobilize the larvae's CNS more than ~40s; while the whole-larva body was immobilized

Similar to the previous characterization on the narrowed channel (section 2.1), ten 3rd instar *Drosophila* larvae were loaded and immobilized into the segmented channel one at the time in order to characterize the device. Next, the image sequence (2 f/s) of whole-larva body was recorded until larva could release itself from the trap. Subsequently, the displacement of the larva's CM along the x-axis vs. time was calculated. Finally, the release

time of each larva was obtained as shown in FIG. 4. 5b.

The results indicate that the average immobilization time for segmented channel was ~70s, which is a significant improvement over the narrow channel design. This time is generally sufficient for typical stimuli responsive assays where the larva is exposed to a stimulus and the response of the neural system is recorded. However, it was also found that this immobilization design does not fully immobilize the CNS of the larva even though the outer body shell was immobilized. In order to characterize the movement of the CNS, ten 3rd instar larvae of the genotype ChaT-Gal4/CyO; UAS-GCaMP5G/TM3 (Bloomington 56500) that have genetically engineered calcium indicators of neural activity were immobilized in this chip and imaged under fluorescent microscope. The image sequence (2 f/s) of CNS was recorded until larva left the field of the view (700µm length and 500µm width). Next, the CNS movements of the larvae were calculated by using the custom-made image processing code on LabVIEW© software which is shown in FIG. 4. 5c.

The results show that even though the outer bodies of the larvae were immobilized, the CNS was capable of moving by ~ 250µm or more in some cases, which may be due to local muscle contractions. Although, the CNS movement was dampened by the segmental protrusions in comparison to narrowed channel, its movement is still significant to affect imaging of internal organs. In order to quantify the immobilization for CNS imaging, the release time was obtained when the displacement of CNS was greater than 200µm from its original location. The results plotted in FIG. 4. 5d showed that the narrowed channel with 2D segmental pinning was able to immobilize the CNS for only ~40s. Therefore, compared to narrow channel, the 2D segmented channel allowed us to immobilize whole-larva body more effectively by using the indented segments in the trap. Those protrusions could latch the muscle abdominal segments and consequently improve the larva immobilization. However, this design was still not able to completely immobilize the CNS for more than 40s.

3.3. 3D segmental pinning

The previous design using 2D segmental protrusions in the narrow channels provided an effective way to immobilize the body of the larva sufficiently for imaging. However, due to the digging and burrowing behaviour exhibited by the larva, the internal organs such as the CNS capsule, heart and gut could freely move inside the hemolymph-filled body cavity, regardless of the outer body immobilization. Therefore, a new design that incorporates 3D segmental protrusions was developed to further curtail the borrowing or digging induced motion thereby preventing the movements of internal organs inside the larva for longer period, which was the ultimate goal of the immobilization device. The 3D segmental pinning design (schematically shown in FIG. 4. 6a-b) consisted of an inlet port for animal loading into the device, a channel for transporting the animal towards the narrowed trap that was designed to immobilize the larvae for imaging and an outlet for ejecting the tested animal upon completion of each experiment. The trap consisted of a narrowed channel (770×700 μm2 cross-section with 500 μm length), primary (200μm width and 450μm depth) and secondary gates (100μm width and 425μm depth) as well as a stopper (100μm width and 100μm depth). The size of a 3rd instar larva is approximately 1mm × 3.5mm (diameter × length), which indicated that larva's body was compressed from ~1mm diameter to ~0.7mm (30%) by loading into this trap. The primary and secondary gates were designed to pin the 3rd instar larvae at two locations on its body while the rest of it was encapsulated in the narrowed channel. The dimension of the secondary gate was designed such that only the nose region of the immobilized 3rd instar larva could protrude through the gate. This stopper was used to prevent the larvae from escaping the trap when a small pressure (0.3bar) was sustained on the posterior side for complete immobilization.

Similar to the previous characterization on the narrowed channel and 2D segmental pinning (section 2.1 and 2.2), ten 3rd instar *Drosophila* larvae were loaded into the 3D segmental pinning chip and immobilized one at the time in order to characterize the device. Next, the image sequence (2 f/s) of whole-larva body was recorded for 350s. The image processing showed that the whole body motion of larvae was almost non-existent which indicated that the chip was able to completely immobilize the larvae during the imaging

process.

In order to study the movement of the CNS, when the larva is immobilized inside the 3D segmental pinning chip, ten 3rd instar larvae were immobilized in this chip and imaged under fluorescent microscope. Next, the image sequence (2 f/s) of the CNS was recorded for 350s and the CNS movements were calculated by using the custom-made image processing code on LabVIEW© software. The longitudinal motions of the CNS were plotted in FIG. 4. 6c. The results indicated that the device could keep the CNS completely inside the field of view (700 *x* 500μm2). Nevertheless, the CNS had minor forward or backward movements inside the field of view. The upper and lower lines (blue) in the graph represent the standard deviation of the data points obtained from the 10 larvae tested. The black line shows the average CNS motion for the larvae, the fluctuation of which is under 10 μm over 350s. The larvae were unloaded for further analysis such as viability test and behavioural studies. To unload the larva, a Tygon tube was connected from the inlet to a Petri dish. Then, a 2bar pressure pulse with duration of 1s was applied from the outlet to the inlet. This process was suitable to release the larvae from the trap and wash them out from the device to a petri dish.

In comparison to the narrowed channel and 2D segmental pinning design, the 3D segmental pinning design significantly improved the whole-larva body immobilization. In addition, the 3D pinning design was successfully able to restrict the motion of the CNS to 10±30μm over 350s which is a first for live un-anaesthetised imaging of these animals. It is important to note that this movement is ~10% of the CNS movement when the larva is glued onto a substrate – a method that is commonly used. It also uses only mechanical ad completely reversible means for immobilization. A possible explanation for such robust immobilization could be that the design of primary and the secondary gates efficiently prevented the wave of muscle contraction from building up which prevented any motion of the internal organs. As a result, the 3D segmental pinning design allowed us to successfully immobilize *Drosophila* larva with minimal internal CNS movements for its subsequent live neuronal imaging under various external stimulations.

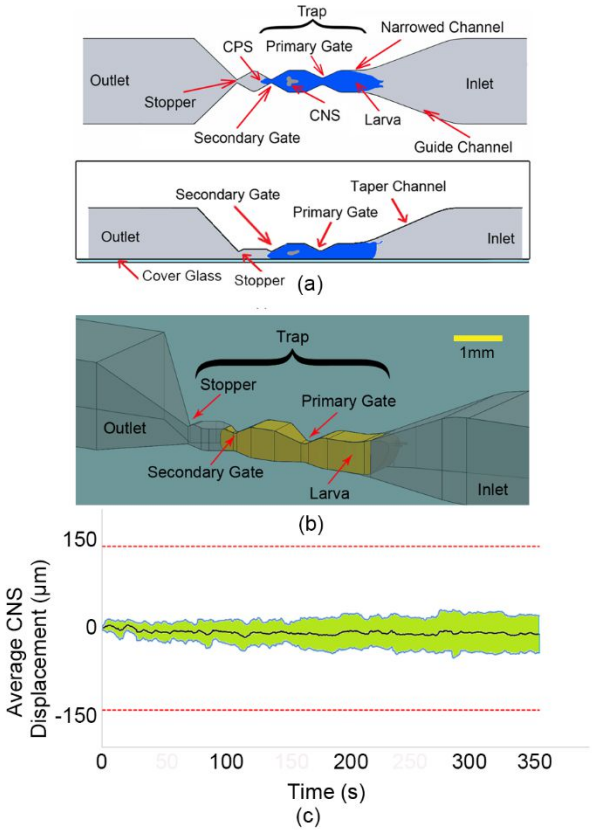

FIG. 4. 6: (a-b) Schematic design of the 3D segmental pinning chip – top view (top image) and side view (bottom). (c) The CM movement of the larva's CNS for 10 different larvae over time, inside the 3D segmental pinning chip. The black line shows the average CNS movement of 10 larvae, while the two blue lines indicate the standard deviation for each average data point.

Although, the various immobilization designs described in this paper could either partially or completely immobilize both internal and external movement of the larvae, such a confinement may affect their viability due to the high mechanical stress on the body [3]. In order to study the impact of mechanical stress caused by immobilization mechanisms on the viability of the larvae, a set of experiments was performed. A total of forty five 3rd instar larvae were picked from their food vial, washed with DI water one at a time, and prepared as described in section 2.1. Next, the larvae were loaded into the microfluidic devices (15 larvae for each design) using the loading method described in section 3.1. The larvae were kept in the channel until they could release themselves from the immobilization

channel. The total time that the larvae were immobilized and were kept inside the loading channel was 350s. In the case of larvae loaded into the 3D segmental pinning chip, they were taken off from trap after 350s, by applying a 2bar pressure pulse with duration of 1s from the outlet to the inlet. Subsequently, the unloaded larvae were transferred into the food media (one food well per chip) to study the viability of the larvae. In order to compare the result with a control sample, 15 fresh larvae were placed into the DI water bath for 350s and then transferred into the food media. The viability test was repeated for three times and the results are shown in FIG. 4. 7. The viability study of the larvae after 7 days indicated that the narrow channel and 2D segmental pinning chip did not have a significant effect on the viability of the larvae in comparison with the control. However, the viability of the larvae loaded into the 3D segmental pinning chip was ~40% lower and statistically significant ($p<0.005$) from the control group as shown in FIG. 4. 7. This reduction in viability might be due to two potential reasons. One reason is that the 3D segmental pinning design induced higher mechanical stress on the larvae due to the 3D mechanical pins. The other reason could be because of the unloading mechanism. The larvae could release themselves from the traps inside the narrow channel and 2D segmental pinning design. However, 2bar pressure was required to unload the larvae from the trap in the 3D segmental pinning design, which caused higher mechanical stress on the larvae.

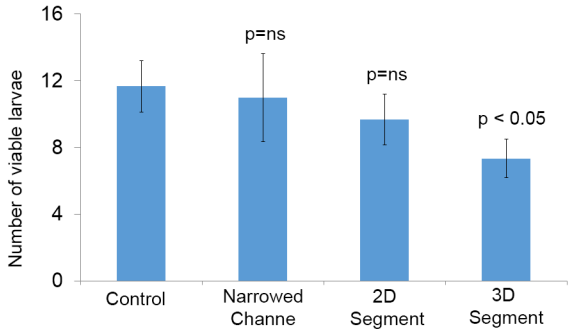

FIG. 4. 7: The viability test of the larvae loaded into the microfluidics devices. The impact of the 3D segmental pinning chip on the viability if the larvae is more significant compared to other narrowed channel and segmented channel design.

3.4. Comparison with other immobilization methods

Currently, dissection, anesthetization and gluing are three common methods for the immobilization of the *Drosophila* larvae. The first two methods could significantly affect the neuronal response of the larvae. The dissection of the larvae could allow one to firmly immobilize the larva and remove undesired organs from the larva's body for capturing a clear image form the organ of interest. However, it is associated with a large amount of damage to the tissues, axons and neurons. Therefore, it could not be used for live imaging and neuronal studies of the larva, while the larva is exposed to external stimulation. Furthermore, once dissected there is a limited time window for an assay before the responses degrade. Alternatively, anaesthesia such as ether and chloroform can be used to immobilize the larva. Although this technique is effective and keeps the larva intact, the use of anaesthesia will significantly affect and could alter the functioning of the neuronal response.

Gluing of the larva on to a substrate is another widely used method that could be used for imaging the neuronal response of the larva. Tissue glue and double side tape are two common adhesives used. In order to compare the performance of the immobilization designs described in this paper with the gluing technique, a number of larvae (n=10) were glued to glass substrates using tissue glue (Nexcare™ Skin Crack Care, Catalog Number 112, UPC 00051131861015) as shown in FIG. 4. 8a. Then, displacement of larvae's whole body and the CNS have been recorded and were compared (see FIG. 4. 8b) to the three microfluidic immobilization designs that were investigated in this paper. The results showed that the whole body of the larvae could be immobilized completely with almost non-existent net displacement by gluing. Additionally, the CNS of the larvae glued to the substrate stayed within the field of the view; however, the CNS had significant motion with an average range of approximately 300μm. Although, the 2D segmental pinning design could more effectively immobilized the CNS in compared to the narrowed channel, the duration of the immobilization (~40s) would not be enough for many in vivo assays[13]. In contrast, 3D segmental pinning design could strongly immobilize the whole body movement and keep the CNS inside the field of view with average range of motion of only

40μm.

In order to achieve high quality images of the internal organs over long periods of time, their complete immobilization is essential. Although, the gluing method could immobilize the body wall and keep the desired organ in the defined field of view, this might not be sufficient for capturing high resolution images of the internal organs such as CNS. The image sequences of the larvae's CNS, when they were glued to the substrate showed a large number of random pistonic motion. These motions could significantly reduce the resolution of the images. The time sequence images of the CNS for the gluing technique and 3D segmental pinning chip have been shown in the FIG. 4. 8c. To compare the performance of the 3D segmental pinning chip and gluing technique on the range of the larvae's CNS motion, the location of the CNS (its centre of mass) have been recorded in the 1100μm *x* 700μm field of the view, while they were immobilized in the 3D segmental pinning chip or glued to the substrate. Next, the average and the standard deviation of the CNS location in the x-axis have been calculated. Since the larvae could not release themselves from both 3D segmental pinning chip or glue, their CNS experience only a random pistonic motion in the field of view, which resulted in almost non-existant motion in both methods. However, the range of larvae's CNS motion in the 3D segmental pinning chip was significantly smaller than the gluing technique. This was determined by comparing the standard deviation of the CNS motion along the x-axis as shown in the FIG. 4. 8d for the number of 10 larvae. Consequently, only the 3D segmental pinning chip was effective and completely immobilized the CNS of the *Drosophila* larvae for high resolution imaging, with minimum tissue damage (compared to dissection techniques and gluing if they want to be used for further study and viability assays) and neuronal effects (compared to both dissection and anesthetize techniques) on the larvae. Additionally, the microfluidic based design could potentially allow one to apply this technique for various high throughput live imaging protocols, while the larvae could be exposed to various external stimulates such as sound, chemical, light and electrical fields.

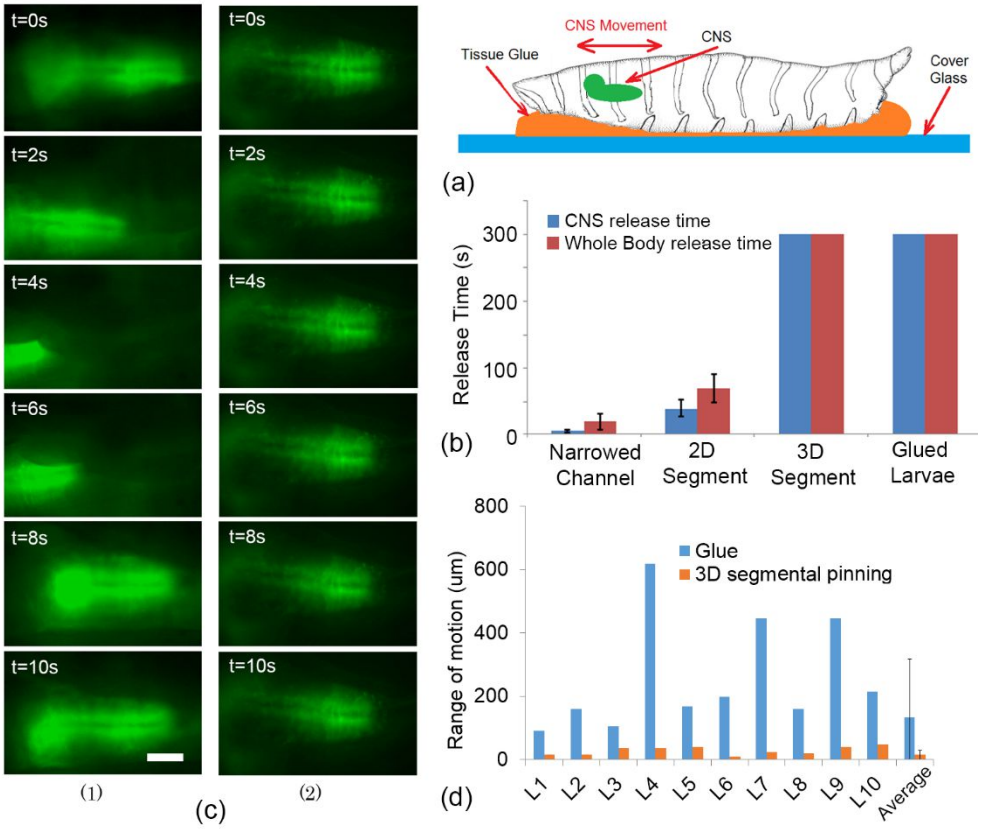

FIG. 4. 8: (a) Schematic of the larva immobilization using tissue glue. A droplet of tissue glue has been placed on a cover glass and the larva was placed on the droplet. After a few minutes, the larva will be glued to the substrate. (b) A comparison of the whole body releasing time and CNS releasing time for three microfluidics chips and the gluing technique. The results were compared over 300s of larvae (n=10) immobilization. (c) The time sequences images (10s) of the larvae's CNS, when they were immobilized by using (1) gluing technique and (2) 3D segmental pinning chip. The CNS experienced a large number of the random Forward/Backward motions, which reduced the resolution of the images in some farms significantly. Scale bar 100µm. (d) The domain of the pistonic CNS's motion for 10 larvae that were immobilized by tissue glue and the 3D segmental pinning chip. The image sequence of the CNSs have been capture in an 1100µm *x* 700µm field of view. In average, the domain of the CNS motion, when the larvae were immobilized by gluing technique, was significantly large. This could lead to different challenges for catering high-resolutiontime-lapse images of the CNS.

References

[1] S. Tickoo and S. Russell, *Current Opinion in Pharmacology*, 2002, **2**, 555-560.

[2] E. S. Heckscher, S. R. Lockery, and C. Q. Doe1, The Journal of Neuroscience, 2012, **32**(36), 12460 – 12471.

[3] E. Bier, *Nature Reviews Genetics*, 2005, **6**, 9-23.

[4] J. B. Duffy, *Genesis*, 2002, **34**, 1-15.

[5] H. Kohsaka, S. Okusawa, Y. Itakura, A. Fushiki and A. Nose, *Dev Growth Differ*, 2012, **54**, 408-419.

[6] A. Schoofs, S. Niederegger, A. van Ooyen, H. Heinzel and R. Spiess, *J. Insect Physiol*, 2010, **56**, 695-705.

[7] S. Mondal, S. Ahlawat and S. P. Koushika, *J Vis Exp*, 2012.

[8] P. Rezai, S. Salam, P. Selvaganapathy and B. P. Gupta, in *Integrated Microsystems*, ed. K. Iniewski, CRC Press, 2011, pp. 581-608.

[9] S. E. Hulme and G. M. Whitesides, *Angew Chem Int Ed Engl*, 2011, **50**, 4774-4807.

[10] Rezai, P., Siddiqui, A., Selvaganapathy, P. R., & Gupta, B. P. (2010). Lab on a Chip, 10(2), 220-226.

[11] S. Mondal, S. Ahlawat, K. Rau, V. Venkataraman and S. P. Koushika, *Traffic*, 2011, **12**, 372-385.

[12] M. Ghannad-Rezaie, X. Wang, B. Mishra, C. Collins and N. Chronis, *PLoS One*, 2012, **7**, e29869.

[13] Ghaemi, R., Rezai, P., Iyengar, B. G., & Selvaganapathy, P. R. (2015).. Lab on a Chip, 15(4), 1116-1122.

[14] Ardeshiri, R., et al. "Cardiac screening of intact *Drosophila* melanogaster larvae under exposure to aqueous and gaseous toxins in a microfluidic device." RSC Advances 6.70 (2016): 65714-65724.

[15] T. V. Chokshi, A. Ben-Yakar and N. Chronis, *Lab Chip*, 2009, **9**, 151-157.

[16] S. E. Hulme, S. S. Shevkoplyas, J. Apfeld, W. Fontana and G. M. Whitesides, *Lab Chip*, 2007, **7**, 1515–1523.

[17] K. Chung, M. M. Crane and H. Lu, *Nat Methods*, 2008, **5**, 637-643.

[18] C. L. Gilleland, C. B. Rohde, F. Zeng and M. F. Yanik, *Nat Protoc*, 2010, **5**, 1888-1902.

[19] F. Zeng, C. B. Rohde and M. F. Yanik, *Lab Chip*, 2008, **8**, 653-656.

[20] J. R. Fakhoury, J. C. Sisson and X. J. Zhang, *Microfluidics and Nanofluidics*, 2009, **6**, 299-313.

[21] S. Zappe, M. Fish, M. P. Scott and O. Solgaard, *Lab Chip*, 2006, **6**, 1012-1019.

[22] Zhang, X.; Scott, M. P.; Quate, C. F.; Solgaard, O. Microoptical characterization of piezoelectric vibratory microinjections in *Drosophila* embryos for genome-wide RNAi screen. Microelectromechanical Systems, Journal of, 2006, 15(2), 277-286.

[23] Delubac, D.; Highley, C. B.; Witzberger-Krajcovic, M.; Ayoob, J. C.; Furbee, E. C.; Minden, J. S.; Zappe, S. Microfluidic system with integrated microinjector for automated *Drosophila* embryo injection. Lab on a Chip, 2012, 12(22), 4911-4919.

[24] Ghaemi, R.; Selvaganapathy, P. R.. In: International Conference on Miniaturized Systems for Chemistry and Life Sciences: A microfluidic microinjection of *Drosophila* embryo in a format using compliant mechanism and electrokinetic dosage control ", 19th International Conference on Miniaturized Systems for Chemistry and Life Sciences October 25-29, Gyeongju, KOREA

[25] G. T. Dagani, K. Monzo, J. R. Fakhoury, C. C. Chen, J. C. Sisson and X. Zhang, *Biomed Microdevices*, 2007, **9**, 681-694.

[26] T. J. Levario, M. Zhan, B. Lim, S. Y. Shvartsman and H. Lu, *Nat Protoc*, 2013, **8**, 721-736.

[27] E. M. Lucchetta, M. S. Munson and R. F. Ismagilov, *Lab Chip*, 2006, **6**, 185-190.

[28] J. Akerboom, T. W. Chen, T. J. Wardill, L. Tian, J. S. Marvin, S. Mutlu, N. C. Calderon, F. Esposti, B. G. Borghuis, X. R. Sun, A. Gordus, M. B. Orger, R. Portugues, F. Engert, J. J. Macklin, A. Filosa, A. Aggarwal, R. A. Kerr, R. Takagi, S. Kracun, E. Shigetomi, B. S. Khakh, H. Baier, L. Lagnado, S. S. Wang, C. I. Bargmann, B. E. Kimmel, V. Jayaraman, K. Svoboda, D. S. Kim, E. R. Schreiter and L. L. Looger, *J Neurosci*, 2012, **32**, 13819-13840.

[29] A. H. Brand and N. Perrimon, *Developmen,* 1993, **118** (2), 401-415.

[30] P. M. Salvaterra, T. Kitamoto, *Gene expression patterns*, 2001, **1**(1), 73-82

[31] J. Nakai, M. Ohkura and K. Imoto, *Nat. Biotechno,* 2001, **19** (2): 137-41

[32] J. Akerboom, J. D, Rivera, M. M. Guilbe, E. C. Malavé, H. H. Hernandez, L. Tian, S. Hires, J. S. Marvin, L. L. Looger and E. R. Schreite, *J. Biol. Chem,* 2009, **284** (10), 6455–6464

Chapter 5

MICROFLUIDIC DEVICES FOR IMAGING NEUROLOGICAL RESPONSE OF DROSOPHILA MELANOGASTER LARVA TO AUDITORY STIMULUS.

Complete citation:

Ghaemi, Reza, Pouya Rezai, Balaji G. Iyengar, and Ponnambalam Ravi Selvaganapathy. "*Microfluidic devices for imaging neurological response of Drosophila melanogaster larva to auditory stimulus*." Lab on a Chip 15, no. 4 (2015): 1116-1122.

Relative Contributions:

Ghaemi, R.: Performed all experiments, interpretation and analysis of the data and wrote the drafts of the manuscript including all figures and text.
Rezai, P.: Helped in the design, assisted for performing the auditory experiments and revised the final draft.
Iyengar,B.G.: Designed the FlexiChip, assisted for performing the auditory experiments and revised the final draft.

1. Introduction

Very recently, behavioral responses of Drosophila larva in reaction to mechanical stimuli (vibration and sound) have been studied [1]-[2]. Zhang et al. [1] used Ca^{2+} imaging and electrophysiological methods and found that Drosophila larvae's Cho and class IV DA neurons responded optimally to sound waves at 500Hz frequency. In these studies, the immobilization for Ca^{2+} imaging was achieved by compressing the larvae (in saline) between coverslips. This is a manual process and the degree of compression, the access of the larva to the external stimuli as well as the orientation of the animal are all variable and dependent on the operator. It is also conceivable that the overt whole-body mechanical compression could be disruptive for the full-range of endogenous sensory-motor activities to take place. To address this problem, the microfluidics immobilization mechanisms developed in the previous chapter could be used. Therefore in this chapter, two lab-on-chip designs that standardize the immobilization of the larva while still allowing access to external stimuli were demonstrated and for the first time, an on-chip study of *Drosophila* larva's CNS activity evoked by acoustic signals was conducted. Use of acoustic signals enabled fast, automated, remote and tunable stimulation of specimens. Specifically these responses were investigated fluorescently at the ventral cord of the CNS, an anatomical structure where a large majority of sensory afferents synapse with interneurons. A new genetically encoded Calcium sensor GCaMP5 [3] was expressed in all sensory and cholinergic interneurons. The devices are engineered to stabilize the CNS specifically from ongoing motor movements and the resulting internal hemolymph displacements. It was demonstrated that localized anchoring of the larval CPS permits functional imaging of CNS in response to auditory stimuli. Our larval-lab-on-a-chip platforms will also be useful for studying CNS responses to other sensory cues (light, chemosensory, tactile, electric/magnetic fields).

2. Methods

The neurological response of Drosophila larvae to auditory stimuli was studied using two different lab-on-chip designs. Device design and fabrication, experimental procedures, data acquisition and processing as well as animal preparation are described in this section.

2.1. Design of the Microfluidic chips

Drosophila larva's burrowing and locomotory behaviors make the CNS capsule move inside the hemolymph-filled body cavity because it is loosely anchored (FIG. 5.1). In order to immobilize the CNS of the larva and to subsequently study their neurological responses to auditory stimulus, the two chips, named the pneumatic chip and the FlexiChip were designed.

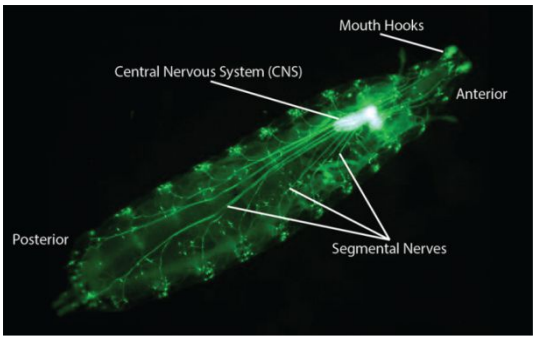

FIG. 5. 1. An epifluorescent image of a 3rd instar larva expressing GFP in all cholinergic neurons as driven by Cha-Gal4, UAS-GFP transgenes. The Central Nervous System (CNS) zone is indicated, its neuronal activity was monitored by expressing a UAS-GCaMP5 transgene.

2.1.1. Pneumatic chip

The Pneumatic chip was designed for automated loading, immobilization, testing and unloading the animals. The first chip (schematically shown in FIG. 5. 2) consisted of an inlet port for animal loading into the device, a channel (inlet in FIG. 5. 2) for transporting the animal towards the tapered trap that was designed to immobilize the larvae for imaging and an outlet for ejecting the tested animal upon completion of each experiment. The trap consisted of a narrowed channel (770×700 μm^2 cross-section with 500 µm length), primary (200µm width and 450µm depth) and secondary gates (100µm width and 425µm depth)

and a stopper (100µm width and 100µm depth). The primary and secondary gates were designed to pin the 3rd instar larvae at two locations on its body while the rest of it was encapsulated in the narrowed channel. We found that without the two-point pinning, the CNS could move longitudinally inside the body despite the complete encapsulation of the larval body in the trap, thereby compromising clear imaging of the neuronal activities in the CNS. The dimension of the secondary gate was designed such that only the nose region of the immobilized 3rd instar larva could protrude through the gate. This gate was used to prevent the larvae from escaping the trap when a small sustained pressure was used on the posterior side for complete immobilization (see section 2.4.1).

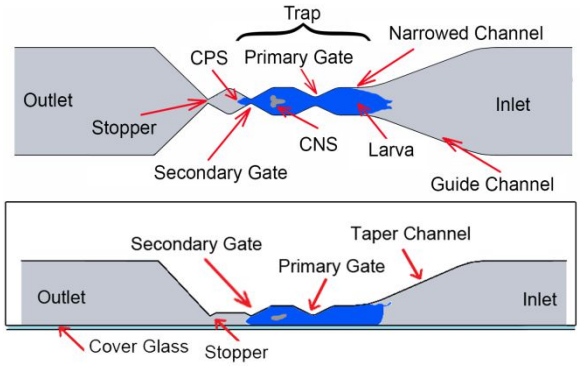

FIG. 5. 2: Schematic design of the pneumatic chip (not to scale). The inlet channel was 25 mm long, 3 mm wide and 2 mm deep with an inlet port for animal loading located at its end. The outlet channel was 8 mm long, 3 mm wide 2 mm deep for ejection of tested animals.

2.1.2. FlexiChip

In order to study the influence of the device design on the auditory response of the larvae, another chip (FlexiChip) with different mechanical and acoustic properties that facilitated manual animal loading was used. Schematic of the FlexiChip (FIG. 5. 3) summarizes its basic design and operation. The key features of the FlexiChip were a main channel that fits the 3rd instar larva (similar to the pneumatic chip) and a clasping mechanism (clip) that was designed into the PDMS substrate so as to clamp the head of the larvae (FIG. 5. 3). Both features are included into the 3D printed mold. The clip mechanism opens when the PDMS is flexed and closes shut when the flexion is removed. The clip-gate also contains a 100 µm diameter glass wire on the top to create an enclosed hole or a burrow-like opening that

encourages the larva to enter it, the glass wire also stabilized the anchoring upon clip closure. The auxiliary channels are available to keep the preparation moistened, or for the introduction of electrical or mechanical probes for body-wall stimulation. Arrowhead in FIG. 5. 3 indicates the approximate location of the CNS ventral cord (VC) that resides just below the ventral body-wall of the larva so that live-imaging could be carried out, often with almost no extraneous tissue obstruction. FlexiChip allowed the larva to continue breathing while being subjected to various types of sensory stimulations.

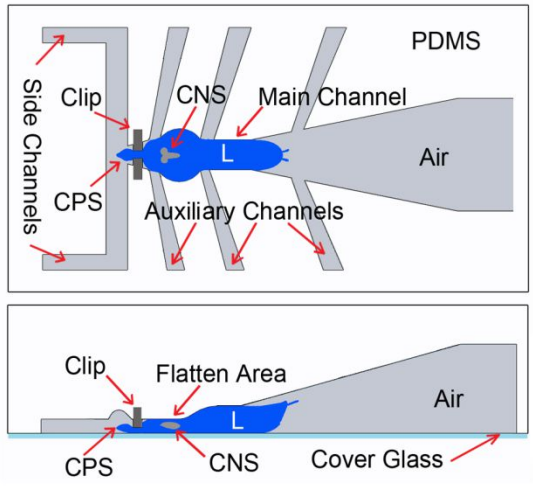

FIG. 5. 3: Schematic design of the FlexiChip (not to scale)

2.2. Device fabrication

Devices were fabricated by 3D printing of two plastic master molds that dimensionally corresponded to the design discussed in section 2.1 for the pneumatic chip and the FlexiChip. Following master mold fabrication, soft lithography [4] was used for conventional PDMS (10:1 ratio base:agent, Sylgard SYLGARD® 184) casting, curing (70C, 2hr), bonding to glass slides (80s, 50W, plasma oxygen) and installation of inlet/outlet tubes (for pneumatic chip, Silicone Tubing, 3/16"ID x 5/16"OD, Cole-Parmer Canada Inc.). The glass wire in the FlexiChip was placed into the 3D mold at the location of the clip before casting the PDMS into the mold.

2.3. Experimental setup

The experimental setup (FIG. 5. 4) consisted of a sound-insulated box (custom made to isolate environmental noises using acoustic sound damping foam UL 94, Parts-Express, USA), an acoustic signal generation system (function generator (AFG3022B, Tektronix, CA), amplifier (RAMSA WO-1200, Panasonic, CA) and speaker (Eminence Beta-12CX coaxial 12", Parts-express, USA)), an optical/fluorescent imaging system (Lumascope 500, Single color 488nm Ex. Fluorescence, 40x magnification, Etaluma, CA), the microfluidic device and a software control system (LabVIEW© , flyCapture2© and Imagej© software).

The function generator connected to the amplifier was controlled through a custom LabVIEW© code and was used to generate the desired pure-tone sinusoidal voltage signal inputs to the speaker. The speaker was installed on the roof of the sound insulating box. Various voltage frequency and intensity levels were generated and amplified to the speaker and the corresponding sound frequency (50-5000Hz) and intensity (95-115dB) produced in the box were measured using a mini sound level meter (DT-85A, CEM) This was done to calibrate the speaker and the sound insulating box. Frequency ranges were selected to cover the hearing range of response of *Drosophila* [1] and intensity levels were selected using preliminary experiments that produced a response in the CNS.

The microscope was positioned inside the box right beneath the speaker with a 15cm distance between its focal plane and the speaker. The microscope was controlled by software and used in the optical mode for loading the animal and in the fluorescent mode for imaging GCaMP5 activities in the CNS of an immobilized larva.

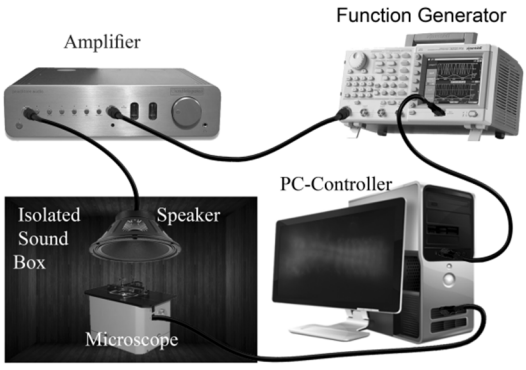

FIG. 5. 4: Experimental Setup used to examine the auditory response of Drosophila larvae. Insulation sound box with internal walls covered with sound damping foams was used to accommodate the microscope right underneath the speaker. The speaker was connected to a function generator (FG) through an amplifier for sound actuation (sinusoidal voltage output from FG). Both the microscope and the FG were connected to a PC for automated control of image acquisition and signal generation (frequency and peak-peak voltage) respectively.

2.4. Animal loading

2.4.1. Pneumatic chip

Drosophila larva (3rd instar) was picked from the food medium using a soft brush, washed with DI water and loaded into the chip at the inlet. Then, the larva was pneumatically inserted into the entrance region of the trap (FIG. 5.5a) in 10s via the inlet channel. The larvae often oriented themselves and crawled voluntarily with no external pressure half-way into the trap up to the primary gate (FIG. 5.5b-d) which helped in proper orientation and imaging of the CNS. This could take up to 30s but robustly produced desired orientations after immobilization. The animal was then pneumatically pushed further inside the trap (using a 0.8bar continuous pressure) and stopped automatically when the head of the larvae reached the secondary gate in less than 3s (FIG. 5.5e). After animal loading and immobilization, a continuous 0.3 bar pressure was applied and maintained at the inlet port to inhibit any further CNS longitudinal movements and to prevent the larva from crawling back and moving out of the trap. The animal was viably kept inside the aqueous environment for the entire duration of the experiment (215s, see section 2.5). Using the shown configuration, we successfully immobilized *Drosophila* larva with minimal internal CNS movements for its subsequent live neuronal imaging under various acoustic wave conditions inside the insulating box.

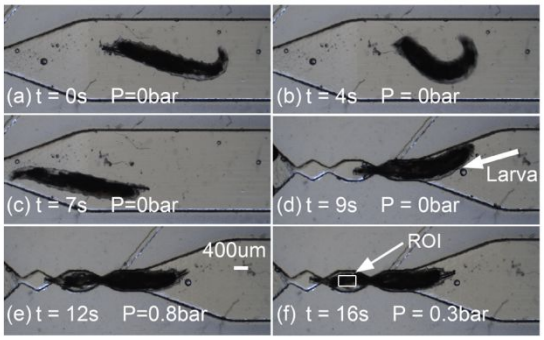

FIG. 5. 5: Steps to load the larva using the pneumatic chip. (a-d) larva swam freely into the trap, (e-f) larva was pneumatically moved into the trap and immobilized. Time-lapsed fluorescent imaging was then conducted on the CNS located inside the Region of Interest (ROI)

2.4.2. Flexichip

The loading of the larva into FlexiChip was performed by bending the chip laterally (FIG. 5.6a the bending opened the clip (double-headed arrow) (FIG. 5.6b) so that the CPS area could be inserted into the gap (arrow in FIG. 5.6c) with larva's ventral side facing upwards. When a drop of water was placed at the clip area the larva automatically attempted to burrow into the clip area. Upon releasing the bend, this facilitated the stable anchoring of the anterior segments of the larva that contains the burrowing apparatus.

Afterwards, a cover-glass was placed on top of the larva (FIG. 5.6d) before visualization of fluorescent activities in the ventral cord aspect of the CNS where a large majority of afferent sensory inputs from the body wall arrive. The larval posterior-end protruded into a funnel shaped outer chamber that was open to ambient air. This allowed respiration to continue through posterior spiracles during live imaging. The procedure for loading the larva into the chip takes approximately 5min.

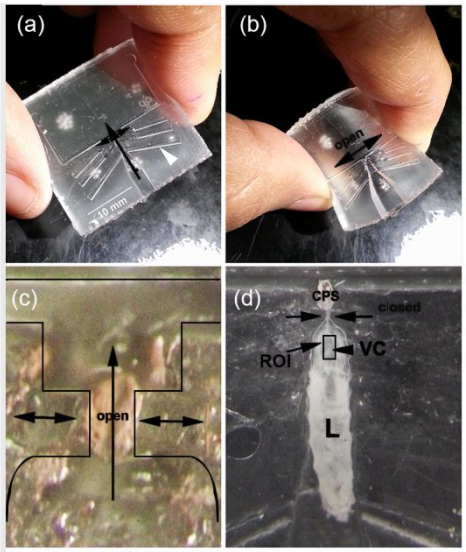

FIG. 5. 6: Steps to load the larva using the FlexiChip. The chip is bent (b) so that the clip (c) opens. Then, the animal is inserted into the gap and the chip is released and sealed by a coverslip (d). Time-lapsed fluorescent imaging was then conducted on the CNS located inside the Region of Interest (ROI)

2.5. Automated animal testing

After the animal was properly loaded into the trap and immobilized as shown in the Figs. 5 and 6, the auditory response of the larva was examined at the abdominal ganglia region of the ventral cord. A custom-made LabVIEW© code controlling the function generator was used to generate a step-like periodic series of acoustic waves (5s On and 5s off) while the animal's CNS fluorescent signal activities were recorded in a movie format using the microscope. Each on-portion cycle of the applied wave corresponded to one frequency (50, 100, 200, 500, 1000, 2000 or 5000 Hz) and one intensity (95, 105 or 115 dB) level. The experiment was continued automatically until the entire 21 frequency-intensity combinations were tested. The animal was then washed off the chip and another one was loaded to repeat the experiments. The movies were then analysed as discussed below for quantification of neuronal activities.

2.6. Data acquisition and processing

Movies recorded for each animal were analyzed by ImageJ© software (National Institutes of Health, USA) to quantify the fluorescence intensity variations in the CNS in

response to the applied acoustic signals. The RGB image sequences for each video were converted to 8-bit black and white images. After subtracting the background with rolling ball radius of 100 Pixels, a Region of Interest (ROI in FIG. 5. 5f and 6d) covering the CNS was selected and the mean grey value for the entire image stack was measured inside the ROI and recorded in an Excel file. The recorded time-lapse intensities were normalized by the average of the initial two seconds (2 seconds before sound being applied) of each experiment.

It is important to note that the inherent movement of the animal also results in an increase in CNS activity that may lead to elevated baseline reading. Movement was measured as the change in the center of mass of the CNS and experiments that had high CNS movement were not included in the analysis.

2.7. Animal preparation

Larvae of the genotype w, Cha-Gal4/CyO; UAS-GCaMP5/TM3, Sb were used for imaging CNS activity in response to auditory stimulations. Hetereozygotes and homozygotes were not separated before testing. This genotype was generated through a standard genetic crossing scheme. 3rd instar stage larvae were isolated using a fine brush and washed with distilled water and dried on a tissue paper before loading into the chips.

3. Results and discussion

3.1 Acoustic response of *Drosophila* 3rd instar larva

After immobilizing the larva (3rd instar) inside each of the PDMS devices as shown in FIG. 5. 5 and 6, neuronal activities in the CNS in response to a sound wave (5s duration, 200Hz frequency and 105dB intensity) were measured using the experimental setup described before (FIG. 5.4). We measured the frequency and intensity of the sound inside both of the devices and found them to be the same as that outside. As shown in FIG. 5. 7 (response of immobilized larva in the pneumatic chip), animal's CNS activity increased by

21% (reported by an increase in average fluorescent intensity) upon exposure to the sound signal and returned to its original state within 0.5s after the signal was turned off (data not shown due to similarity to FIG. 5.7a). This type of response was observed consistently for 5 animals tested at the same acoustic conditions and each time it was tested.

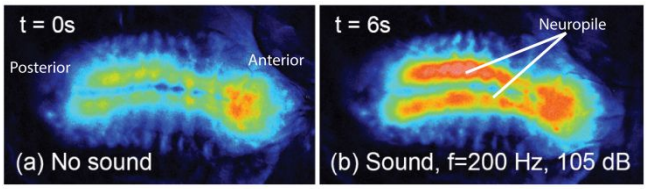

Fig 7: Snapshots of the fluorescent activities in the CNS of a larva (a) before and (b) while it was exposed to a 5s duration sound wave (200Hz and 105dB) in the Pneumatic Chip

3.2 Investigation of the effect of sound frequency and intensity on Drosophila larvae CNS activities

The interesting observation of a significant CNS activity in response to a sound signal (FIG. 5. 7) encouraged us to investigate this phenomenon further in detail. Hence, we recorded the CNS activities of Drosophila 3rd instar larvae in response to sound signals of various intensity (95-115dB) and frequency (50-5000Hz) levels using both the pneumatic chip and the FlexiChip (FIG. 5. 8, averaged for n=5 animals).

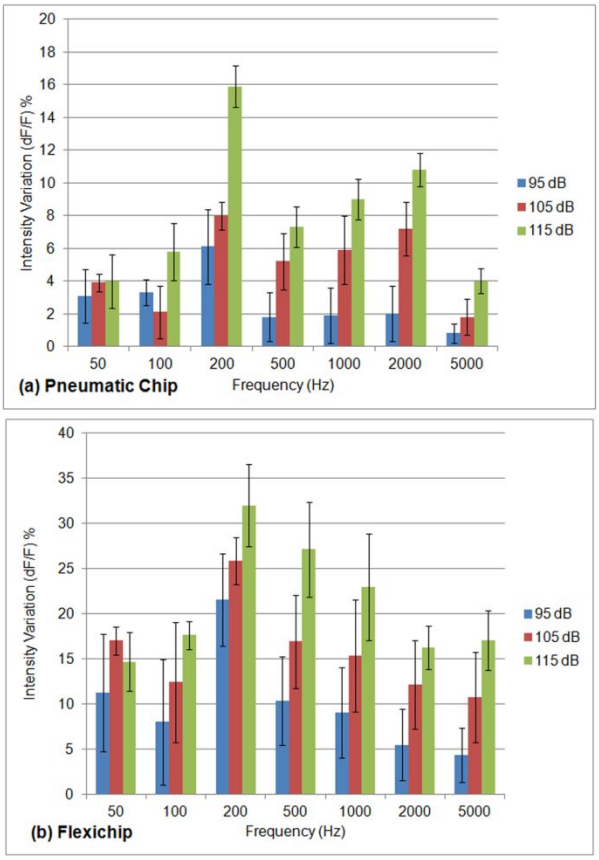

FIG. 5. 8: CNS response of fly larvae (n=5) to various sound frequency and intensity levels tested inside (a) Pneumatic Chip and (b) FlexiChip. A peak in response at 200Hz was observed in both chips with reduction in CNS activities when the frequency of signal was decreased below or increased above 200Hz. Increase in sound intensity resulted in increase in CNS activities

As shown in FIG. 5. 8, animals tested in both chips demonstrated an increase in CNS activities when the frequency of the sound signal was increased from 50Hz to 200Hz. Further increase in frequency resulted in reduced CNS activities as compared to 200Hz condition. In addition to a peak in response at 200Hz, a secondary but less significant peak in CNS response was also observed at 2000Hz and only inside the pneumatic chip (FIG. 5.8a). This peak was more significantly pronounced at higher intensity levels. The level of mechanical vibrations induced by the sound waves at frequencies less than 50Hz on the chip did not allow clear imaging of the CNS. The CNS response continued to decrease further beyond 5000Hz (data not shown). Increase in sound intensity from 95dB to 115dB, resulted in corresponding increase in CNS activity.

The peak observed in the CNS response at 200Hz sound waves is in contrast to the recently reported observation that the optimal neuronal response to auditory stimulus in the larva occurs at 500 Hz. We noted two major differences between our experimental design and that used by Zhang et al. [1]. First, in Zhang et al. [1], the behavioral, calcium imaging and electrophysiological measurements involved the placement of the animals (or semi-intact preparations) directly on top of a speaker that delivered the auditory stimulus which may have coupled some of the vibrations to the larva as tactile stimulations. The use of whole body compression provides sufficient contact of the substrate to activate Cho sensory neurons that are spread throughout the body. Second, our devices have physical separation of the speaker from the device ensuring that it is the sound waves that cause the response while also providing a better simulation of sound cues that occurs in nature. Since the larva is a burrowing animal, it is likely that the sensory neurons in the posterior abdominal segments are better tuned to a sound frequency that matches the wing beat frequency of the predatory wasp. We also test two different designs to separate out any possible tactile stimulation effects.

References

[1] W. Zhang, Z. Yan, L. Y. Jan and Y. N. Jan, *Proc Natl Acad Sci U S A*, 2013, **110**, 13612-13617.

[2] T. Ohyama, T. Jovanic, G. Denisov, T. C. Dang, D. Hoffmann, R. A. Kerr and M. Zlatic, *PLoS One*, 2013, **8**, e71706.

[3] J. Akerboom, T. W. Chen, T. J. Wardill, L. Tian, J. S. Marvin, S. Mutlu, N. C. Calderon, F. Esposti, B. G. Borghuis, X. R. Sun, A. Gordus, M. B. Orger, R. Portugues, F. Engert, J. J. Macklin, A. Filosa, A. Aggarwal, R. A. Kerr, R. Takagi, S. Kracun, E. Shigetomi, B. S. Khakh, H. Baier, L. Lagnado, S. S. Wang, C. I. Bargmann, B. E. Kimmel, V. Jayaraman, K. Svoboda, D. S. Kim, E. R. Schreiter and L. L. Looger, *J Neurosci*, 2012, **32**, 13819-13840.

[4] Y. Xia and G. M. Whitesides, *Annu. Rev. Mater. Sci.*, 1998, **28**, 153-184.

Chapter 6

BENDING *DROSOPHILA* LARVA ENABLES IMAGING OF IT'S BRAIN AND NERVOUS SYSTEM AT SINGLE NEURONAL RESOLUTION

Complete citation:

Ghaemi, Reza, Meryl Acker, Ana Stosic, Roger Jacobs and Ponnambalam Ravi Selvaganapathy. "*A Microfluidic devices for imaging of Drosophila larva's nervous system at single neuronal resolution*", Under review for submission to journal of Lab on a Chip.

Relative Contributions:

Ghaemi, R.: Performed all experiments, interpretation and analysis of the data and wrote the drafts of the manuscript including all figures and text.
Stosic, A.: Assisted in performing the confocal imaging of the samples and sample preparations.
Acker, M.: Helped in performing the confocal imaging and performed genetic crossing of the samples.

1. Introduction

The immobilization of the whole larva or at least the target organs is the main requirement for capturing high-resolution image of the neurons. Due to robust digging/burrowing behaviour in the *Drosophila* larva and the lack of the intact immobilization methods, live high-resolution imaging of the neuronal activities in *Drosophila* CNS is challenging. In previous chapter, two microfluidics devices for intact live imaging of the *Drosophila* larva's CNS were developed [1]-[2]. The devices mechanically immobilized the larvae using the 3D clams designed in the microchannel and image the whole-CNS when it was exposed to auditory stimulates. In these devices, the immobilization of the CNS was just enough for the whole-CNS imaging and single neuronal imaging of the neurons were not feasible due to the micro-movement of the CNS inside the capsule body. Recently, two microfluidic devices have been developed for single neuronal image of the *Drosophila* larva's neuronal network. One used the combination of dissection and mechanical clamp to immobilize the larvae. While, the other used anaesthesia and membrane compression. Giesen et al.[3] partially dissected the larva in a semi-intact manner, leaving the brain and ventral nervous system (VCS) connected to the mouth hook. In this design, the larva's mouth was placed inside a microfluidic channel for exposure to a chemical stimulus , while the neuronal activities of the CNS and brain was imaged using a genetically encoded calcium sensor at single-cell resolution. Chaudhury et al. [4] designed an anaesthesia-based microfluidic device for high resolution in vivo imaging of *Drosophila* neuronal system. Unlike chemical anaesthesia, a combination of mechanical compression and cryo-anesthesia (low-temperature micro-environment) have been used to immobilize individual larvae. Using this device, they were able to capture high resolution imaging of larval neuromuscular junction (NMJs), VNCs and axons in an intact format. However, similar to other methods using anaesthesia, reducing the temperature of the environment to ~5^{o} can affect the true physiological response of neurons in response to the external stimulus. Small organism such as *Drosophila*, must rely on behavior to maintain body temperature within a physiologically permissive range [5]. Therefore, they cannot endogenously regulate body temperature when they are immobilised by the cold chamber in this design. This could not

only affect the neuronal response, it also can be harmful for the viability of the larva. In this chapter, we demonstrate a simple microfluidic device and employ an interesting strategy to completely immobilize the brain and the CNS of a live, fully-functioning *Drosophila* larva that enables, for the first time, imaging throughout these organs at single neuron resolution., none of the methods available currently is capable of immobilization of the brain and the CNS of a live fully functioning *Drosophila* larva sufficiently intact in order to image at a single neuron resolution. It is expected that this device will have broad applicability in any study the brain or CNS of the larva and in combination with techniques such as light sheet microscopy is capable of imaging the whole brain at the single neuron level.

2. Design of the Microfluidic chip

In order to halt the motion of the internal organs in the larva's body, we developed a microfluidic device with a unique clamping trap that pins and bends the larva at $1/3^{th}$ of its body length from the head. The microfluidic chip (see FIG. 6. 1) consists of three major sections: loading channel (inlet, outlet, orientating channel and acceleration track), immobilization trap (bent trap) and chemical exposure channel.

2.1. Loading channel

The loading channel has been designed to transport, orientate, accelerate the larvae for immobilization and unload them from the bent trap. The larvae were manually placed into the inlet port using a brush and then moved inside device by flowing DI water into the inlet channel (FIG. 6. 1b). In order to capture clear images from the CNS and brain of the larvae, the ventral side of the CNS should be placed in front of the lens before loading the larvae into the bent trap. The desired orientation of the larva can be achieved before loading by the orientating channel, where a tapered channel connected the inlet channel to a semi-narrow channel (600μm × 700μm) with the length of 2mm. In this mechanism, when the head of the larva was exposed to the orienting channel, the larva often oriented themselves and crawled voluntarily half-way into the channel. Therefore, the ventral side of the larvae was placed in front of the lens and assisted one in proper orientation of the CNS. After orientation, the long section in the acceleration track allowed the applied pressure to

accelerate the larva and gain momentum such that it will go beyond the bend and position itself. This feature allowed positioning of the larva inside the bent channel with minimal pressure application.

2.2. Immobilization trap

Anatomy of the *Drosophila* larva contains a mouth-hook, two thoracic segments (T2, T3), eight abdominal segments (A1-8) and tail. The *Drosophila* larva's forward and reverse crawling (positioning motion) is caused by muscle contraction patterns in abdominal segments. According to this anatomy and locomotion pattern, the immobilization trap consists of three sections to fully immobilize the larvae: 2D segmental pinning, a bent channel and a stopper. In the first section, three equispaced 2D protrusions have been added to a channel, which could be served as pinning points for the abdominal muscle of the larva. The spacing between the protrusions were closely matched with abdominal segment lengths on the larva's body as indicated in FIG. 6. 1a). Therefore, the 2D segmental pinning could provide segmental constrictions along the larva's body to disrupt transmission of abdominal constriction, which could stop the larva's body-wall movement. In order to capture intact high-resolution images of the targeted neurons, tissue or cells, the larva's internal movement needs to be stopped as well. This was achieved by bending the larva's body for 90^{o} using a bent channel, which has a divergence indent at its corner. The height of the channel after the bending was decreased (from 700µm to 300µm) to form a stopper, which could define the location of the bending along larva's body.

2.3. Chemical stimulus channels

Drosophila larva can sense various environmental cues (e.g. mechanical, visual and chemical) and transmit signals to the central nervous system (CNS) to generate response signals for stereotypic motor behaviors. Larvae can do that by using different types of sensory neurons that are formed in a sectional arrangement. In this device, a chemical delivery channel has been design to expose the larvae into the targeted chemical stimulates, which is perpendicular to the immobilization channel. The configuration of the design allow one to precisely deliver the solution into the mouth-hook of the larvae, however, it could be redesigned for different location along the larva's body as it might be required in

various chemotaxis assays.

2.4. Unloading the larva

In order to unload the larva from the bent tarp after immobilization and imaging, a pressure pulse of 1.5bar was applied into the outlet and the larva was ejected from the inlet, which is the reverse of the loading process. In this process, the inlet and outlet of the chemical stimulus channels should be closed.

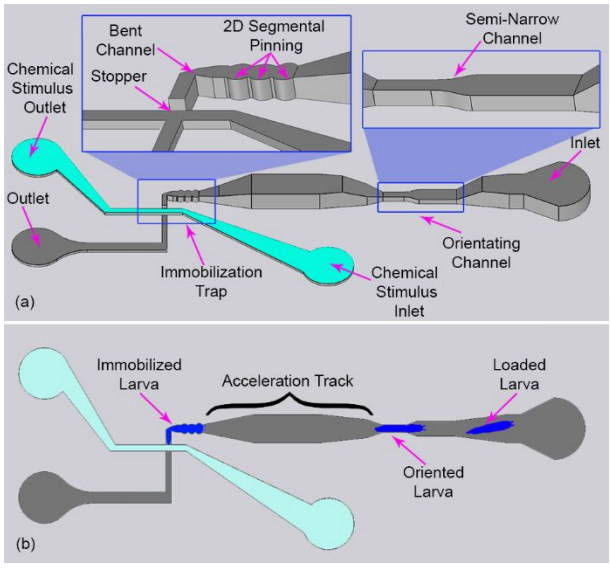

FIG. 6. 1: Schematic of the bent chip. A L-Shape narrowed channel has a divergence intend at its corner. Introducing of the larva into the narrow channel via a controlled pneumatic pressure, pinned and then bent the larva inside the trap.

3. Method

3.1. Device fabrication

The devices for immobilization and high resolution imaging of 3rd *Drosophila* larvae were fabricated by dye casting of Polydimethylsiloxane (PDMS, Sylgard SYLGARD® 184, Dow Corning, USA). To do this, first, the microfluidic channel mold design (see FIG. 6. 1a) was

created in a mechanical CAD software (Inventor) and then 3D printed (Projet HD 3000 from 3D Systems, Material: VisiJet® EX200 Plastic). Next, two 1cm silicone tubes (3/16"ID x 5/16"OD, Cole-Parmer Canada Inc.) were placed on the reservoirs as the inlet/outlet. Similarly, two 1cm tubes (1/8"ID x 1/4 "OD) were placed on the inlet/outlet reservoirs of the chemical stimulus channels. Afterward, uncured PDMS (10:1 ratio base:agent) was poured on the mold. The PDMS cured at 85ºC for 1hr and then it was peeled off from the master mold. Finally, the PDMS chip was bonded (80s, 50W, plasma oxygen) to the glass slides (75mm x 25mm with thickness of 1mm) and/or cover glass (50mm x 22mm with thickness of 0.2mm) to seal the channels.

3.2. Larva preparation

For the both epifluorescent and confocal microscopy, the larvae with genotype of ChaT-Gal4/CyO; UAS-GCaMP5G/TM3 (Bloomington 56500) and Elav-Gal4; UAS-GFP were used. The stock were raised at room temperature on yeast fly food. In the ChaT-Gal4/CyO; UAS-GCaMP5G/TM3 strain, all sensory and central neurons that express the Choline Acetyltransferase gene express the GCaMP5 calcium sensor. In order to collect 3rd instar larvae, the larvae that were outside of the food and crowed up on the wall, have been picked by brush and washed by DI water.

3.3. Experimental setup

The experimental setup consisted of four aspects: Fluidic system, optical systems, microfluidic device and acquisition software. The fluidic system, which was used to introduce the larva into the device for imaging, consisted of a pressurized air tank at 4 (bar), pressure regulator (2000 Series Regulator, ARO, Ingersoll Rand, USA) and a solenoid valve (S10MM-30-12-3, 3-Way Normally Closed, Pneumadyne, Inc., USA). Two different optical setups have been used in this research. The first one (epifluorescent microscopy) with wide-field of view, lower resolution and faster frame rate (2f/s) have been used to characterize the design parameters of the bent chip. While, the second setup (confocal microscopy) with higher resolution was used for single neuronal imaging of the larvae.

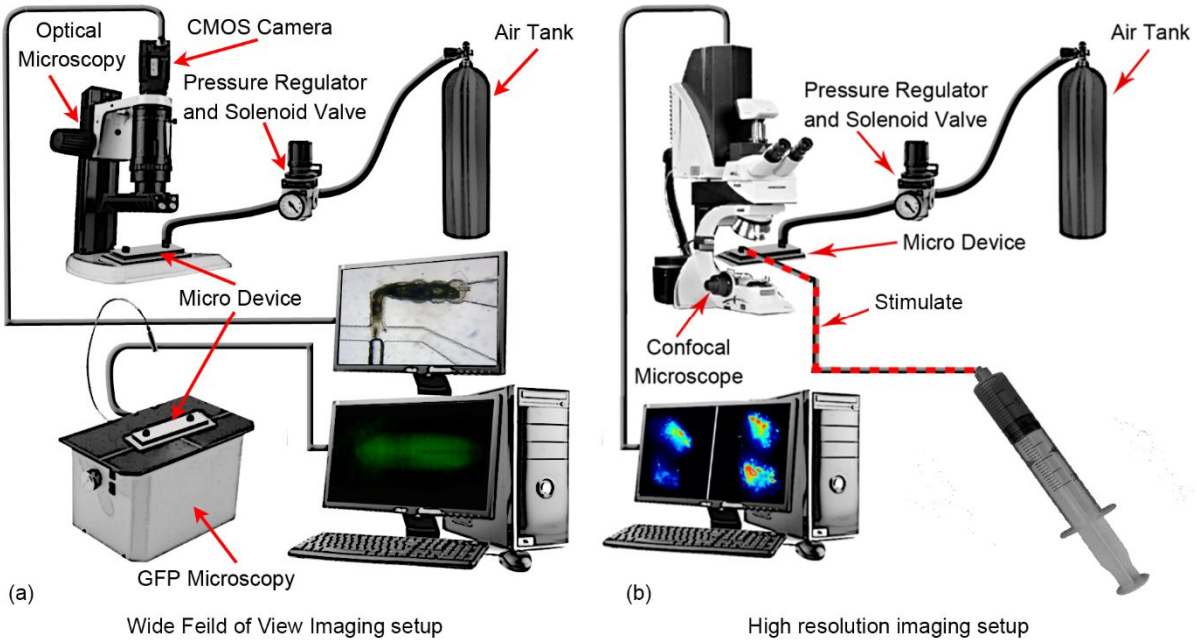

FIG. 6. 2: (a) wide-FOV experimental setup used for larva loading, image sequence recording and processing. (b) High-resolution experimental setup used for larva loading, image sequence recording and processing

3.3.1. Wide field of view imaging

Epifluorescence Microscopy (Lumascope 500 - Etaluma, Inc.) was used to image the entire larva's brain and CNS to characterize different design parameters of the bent chip (see FIG. 6. 2a). The microscope allows one to record the required time-lapse images of the organs of interest. A 1000µm *x* 700µm field of view (20x objective lens) was used to completely cover the brain and CNS. Image sequences (2 f/s) captured for each larva were analysed by Labview© software to measure the movement of the whole body and CNS movement during the time that larva was immobilized. The RGB image sequences for each video were converted to 8-bit grey scale images. Then, the pixel value of 255 was assigned for the larva's brain and CNS, while the background was adjusted to the pixel value of 0. Subsequently, the pixel centre of mass of the both larva's body and its CNS were measured for the entire image stack. Finally, the recorded data were recorded in a spreadsheet file.

3.3.2. High Resolution imaging

Confocal microscope (Leica SP8 Spectral Confocal) was used to capture high resolution images of the single neuronal activities in the *Drosophila* larva's brain as shown in FIG. 6. 2b. In order to record live Ca^{2+} activities of the larva's brain and CNS, the larva was loaded into the microfluidic device. Next, live fluorescent images (GFP images) of the targeted neurons were recorded, while the larva was exposed to chemical stimulates.

3.4. Data analysis and statistics

Two different analyses have been used to compare the effect of design parameters on the larva's immobilization: Statistical analysis and movement analysis. In the statistical analysis, a ±25µm window along the CNS axis has been defined as the desired field of view for single neuronal imaging. In the analysis, the total number of the frames that the CM (Center of mass) of the CNS were inside the field of view, were counted. Therefore, a binomial distribution of the frames can be calculated by:

$$P_{in} = \frac{Number\ of\ the\ frames\ inside\ the\ FOV}{Total\ number\ of\ frames}$$

$$P_{Out} = \frac{Number\ of\ the\ frames\ Outside\ the\ FOV}{Total\ number\ of\ frames}$$

Where, $P_{in} + P_{Out} = 1$. In this analysis, the large value of P_{in} shows stronger immobilization. As a result, this analysis could allow one to quantify the strength of the immobilization mechanisms for time-lapse imaging of the brain and CNS.

Alternatively, movement analysis have been used to calculate the range of CNS's spontaneous motion, while it was immobilized in the chip. In this analysis, first, the location of the CNS been recorded in the 1100µm *x* 700µm field of the view (600s with 2f/s), while they were immobilized in the microfluidic chips. Next, the average and the standard deviation of the CNS location along the CNS axis was calculated. Since the larvae could not release themselves from the microfluidic chips, their CNS experience only a spontaneous pistonic motion in the field of view, which is associated with a mean value (µ) a standard deviation (σ). Although, the mean value of the location of the CM was approximately equal to zero, the standard deviation is reflective of the degree of

immobilization and varies for the various immobilization schemes under consideration. Therefore, the strength of the immobilization systems can be quantified by calculating the standard deviation of the CNS's location. The range of the spontaneous motion also can be defined by $\pm\sigma$.

4. Results and discussion

4.1. Bending immobilization for Single neuronal imaging of CNS

Drosophila has been used as a model organism for over 90 years and is currently used to study various neuronal diseases such as Parkinson, Alzheimer and Seizure. The neuronal system of *Drosophila* larva is structurally simple and contains ~10,000 neurons. This coupled with its genetic tractability make this organism attractive to study the mechanisms of various neurological diseases. Emerging optical imaging techniques (confocal, two photon and light sheet microscopy) and genetically encoded fluorophores have recently enabled biologists to record real-time neuronal events in larva's CNS and brain. However, in order to perform such high resolution imaging on live, intact, fully functioning larva, it should be completely immobilized. The microfluidic device designed in this research was used to immobilize 3rd instar larvae to record neuronal image of the *Drosophila* larva's CNS.

The bent trap was used to stop the pistonic movement expressed in the larva's locomotion. In order to demonstrate the functionality of the bent trap on the immobilization of the mobile larvae, images of neurons on the CNS and body-wall of the 3rd instar larva were recorded while it was immobilized into the bent trap. In this process, first, a 3rd instar larva was loaded into the inlet of the device, where it oriented itself and crawled voluntarily into the semi-narrow channel (See FIG. 6. 3a-d and supplement video S1). This positioned the ventral side of the larva close to the bottom glass surface (or Cover glass), appropriately orientating the CNS for imaging. As the larva crawled into the channel and its head passed the end of the orientating channel (usually takes less than 45s), a pressure pulse of 150kPa was applied to accelerate the larva and insert it into the bent trap, as shown in FIG. 6. 3e. In this configuration, approximately 1/3rd of larva, including its CNS and brain, passed the bent neck. The posterior end of the larva was simultaneously immobilized by the 2D

segmental pinning locations in the channel leading to the bent trap. Next, Epifluorescent images (excitation: 475±18nm, emission: 530±22nm) of larva's body-wall neurons and CNS were captured. The larvae of elav-gal4; UAS-GFP and Cha-Gal4/CyO; UAS-GCaMP5G/TM3 strains have been used to image the body-wall neurons and CNS respectively as shown in FIG. 6. 4. Elav-gal4; UAS-GFP drives GFP expression in all neurons in larva's body including body-wall sensory neurons and neuronal muscular junctions [6]. The epifluorescent images (FIG. 6. 4a-f) showed that the body-wall neurons of Elav-gal4; UAS-GFP larva can be clearly imaged using the bent device. In these pictures, all three part of the neurons (cell body, dendrites and axon) were clearly imaged at three different sections along the body including larva's mouth (FIG. 6. 4a), A2-A4 (FIG. 6. 4b-d) and A7-A9 (FIG. 6. 4e-f) abdominal segments. The shape and path of axon indicated different types of sensory neurons and neuronal muscular junction that were patterned in a segmental configuration. This allows *Drosophila* larvae sense various environmental cues (e.g. mechanical, temperature and chemical) and relay information to the Central Nervous System (CNS) to help elicit stereotypic motor behaviors. The larva of Cha-Gal4/CyO; UAS-GCaMP5G/TM3 mark the expression of Cha (choline acetyltansferase) gene, which is required for acetylcholine synthesis and is localized to cholinergic neurons[7]. It can be seen from FIG. 6. 4g, that the three parts of the CNS including ventral nerve cord (VNC), subesophageal ganglion/tritocerebrum (SOG) and centre brain are completely disguisable and easily imaged when the larva is immobilized in the bent trap. It should be noted that no other immobilization scheme that doesn't use anaesthesia or dissection is able to image these areas of the CNS and brain with this level of clarity for long term (imaging processes that should be performed on larva more than 2hrs) imaging. The wide field of view (FOV) imaging setup used in this experiment conducted under an epifluorescent microscope, does not provide the ability to capture images at the level of single neuron in the brain. Therefore high resolution Confocal imaging setup was used to determine whether the immobilization device will allow high resolution imaging directly from the CNS and the brain.

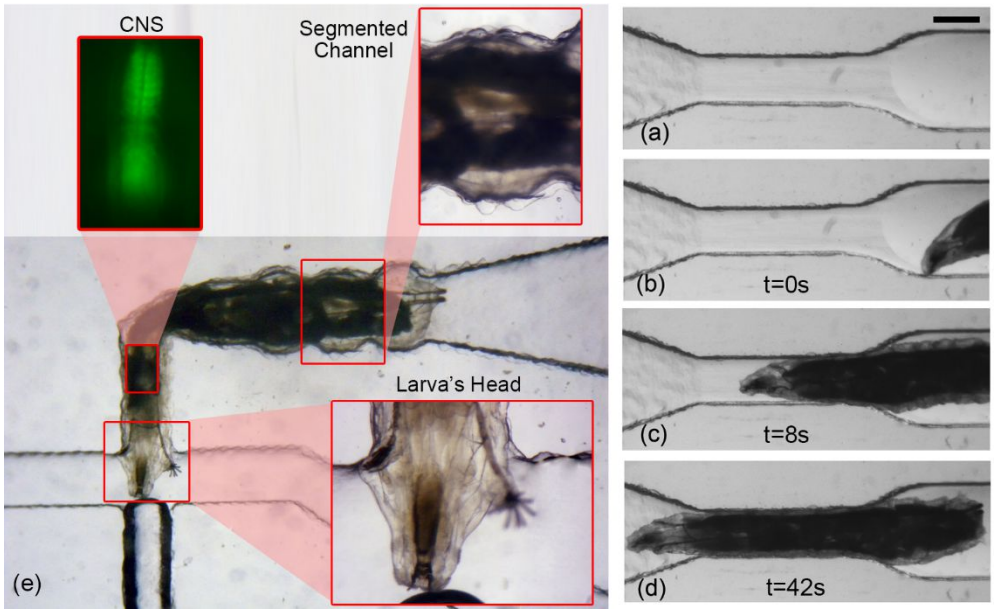

FIG. 6. 3: The steps of the self-orienting behavior of *Drosophila* larva when it was introduced to the orienting channel (a). The larva looks for the tapering shape design in the channel (b) and then moved completely into the channel (c-d), while its ventral side was downward on the glass substrate. Scale bar 600µm (e) the larva that is loaded into the bent trap. When, the larva aligned itself in the orienteering mechanism before the trap, a pressure pulse of 150kPa loaded the larva into the bent trap. This configuration completely immobilized the larva with the proper orientation for CNS imaging.

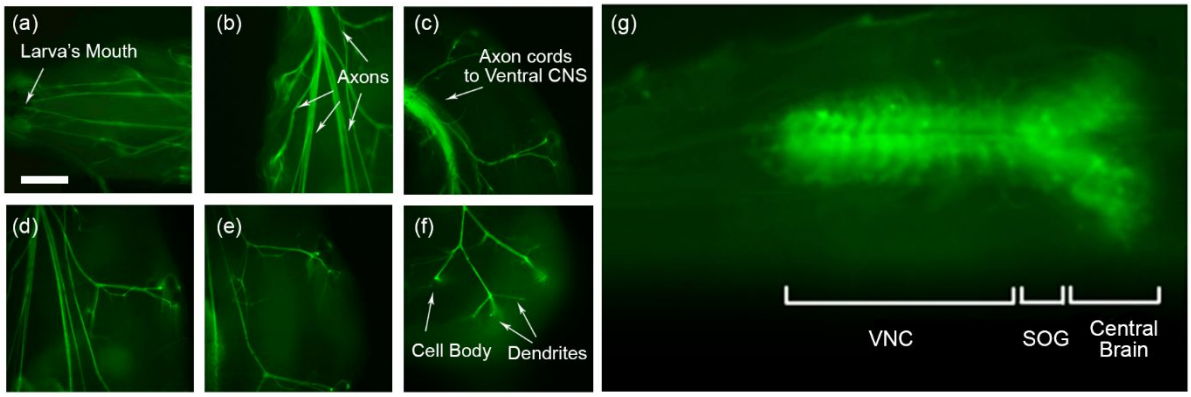

FIG. 6. 4: GFP images of single body-wall neurons and central nervous system (CNS) of *Drosophila* larva by using the bent chip. (a-f) body-wall neurons of elav-gal4 :: UAS-GFP larvae at three different sections along the body including larva's mouth (a), A2-A4 (b-d) and A7-A9 (e-f) abdominal segments. (g) Central nervous system (CNS) of Cha-Gal4/CyO; UAS-GCaMP5G/TM3 larva.

In order to achieve high resolution imaging of neurons in the CNS, a 3rd instar larva of Cha-Gal4/CyO; UAS-GCaMP5/TM3 strain was immobilized in a device with a bent trap and imaged using a confocal microscope. The images of the neurons in various location of the CNS were recorded and shown in FIG. 6. 5. The projection images of neurons in *Drosophila* mushroom bodies (FIG. 6. 5a-c) have been obtained from 20 stacks with thickness of 5µm. In this process, the field of view was set to 512pix x 512pix, where the scanning of the individual slice by speed of NNN Hz took 5s (100s in total) and the brain was immobile during imaging to get a clear image. These images specifically showed the Cha neurons that were distributed around the CNS. The size of the neurons (cell body) were approximately in the range of 5µm to 15µm. Higher magnification images of the neurons inside the VNC of CNS recorded from 12 stacks with thickness of 2µm and their projection are shown in FIG. 6. 5c-d. In this process, the field of view and scanning speed were set 512pix x 512pix and 200 Hz, which resulted 5s scanning time for each slice. Similarly, the targeted neurons were selected from the mushroom bodies of the larva's brain. The 3D video reconstruction of the stacks have been created and shown in supplemental video S2-S5. The larvae from the same strain have used to image the body-wall neurons. The expression of *Cha* gene have been reported in different neuronal receptors on the body wall of the larva. The bent trap has been also used to immobilize the larva for body-wall neuronal imaging at single neuronal resolution as shown in FIG. 6. 5f-g. In order to completely cover entire structure of the neuron including cell body, dendrite and axon terminals, the total number of 5 stacks with a thickness of 10µm have been captured form a body-wall neuron located on the ventral side of T3 thoracic segment and A1 abdominal segment. Currently, the larva should be dissected (completely or partially) or anesthetized in order to capture single neuronal images of the CNS and body-wall neurons. However, dissection completely disconnect the CNS from the rest of the neurons in the body, which are mainly required to sense the external stimulates (e.g. light, temperature, pressure) and rely the information into the CNS and brain. Anaesthesia (e.g. exposing to ether, CO_2 and cooling the larva) also influence the neuronal behaviour and it can stop or reduce the neuronal activates. In our previous work, the effect of anaesthesia on the neural response of the larva to auditory

stimulus was studied and the results showed that the neuronal response to sound as measured by the intensity of the fluorophore (GCaMP5) was significantly decreased in anesthetized larvae (exposing to ether solvent for 2 minutes) compared to unanesthetized condition. Therefore, the side effects associated with these two methods could not allow one to record the true physiological response of *Drosophila* larva. In contrast, immobilization of larva achieved by mechanical clamp could prevent the neuronal and tissue damages that caused by dissection, and keep the neuronal system in the more conscious state compared to the time when they are anesthetized. Additionally, this platform could potentially allow one to record neuronal events at different organs (e.g. gut, intestine) simultaneously, while they have true physiological connection to each other. This could not be achievable using dissection protocols as they usually isolate a single organ, where the connection between the organs will be lost. As the results shown in FIG. 6. 5, clearly demonstrate that the bent trap has the usual ability to completely immobilize a live larva and its internal organs sufficiently to enable accurate and high resolution imaging of its CNS and brain at a single neuron resolution.

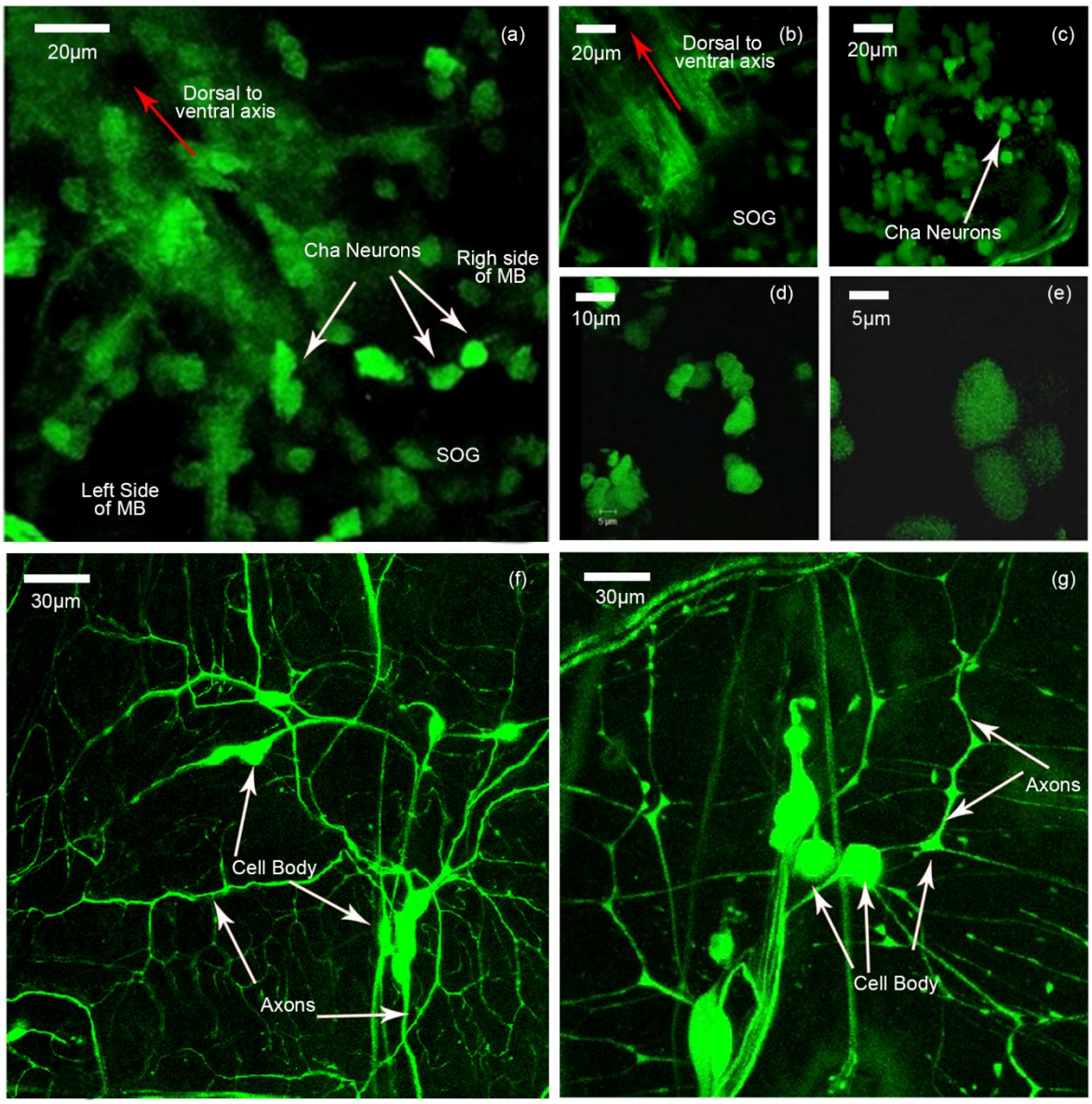

FIG. 6. 5: High resolution images of the neurons inside the *Drosophila* larva's brain, CNS and body wall. Neurons in *Drosophila* mushroom bodies (MB) in two different height (c-e) and ventral cord (c). Higher magnification images of the neurons inside the mushroom bodies of the brain (d-e). The images of the body-wall neurons located on the ventral side of T3 thoracic segment (f) and A1 abdominal segment (g).

4.2. Characterization of the immobilization mechanism

4.2.1. The strength of the immobilization mechanism

In order to quantify the strength of immobilization mechanism, the movement of the CNS has been recorded over time and its range have been compared with the design criteria

required for high resolution imaging. To calculate the range of motion, firstly, image sequence (2f/s) of the CNS has been captured for 500s using the wide field of view imaging system described in section 3.1.1. Next, the larva's CNS movement (its centre of mass) has been calculated using a custom-made LabVIEW code and plotted in FIG. 6. 6a. Then, the average and the standard deviation of the CNS displacement in the x-axis have been determined. The larva's CNS experience only a random pistonic motion in the 1100µm *x* 700µm field of the view, which resulted in almost non-existent motion. The results obtained from ten larvae indicated that the range of larvae's CNS spontaneous motion in the bent trap were always smaller than 10µm over 500s imaging (see FIG. 6. 6b), which was significantly smaller than the maximum allowed motion (any motions move the neurons out of the 50µm x 50µm FOV) for high resolution imaging of single neuron. This was determined by calculating the standard deviation of the CNS motion along the x-axis as shown in the FIG. 6. 6b for the number of ten larvae. Compared to other intact mechanical immobilization schemes (Ghaemi et al. [1]-[2]) this represents a significant reduction in long term motion of CNS and sufficient to image the same neuron over long duration of time. The reason for the complete immobilization in this format can be attributed to several factors. First, the bent trap not only provides a way to pin the larva but also bends it which could result in breaking up of the locomotory wave of muscle contraction that results in movement of not only the body but also of its internal organs. The second could be due to the increased friction at the bend encountered by the larva whenever it tries to move and release itself. As a result, the bent trap design allowed us to successfully immobilize *Drosophila* larva with minimal internal CNS movements for its subsequent live single neuronal imaging. Consequently, the bent trap was effective and completely immobilized the internal organs such as CNS for intact single neuronal imaging of the *Drosophila* larva. This method caused the minimum tissue damage compared to dissection and gluing immobilization technique. Additionally, it has fewer neuronal effects as compared to anesthetize techniques. Moreover, the method of immobilization is based on microfluidics techniques, which could be applied for various intact high throughput live imaging protocols.

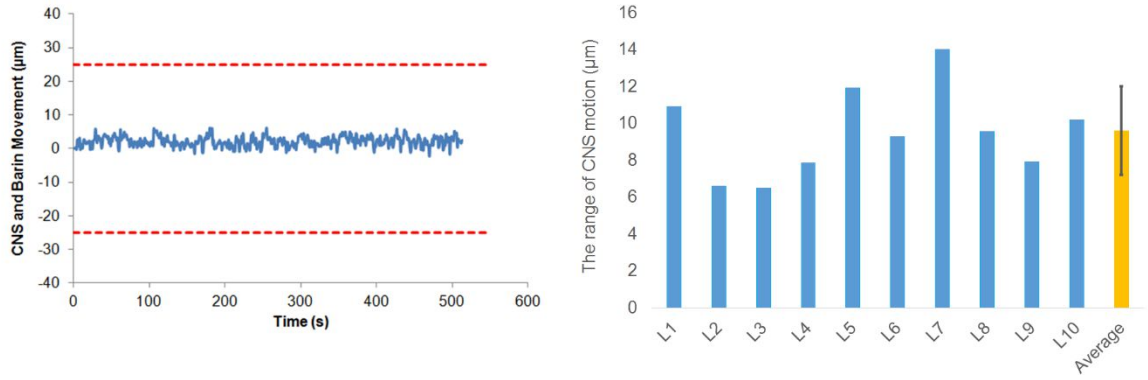

FIG. 6. 6: The CM movement of the larva's brain and CNS, inside the bent chip.

In order to characterize the immobilization mechanism, the wide field of view imaging system has been used in the previous experiment. Although, this system was suitable to fully cover the entire CNS in the FOV, the movement of the single neurons could not be visualized in pictures. In order to validate the data obtained by the wide field of view imaging system (see FIG. 6. 6b), the movement of a single neuron in the VNC of CNS has been recorded over time using the high resolution imaging system (Confocal microscopy) and its range of motion have been compared with results obtained with low resolution imaging system. To do this, image sequences (1stack/min) of a single neuron in the VNC of CNS were recorded for over 10min.The size neurons in the *Drosophila* larva's CNS are 5-15µm. Therefore, a field of view (FOV) with a size of 50µm × 50µm was chosen for long term imaging experiment. The movement of the neuron was calculated from the images by using the custom-made image processing code on ImageJ© software and its trajectory plotted in FIG. 6. 7. The result of the movement analysis showed that the bent trap could keep the single neuron completely inside the field of view (50µm × 50µm) over 10 minutes of confocal imaging. The data points indicated the location of neuron in each time from 0 to 10min and the orange line indicated the potential pathway from one data point to the other. The tracked neuron had relatively small and smooth motion over the course of the 10 min as shown in FIG. 6. 7 which is ideal for imaging. The range of the motion in x- and y-axis were approximately 8µm (from +3µm to -5µm) and 2.5µm (from -2µm to 0.5µm), respectively. This corresponds to a range of 16% and 6% along the axis of the channel and

across it compared to the size of the FOV (50µm × 50µm). This could successfully validate the results obtained from the wide field of view imaging system and indicated that the CNS movement analysis could be performed with either systems and the results would be approximately equal.

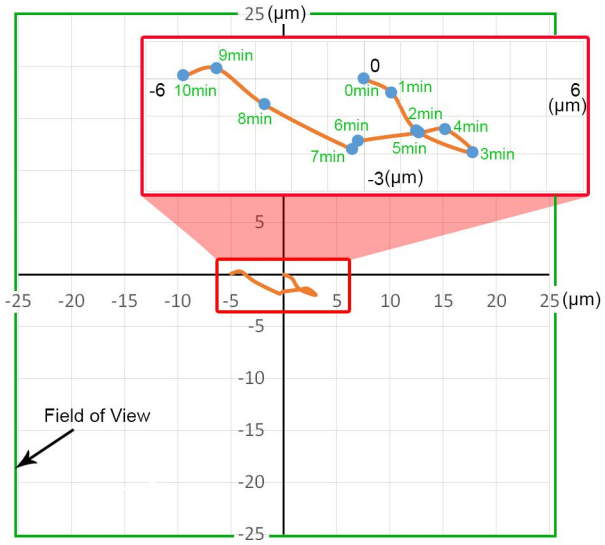

FIG. 6. 7: The pathway motion of a single neuron for 10miutes, when the larva is immobilized inside the bent trap that is calculated by using the custom-made image processing code on ImageJ© software.

In order to understand the mechanism by which the bent trap is able to provide complete immobilization of the larval CNS, the critical parameters such as the angle of the bend and the location of the bending on the larval body was varied and the degree of immobilization measured.

4.2.2. Effect of the bending angle

Three different angles (0°, 45° and 90°) were selected to examine the effect of the bending angle on the immobilization of the larva as shown in FIG. 6. 8a. In these designs, the length of the segmented channel and bent channel were made equal to ensure the same friction length in both of the designs. In this experiment, the larvae were loaded into the device and the image sequences (2f/s) of the brain and CNS were recorded for 600s using the wide

FOV (1100µm *x* 700µm) imaging system shown in FIG. 6. 2a. Subsequently, the movement of the CNS neurons was calculated by a custom-made LabVIEW code. Both movement analysis and statistical analysis (FIG. 6. 8b-c) (n=10) showed that the 90º bending angle was crucial for the complete immobilization of the larva. The range of CNS spontaneous motion was found to be 47µm and 46µm over the duration of 600s for larva immobilized in the bent channels with 0º and 45º bend angles. The movement of the CNS was significantly reduced to only 9.6µm in the 90º bent channels (see FIG. 6. 8b). Similarly, statistical analysis of the probability of the CNS being confined to the ±25µm FOV was found to be only 40% and 51% in channels with a 0º and 45º bend. However, the probability was significantly higher at 98% for channels with a 90º bend (see FIG. 6. 8c). This indicates that the extreme bending (close to 90º) is needed for complete immobilization of the larva and its internal organs.

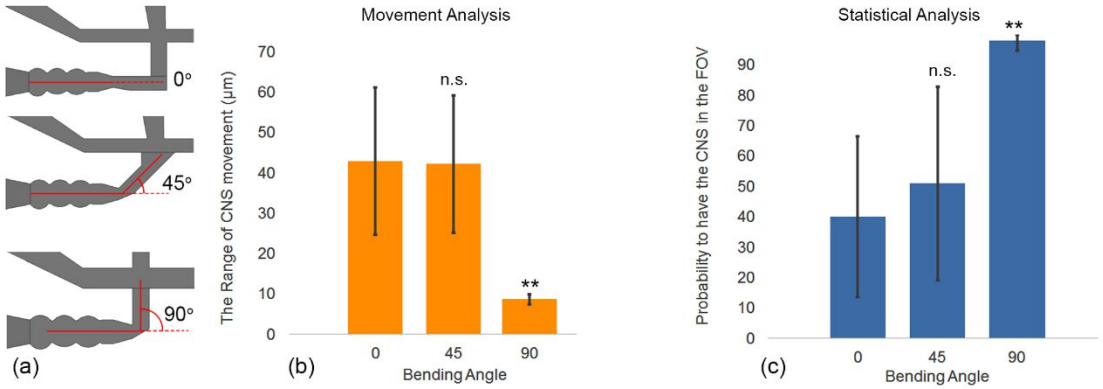

FIG. 6. 8: (a) schematic of the microfluidics tarps with three different bending angles. Movement (b) and statistical (c) analysis of the immobilization chips.

4.2.3. Effect of the bending location

The bending location defines as the point where larva's body was bent by the trap. In order to test whether the location of the bend was an important factor in immobilization, a number of designs of the bent trap were developed with different lengths so that it would bend the trapped larva at different locations (abdominal segment of T2, A2 and A4 (see FIG. 6. 9)) along its body. Furthermore, a straight trap, which consists of three equispaced 2D

protrusions added into a straight channel, was also included as the control case. Similar to the section 3.2.2., ten larvae were loaded and imaged for 600s in each devices and the range of the CNS spontaneous motion has been obtained in each design and compared in FIG. 6. 9. The results of movement analysis showed that the range of the CNS spontaneous motion in the straight trap was significantly larger than the three other designs and the CNS of all ten larvae left the 1100μm *x* 700μm field of view, approximately after 1min. Bending the larva body at T2 location resulted in moderate immobilization with the movement of CNS restricted to 43±15μm. The degree of immobilization was found to be similar to that of the 0^o and 45^o traps. Therefore bending at T2 is clearly not sufficient for single neuron resolution imaging. Notably, bending to the larva's body at A2 and A4 abdominal segment produced a remarkable degree of immobilization with the movement of CNS restricted to 8.6±1μm and 6±1μm, respectively and within the FOV of 50μm × 50μm making it suitable for high resolution imaging. These results indicate that the bending of the larva body close to its mid-section results in interruption of its peristaltic muscle movement and leads to trapping and complete immobilization of the larva. It was also noted that the immobilization at A4 was statistically ($p<0.001$) better that at A2. One reason for it could be the length of the larva post bend in contact with the narrowed channel. This could lead to more body-wall friction and body compression on the larvae's body and cause less CNS movement, consequently. The length of the larva that should be loaded into the narrowed channel in A4-bent trap is noticeably longer than A2-bent trap. This could increase the hydrostatic resistant of the microfluidics system during both loading and unloading process. As a result, it required relatively higher pressure to load the larva into the A4-bent trap, which could be more damaging to the larvae and it can affect their viability during imaging and after unloading. The higher level of the pressure could also be more destructive to the microfluidics device. Therefore, the trap that bent the larva at A2 abdominal segment would be optimal for immobilization of larva's CNS with minimum effects on larva's viability.

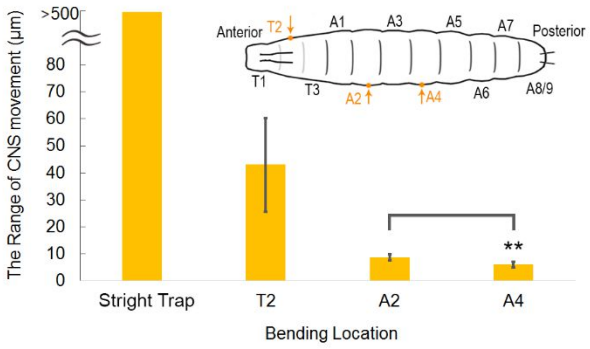

FIG. 6. 9: The range of the CNS spontaneous motion in four traps that had different bending location. The schematic of the larva shows the different abdominal segment of the larva's body, where the orange arrows indicated the location of the bending along the body.

4.3. In-vivo neuronal imaging upon exposure to chemical stimuli

Multicellular electrophysiological measurements of *Drosophila* larva's taste system is technically challenging and the results obtained from this method cannot reveal how many chemosensory neuron are housed in which sensillum [8]. This could be addressed by live calcium imaging of the chemosensory neurons at single neuron resolution using genetically encoded calcium indicator GCaMP5. However, larvae need to be strongly immobilized for high resolution imaging and exposed to defined chemical stimuli. This assay can be performed using the bent chip. In order to demonstrate the unique capabilities of this immobilization scheme, in-vivo imaging of multiple neurons at ventral nerve cord (VNC) in the CNS was performed and their response to chemical exposure studied. *Drosophila* larva can sense various sensory input such as light, sound, chemicals (e.g. odours, taste) and mechanical touch using different neuronal receptors. Essential information about the nutritional value, chemical composition and putative toxic compounds of food substrates can be sensed by specialized gustatory receptor neurons (GRNs), in *Drosophila* larva's sensor network. In order to fully understand the sensory coding in larva's CNS, intact live imaging of the neuronal responses to defined sensory stimulates would be a practical approach. However, such an approach has not been possible till now due to the difficulty in simultaneous immobilization of the larva for intact live imaging of it's CNS at single-neuron resolution while delivering accurate and reproducible stimuli to its sensing organs.

In this experiment, the microfluidic device with the bent trap was used to completely immobilize the larva for intact live imaging and simultaneously position its mouth in a perpendicular channel that can allow precise and accurate exposure to chemical stimulus. A 3rd instar GCAMP5 larva (Cha-Gal4/CyO; UAS-GCaMP5G/TM3) was immobilized into this chip and it's CNS was imaged while its mouth region was exposed into 20mM sodium azide (NaN_3) for 5s. The confocal image (10 stacks) of the larva's CNS neurons was captured 50s before and 5s after exposure and are shown in FIG. 6. 10a. The results indicated that the intact images of the larva's ventral nerve cord of CNS at single-neuro resolution could be recorded by immobilizing the larva via bent trap. The larva's neuronal activities in the ventral nerve cord of the CNS was significantly increased as the olfactory receptor neurons (ORNs) and gustatory receptor neurons (GRNs) of the larva was exposed to 20mM NaN_3. The mean intensity of the individual neurons have been measure before and after NaN_3 exposure and plotted in FIG. 6. 10b. The blue and orange hatched bars, which represents the average of ten data point, showed that the activity of the neurons have been statistically ($p<0.0005$) increased from 23.5 to 37.5 (~60% increase). Cha (choline acetyltansferase) is required for acetylcholine synthesis and is localized to cholinergic neurons. Acetylcholine is the major excitatory neurotransmitter of the *Drosophila* CNS and is involved in mediating olfactory information (though the synthesis of acetylcholine in mechanosensory as well as chemosensory- related neurons). Therefore, the UAS-GCAMP5 shows the physiological response of Cha-expressing neurons to NaN_3, which is a potent metabolic toxin with a multitude of dosage dependent effects and can cause permanent neuronal damages. Recently, live imaging of neuronal responses to chemical stimuli has been performed via a semi-intact protocol, which used the calcium sensor GCaMP5 expression in distinct types of *Drosophila* chemosensory neurons [3]. The live images of the larva's suboesophageal ganglion (SOG) successfully showed the calcium activity ($dF/F > 50\%$) of the IR76b-positive neurons as the larva's head was exposed to defined chemical stimuli. The results presented in in FIG. 6. 10b also showed increased in the neuronal activity more than 50%, which indicated that the same neuronal activity in *Drosophila* chemosensory neurons can be measured using the bent chip. As a results, the bent chip is

the first microfluidics chip that could allowed one to record the live activities of the larva's chemosensory neurons in the fully intact format, when it was exposed to a defined chemical stimuli.

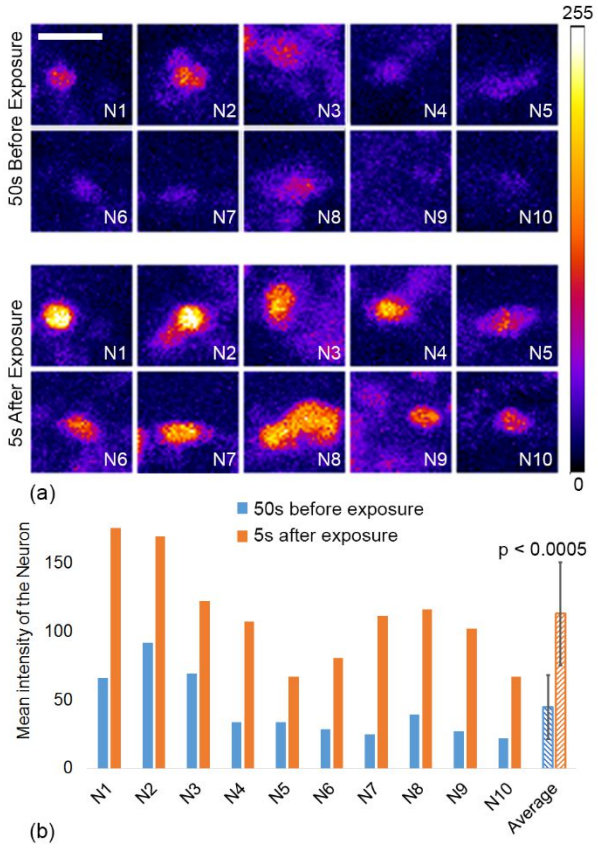

FIG. 6. 10: Neuronal activities of *Drosophila* larva during chemotaxis response. (a) The calcium activity of the single neurons from one larva in response to the sodium azide 50s before and 5s after exposure. Scale bar 5µm. (b) The mean intensity of the neurons for ten different neurons in the VNC of the larva's CNS. The hatched bars represents the average of the data points in each image sets.

References

[1] Ghaemi, R., Rezai, P., Iyengar, B. G., & Selvaganapathy, P. R. (2015). Microfluidic devices for imaging neurological response of *Drosophila* melanogaster larva to auditory stimulus. Lab on a Chip, 15(4), 1116-1122.

[2] Ghaemi, R., Rezai, P., Nejad, F. R., & Selvaganapathy, P. R. (2017). Characterization of microfluidic clamps for immobilizing and imaging of *Drosophila* melanogaster larva's central nervous system. Biomicrofluidics, 11(3), 034113.

[3] Van Giesen, L., Neagu-Maier, G. L., Kwon, J. Y., & Sprecher, S. G. (2016). A microfluidics-based method for measuring neuronal activity in *Drosophila* chemosensory neurons. nature protocols, 11(12), 2389-2400.

[4] Chaudhury, A. R., Insolera, R., Hwang, R. D., Fridell, Y. W., Collins, C., & Chronis, N. (2017). On chip Cryo-Anesthesia of *Drosophila* Larvae for High Resolution In Vivo Imaging Applications. Lab on a Chip.

[5] Dillon, M. E., Wang, G., Garrity, P. A., & Huey, R. B. (2009). Thermal preference in *Drosophila*. Journal of thermal biology, 34(3), 109-119

[6] Yao, K. M., & White, K. (1994). Neural specificity of elav expression: defining a *Drosophila* promoter for directing expression to the nervous system. Journal of neurochemistry, 63(1), 41-51.

[7] Nässel, D. R., Enell, L. E., Santos, J. G., Wegener, C., & Johard, H. A. (2008). A large population of diverse neurons in the *Drosophila* central nervous system expresses short neuropeptide F, suggesting multiple distributed peptide functions. BMC neuroscience, 9(1), 90.

[8] Oppliger, F.Y., Guerin, P.M. & Vlimant, M. Neurophysiological and behavioural evidence for an olfactory function for the dorsal organ and a gustatory one for the terminal organ in *Drosophila* melanogaster larvae. J. Insect Physiol. 46, 135–144 (2000)

Chapter 7

CONCLUSION AND RECOMMENDATIONS

1. Summary of the thesis

In this thesis, various microfabricated devices were developed to address the key challenges associated with conventional *Drosophila* assays. These challenges include low throughput, low efficiency, complex procedure and technological barriers (e.g. precise positioning and accurate delivery of reagents), in both embryonic and larva stages. The microfabricated devices developed in this thesis could simplify the procedure of the assays, increase the throughput and allow one to perform the assay in an automatic manner.

A novel microdevice for microinjection of the *Drosophila* embryo has been developed. Unlike a conventional microinjector, this microdevice enables insertion of the needle that is precise and results in minimal damage over a wide range of depth (up to 200μm) inside the embryo with the resolution of 5μm. In this design, a simple 1-DOF compliant mechanism has been used for microneedle actuation, which significantly simplified the needle alignment and insertion procedure compare to a conventional microinjector. The reagent delivery was achieved via pressure driven flow, with the resolution of 10pL. The microinjector have been used to study the effect of the NaN_3 on the migration velocity of the cardioblasts cell in *Drosophila* embryo. As the results indicated, the CB migration velocity was decreased as the concentration of the NaN_3 were increased from the 10mM to 100mM. Additionally, a dose-dependent response to sodium azide was shown, which demonstrated that this platform could be a suitable microinjection system for drug delivery experiments.

Additionally, a series of microfluidic clamps for intact immobilization of the larva were investigated and an optimized structure for rapid mechanical immobilization of *Drosophila* larvae for CNS imaging was established. The optimal design had 3D segmental pinning, which was able to restrict CNS movement to maximum of 10±30 µm. The stability of the CNS location inside 3D segmental pinning chip allowed one to visualize neuronal activities using a genetically encoded calcium indicator probe (GCaMP5) without the use any anaesthetic drugs that could affect animals' neurophysiological status. However, the viability of the larvae load into the 3D segmental pinning chip, was reduced in comparison to the control.

In the second phase, the optimal immobilization mechanisms (Pneumatic Chip) developed in the first phase have been used for immobilization and live-intact fluorescence functional imaging of *Drosophila* larva's CNS in response to controlled acoustic stimulation. However, since this is a closed-configuration chip, access of the larva to sound stimulation was indirect. Therefore, another immobilization chip (FlexiChip), which allowed for manual loading, unloading and immobilization, has been developed. In this design, the posterior end of the larva inside the FlexiChip was open, thus allowing the larva to respire, and also for the acoustic vibrations to reach the larval body directly. A Genetically Encoded Calcium Indicator (GECI) probe, called GCaMP5, have been used to optically record the response of the CNS to auditory stimuli. We report an optimal GCaMP5 response at 200 Hz. These customized larval lab-on-chip platforms allow the integration of functional imaging with a sensory-motor response.

Both microfluidics clamps used in the previous phase can be used to immobilize *Drosophila* larvae for imaging the CNS in its entirety. However, they do not allow one to capture neuronal responses at single-neuron resolution. High resolution imaging of larva's CNS at single-neuron resolution requires stronger immobilization. In the third phase, an innovative device that exploits the biomechanics of the larva has been developed for immobilization and intact-live imaging of the single neuron in the larva's CNS and body wall. In this novel design, the immobilization of the larva was achieved by bending the larva's body, unlike current mechanical immobilization techniques that

compress the entire or part of the body. The immobilized larvae at the bending trap was completely intact in this new technique and fewer neuronal effects have been caused as compare to dissection and anaesthesia methods. Single neuronal images of the immobilized larvae have been recorded by epifluorescent and confocal microscopy for movement analysis and high resolution imaging, respectively. The movement analysis of the single neuronal in larva's CNS showed that bending trap could successfully keep the neuron inside the 50µm × 50µm field of view. The bending angle and the bending location plays critical roles in the strength of immobilization technique. The trap with bending of 0^o and 45^o could not effectively immobilize the neurons in the field of view as the 90^o bending tarp performed. The bending location of the larvae should be behind the A2 abdominal segment in order to fully immobilize the larvae in the desired FOV. The bending immobilization mechanism was used to imaging the larva's CNS neurons when it was exposed to 20mM NaN_3. The results showed that disregard of the location of the neuron in the CNS, the Ca^{2+} activity were significantly increased as the larvae the larvae was exposed to the sodium azide. This platform could potentially allow one to record neuronal events at different organs (e.g. gut, intestine) simultaneously, while they have true physiological connection to each other.

2. Research contributions

2.1. Applied contributions

2.1.1. Embryo microinjection

I. Conventional microinjection systems required a high degree-of-freedom micropositioner in order to align the microneedle with targeted location and insert it into the embryo. Here, this system was replaces with a simple 1-DOF compliant mechanism for microneedle actuation, which strongly simplified the needle aligning and insertion procedure compare to conventional microinjector. The positing resolution of 5µm was achievable using this system.

II. The microneedle used in conventional microinjection have a steep taper angle of over 30^{o} which can create significant damage to the embryo, if the microneedle was inserted too deeply. In this thesis, microneedles with tip sizes in the range of 3-6 µm and taper length of ~250µm (taper angle < 3.5^{o}) were fabricated to minimize embryo damage, while being large enough to allow reagent delivery into *Drosophila* embryo. This could allow one to precisely insert a long taper microneedle laterally and at various positions inside the length of the *Drosophila* embryo (up to 250µm) with the resolution of 5µm.

III. The current embryo microinjectors use an active system such as suction or fluidic drag force to hold and immobilize the embryo for needle insertion, which adds more complexity to the microinjection process. In this thesis, the device immobilizes the embryos using a form fitting passive immobilization chamber, allows easy needle penetration and enables a wide range of needle motion and positioning inside the embryo, with less complexity compare to active systems.

2.1.2. Immobilization of Drosophila larva for CNS imaging

I. A systematic study of the microfluidic clamps for intact immobilization of the larva without using anesthesia, was performed. As a result, an optimized structure for rapid mechanical immobilization of *Drosophila* larvae for CNS imaging was determined. The clamping and immobilization process were characterized by imaging and movement measurement of the CNS through expression of genetically encoded Calcium sensor. The optimal structure restricts the CNS movement to 10% of the motion from a glued larva and allows motion of only 10±30µm over 350s immobilization which was sufficient for CNS imaging. This study was the first systematic analysis of the mechanical clamps that used for immobilization of the larva in a non-invasive manner.

II. In the conventional larva's assays, the manipulation, position and orientation of *Drosophila* larva is performed manually, which could reduce the throughput and accuracy, increase human errors and complexity of the produce, and require skill operator as a result. The microfluidics format of the clamps designed in this thesis allowed one for

automated loading/unloading, position and orientation of the larva, which led to higher throughput and simplicity of the operation for larva's studies with large number of samples. The larva could pneumatically loaded/unloaded and positioned inside the devices and the converging channel (orientating channels) induced a self-orientating behavior on the larvae, which caused proper alignment of the larvae for CNS imaging.

III. The current microfluidics immobilization mechanism used for larva's internal imaging are closed-configuration chip and the access of the larva to sound stimulation were indirect. Therefore, another immobilization chip (FlexiChip), which allowed for manual loading, unloading and immobilization, has been developed. In this design, the posterior end of the larva inside the FlexiChip was open, which allowed the acoustic vibrations to reach the larval body directly and help them to respire. The FlexiChip provides a simple and quick manual option for animal loading and is suited for smaller studies

IV. The current microfluidic system, which are used for the immobilization of *Drosophila* larva to capture high resolution images of the larva's neuron, anesthetize the larva by exposing them either to CO_2, reduced temperature microenvironment or perform partial dissection. These procedures could affect the true physiological response of the larva's neurons in response to external stimulus. In this thesis, the first microfluidic device for immobilization and intact-live imaging of the *Drosophila* larvae at single-neuron resolution has been developed, which mechanically immobilized the larvae via a bending channel. This device can be used to record the neuronal activities in response to chemical stimulus, while the larva was not anesthetized and is intact. The movement analysis of the single neuronal in larva's CNS showed that bending trap could successfully keep the neuron inside the 50µm × 50µm field of view.

2.2. Fundamental contributions

I. Temporal effects of sound frequency (50-5000Hz) and intensity (95-115dB) on CNS activities were investigated and peak neuronal response of 200 Hz was identified. Our lab-on-chip devices will not only aid further study of *Drosophila* larva´s auditory responses but can be also adopted for functional imaging of CNS activities in response to other sensory cues. Auditory stimuli and the corresponding response of the CNS can potentially be used as a tool to study the effect of chemicals on the neurophysiology of this model organism.

II. In this thesis and for the first time, the fully intact response of the larva's CNS to the chemical stimulate at single-neuron resolution, have been imaged. The larva's neuronal activities in the ventral nerve cord of the CNS was significantly increased for 60% ($p<0.0005$) as the olfactory receptor neurons (ORNs) and gustatory receptor neurons (GRNs) of the larva was exposed to 20mM NaN_3. Compare to the results of other live calcium images ($dF/F > 50\%$) reported in literature, our results (neuronal activity more than 50%) indicated that the same neuronal activity in *Drosophila* chemosensory neurons can be measured using the bent chip. As a results, the bent chip is the first microfluidics chip that could allowed one to record the live activities of the larva's chemosensory neurons in the fully intact format, when it was exposed to a defined chemical stimuli.

III. The microinjector was used to study the effect of toxins on cardiogenesis in *Drosophila* embryos. Using this device, we demonstrate that the cardioblast migration velocity is modified in a dose sensitive manner to varying doses of injected Sodium Azide (NaN_3) and, for the first time, quantify the effect of the toxin on heart assembly. Injection with 40pL of NaN_3 was shown to decrease CB migration velocity and filopodia number at concentrations above 10mM, while embryos injected with the tracer Rhodamine B (0mM NaN_3) displayed no significant difference when compared to uninjected embryos. This device can be potentially used for other embryonic assays, which requires accurate delivery of the regents to a specific location within the embryo.

3. Recommendations for future work

3.1. Light sheet microscopy

The current immobilization devices developed in this thesis were greatly compatible with epifluorescent and confocal microscopy. However, they can be modified for two-photon and light sheet microcopy. Unlike the epifluorescent and confocal microscopy, the excitation and emission light of the light sheet microscopy are perpendicular to each other. Therefore, immobilization devices, which needs to be used in light-sheet microscopy, should give the same flat and clear space (~200μm) on side and bottom of the device for imaging. Currently, this space is only available thought the bottom of the device and the excitation light cannot be deliver uniformly from the side of the device due to the thick layer of PDMS. However, this problem can be addressed by generating new mold, which has features on the side of the clamp to control the roughness and thickness of the PDMS.

3.2. Two-photon laser microscopy for localize neuronal damage

Two-photon microscope laser can used to damage particular neurons in the immobilization larvae and live imaging of its healing process can be recorded. This can be only achieved when the larva is completely immobilized as it was obtain by the bending immobilization mechanism. The applications can go future and these devices can be also used for neuronal imaging of the CNS when it exposed to different stimulates such as heat, light, or electrical/magnetic field.

3.3. Probe-based assays

The immobilization devices can be modified for probe-based assays such as intact electrophysiology or microinjection of the larvae. To do this, some features microprobe holder and probe actuation mechanism should be added to the designs developed in this thesis. Complaint mechanism similar the one that used for embryo microinjection can be incorporated into the existing immobilization mechanism to electrically or chemically perturb the internal organs of the larvae. The longitudinal positioning of the probe or

microneedle can be achieved by actuation of the compliant mechanism. However, its lateral positioning could be more challenging. One can coat (deposit) the probe or microneedle by magnetic film, which can be later manipulated by external focused magnetic after insertion inside the larvae. Therefore, intact electrophysiological recording of the larva's internal organs would be possible.

3.4. Electrokinetic flow for microinjection

The delivery of the reagent inside the embryo was achieved by using pressure pulse driving flow. However, this pressure could displace large amount of the material inside the embryo. This could affect embryo's viability and it could be problematic in the assays that needs high rate of viability such as transgenic process. Electrokinetic flow could be an alternative to address this problem. The ionic reagent can be deliver into the embryo using electrical field induced between the embryo and the reagent chamber. However, minor modifications need to be implemented into the microinjector in order to incorporate the electrical probes into the device.

3.5. Transgenic assays

The embryo microinjector can used for creating transgenic embryos. This can be simply achieved by replacing NaN_3 solution with the desired plasmid.

APPENDIX

1. Mold fabrication

A) SU8 mold fabrication for embryo microinjector

First layer

1. Wash silicon wafer in Acetone and then in Methanol solution each one for 60s.
2. Rinse it with DI water, blow air gas to dry it and put the wafer on 150^{o} C hotplate for 2 minutes.
3. Cool down the wafer and plasma etch in in oxygen plasma etcher at 50Watt for 50 seconds.
4. Spin SU8-100 photoresist on the wafer at 500 rpm for 5s and then Ramp up the speed to 3100 rpm and keep it for 30s to get 90 µm thickness.
5. Soft bake the wafer at 65ºC for 9 minutes and then 95ºC for 27 min.
6. Align the wafer and mask on mask aligner by using the first layer mask.
7. Expose the wafer to UV light for total exposure energy of 150 mJ/cm 2 .
8. Post bake it in 65ºC for 1 min and then 95ºC for 9 min.
9. Put the wafer into SU8 developer and slowly shake it slowly until the features were appeared.
10. Use Isopropyl alcohol (IPA) to check remaining if the residual SU8 as they will have white color after pouring IPA on the wafer.
11. Re-submerge wafer back in developer if white residual appears.
12. Wash it with DI water and blow air to dry the wafer.
13. Hard bake at 120 ºC for 10 minutes.

Second layer

1. Rinse silicon wafer in Isoproponal alcohol (IPA) for 1 minutes, then wash it with DI water and blow air gas to dry it.
2. Spin SU8-3035 photoresist on the wafer at 500 rpm for 5s and then Ramp up the speed to 1650 rpm and keep it for 30s to get 90 µm thickness.
3. Soft bake the wafer at 95ºC for 10 minutes.
4. Align the wafer (the first pattern) with second pattern by using aligner.
5. Expose the wafer to UV light for total exposure energy of 210 mJ/cm 2 .

6. Post bake it in 65ºC for 1 min and then 95ºC for 4 min.
7. Put the wafer into SU8 developer and slowly shake it slowly until the features were appeared.
8. Use Isopropyl alcohol (IPA) to check remaining if the residual SU8 as they will have white color after pouring IPA on the wafer.
9. Re-submerge wafer back in developer if white residual appears.
10. Wash it with DI water and blow air to dry the wafer.
11. Hard bake at 120 ºC for 10 minutes.

B) 3D printed mold fabrication for larva immobilization

1. Draw the 3D model of the final design in Solidworks or an alternative 3D CAD design software.

2. Converted (Save as) the 3D model into a STL format.

3. Use 3D printer (Projet HD 3000 from 3D Systems, Material: VisiJet® EX200 Plastic) to print the design from the STL file in hard plastic part.

2. PDMS Casting

A) Embryo microinjector

1. Set the hotplate on 70ºC or oven on 75ºC.

2. Pour PDMS (10:1 ratio base: regent, SYLGARD® 184, Dow Corning Corporation) on the SU8 mold.

3. Put the molds into the desiccator and degas the PDMS for 5 min.

4. When the bobbles were removed from the PDMS mixture, place the mold into a 75ºC oven for 2hr to fully cure the PDMS. Alternatively, put the PDMS at on hot plate for 2hr. temperature for 24hr if oven was not available

B) Larva immobilization chips

1. Cut 1cm of silicone tubes (3/16"ID x 5/16"OD, Cole-Parmer Canada Inc.) and place on the allocated reservoirs as the inlet/outlet.

2. Pour the uncured PDMS (10:1 ratio base: regent, SYLGARD® 184, Dow Corning Corporation) on the 3D mold.

3. Put the molds into the desiccator and degas the PDMS for 5 min.

4. When the bobbles were removed from the PDMS mixture, place the mold into a 75ºC oven for 2hr to fully cure the PDMS. Alternatively, put the PDMS at room temperature for 24hr if oven was not available.

2. Device assembly

A) Embryo microinjector

1. Peel off the cured PDMS from the mold and tape the surface of the PDMS in order to avoid contaminations.

2. Cut the region between the fixed and the movable blocks with the dimension 2×10 mm^2 to form the compliant mechanism.

3. Cut the PDMS to proper dimensions (~1.5 × 1.5 cm^2), such that all aspects of the microinjector including compliant mechanism, needle channel and embryo chamber is placed into one piece.

4. Plasma bond (air plasma, High power for 70s) the bottom surface of the PDMS chip to a glass slide. In this configuration, the microfluidics channels are open on top surface.

5. Insert the shank of the needle into needle channel on the movable block.

6. Spread a droplet (~1 uL) of the PDMS (4: 1 ratio of the base and crosslinker) on the movable block to fully attach the microneedle to the movable block.

7. After curing the PDMS glue using the flame of the match, drive some reagent through the microneedle to make sure that the needle is still open and then take off the PDMS

B) Larva immobilization chips

1. Peel off the cured PDMS from the mold and tape the surface of the PDMS in order to avoid contaminations.

2. Using 4mm pouch hole, clear the PDMS diffused into the silicon tubes to avid clogging and create open reservoir.

3. Removed the tape and plasma bond (air plasma, High power for 70s) the bottom surface of the PDMS chip to a glass slide to form an enclosed microchannel.

4. Put the device into an 85ºC oven overnight to make a stronger bonding.

یک چند به کودکی باستاد شدیم
یک چند به استادی خود شاد شدیم
پایان سخن شنو که ما را چه رسید
از خاک در آمدیم و بر باد شدیم
خیام

Myself when young did eagerly frequent
Doctor and Saint, and heard great Argument
About it and about; but evermore
Come out by the same Door as in I went.
Omar Khayyam